

Thermodynamics and Kinetics of Advanced Separations Systems – FY 2010 Summary Report

Leigh R. Martin
Peter R. Zalupski

September 2010



The INL is a U.S. Department of Energy National Laboratory
operated by Battelle Energy Alliance

**INL/EXT-10-19986
FCR&D-SEPA-2010-000174**

Thermodynamics and Kinetics of Advanced Separations Systems – FY 2010 Summary Report

**Leigh R. Martin
Peter R. Zalupski**

September 2010

**Idaho National Laboratory
Fuel Cycle Research & Development
Separations and Waste Forms Campaign
Aqueous Separations and Radiochemistry Department
Idaho Falls, Idaho 83415**

**Prepared for the
U.S. Department of Energy
Office of Nuclear Energy
Under DOE Idaho Operations Office
Contract DE-AC07-05ID14517**

DISCLAIMER

This information was prepared as an account of work sponsored by an agency of the U.S. Government. Neither the U.S. Government nor any agency thereof, nor any of their employees, makes any warranty, expressed or implied, or assumes any legal liability or responsibility for the accuracy, completeness, or usefulness, of any information, apparatus, product, or process disclosed, or represents that its use would not infringe privately owned rights. References herein to any specific commercial product, process, or service by trade name, trade mark, manufacturer, or otherwise, does not necessarily constitute or imply its endorsement, recommendation, or favoring by the U.S. Government or any agency thereof. The views and opinions of authors expressed herein do not necessarily state or reflect those of the U.S. Government or any agency thereof.

SUMMARY

This report presents a summary of the work performed in the area of thermodynamics and kinetics of advanced separations systems under the Fuel Cycle Research and Development (FCR&D) program during FY 2010. Thermodynamic investigations into metal extraction dependencies on lactate and HDEHP have been performed. These metal distribution studies indicate a substantial deviation from the expected behavior at conditions that are typical of TALSPEAK process operational platform. These studies also identify that no thermodynamically stable mixed complexes exist in the aqueous solutions and increasing the complexity of the organic medium appears to influence the observed deviations. Following on from this, the first calorimetric measurement of the heat of extraction of americium across a liquid-liquid boundary was performed.

Interesting discoveries have been made during the investigation of the phase transfer kinetics of the lanthanides in the TALSPEAK process. These studies have been performed using macro metal concentrations in the aqueous phase, something that has not been previously studied in detail. It has been determined that under the conditions studied here, the phase transfer kinetics of the light lanthanides is extremely fast, as a result the distribution coefficient is seen to vary until the slowest lanthanide to extract has come to equilibrium. This will have significant effects on process scale-up and requires further attention. These results have also identified that the kinetics of DTPA binding to the lanthanides and actinides is of higher significance than first thought. The continuing work into this area has highlighted the fact that the binding kinetics show very little difference across the lanthanide series indicating that the binding rate is essentially independent of ionic radii or physical properties of the lanthanides. However, americium is seen to complex to DTPA significantly faster than the lanthanide ions. This has led to the suggestion that the nature of the interaction is chemically different between americium and DTPA than the lanthanides and DTPA.

Additional scope than originally planned for FY10 was also completed. Investigations into the use of different buffers for a TALSPEAK type process have been performed with promising results. The use of amino acids as the buffer instead of lactic acid results in significantly faster phase transfer kinetics and somewhat increased separation factors. In addition, the use of amino acids would allow for the process to be operated in a more acidic regime. Finally, investigations into the presence of ternary complexes in TALSPEAK aqueous phases have added additional weight to the argument that inner-sphere ternary complexes do not exist in solution. However, evidence presented here suggests that the lactate may be dehydrating the outer hydration sphere and facilitating phase transfer in this manner.

CONTENTS

SUMMARY.....	iii
ACRONYMS.....	ix
1. INTRODUCTION.....	1
2. APPROACH	2
2.1 Thermodynamics.....	2
2.2 Kinetics.....	3
3. SUMMARY OF RESULTS	3
3.1 Thermodynamics.....	3
3.1.1 Liquid-liquid Distribution of Lanthanides as Mediated by Lactate and HDEHP in Talspeak Solutions.	3
3.1.2 Two-phase Calorimetric Investigation of HDEHP-facilitated Liquid-liquid Distribution of Trivalent Americium.	16
3.2 Kinetics.....	19
3.2.1 Solvent Extraction Phase Transfer Kinetics	19
3.2.2 Solvent Extraction and Phase Transfer Kinetics from other Buffers	24
3.2.3 DTPA Complexation Kinetics.....	27
3.3 Ternary Complexation.....	29
4. CONCLUSIONS AND FUTURE WORK	34
5. PRESENTATION AND PUBLICATION OF RESEARCH	35
6. COLLABORATORS AND PARTICIPANTS	35
7. SUMMARY OF COLABORATORS EFFORTS IN FY 2010.....	35
7.1 LBNL.....	36
7.1.1 Summary of LBNL results	36
7.2 ANL.....	36
7.2.1 Summary of ANL results	37
7.3 SRNL.....	37
7.3.1 Electrochemistry	37
7.3.2 Solvent extraction	38
8. REFERENCES CITED	39
Appendix A Understanding Actinide/Lanthanide Speciation under TALSPEAK Conditions	41
INTRODUCTION.....	42
RESULTS.....	43
Complexation of Nd(III) and Eu(III) with Lactate (10-70°C).....	43
Effect of Temperature on the Complexation.....	43

Direct determination of enthalpy of complexation for Nd(III)/lactate and Eu(III)/lactate complexes at 25°C by calorimetry.....	44
Luminescence Data and the Coordination Modes in Ln(III)/Lactate Complexes	44
Complexation of Nd(III) and Eu(III) with DTPA (10 - 70°C).....	46
Potentiometry for Nd(III)/DTPA and Eu(III)/DTPA (10 – 70°C).....	46
Absorption Spectroscopy for Nd(III)/DTPA (10 – 70°C).....	46
Luminescence Spectroscopy for Eu(III)/DTPA (10 – 70°C)	47
Effect of Temperature on the Complexation.....	48
Effect of Temperature on the Complexation of Cm(III) with Nitrate (10 – 85°C).....	48
 PUBLICATIONS	 50
 FUTURE PLAN.....	 50
Complexation of Cm(III) with lactate and DTPA at variable temperatures	50
The complexation of Ln(III)/An(III) with propanoic acid at variable temperatures, in comparison with lactic acid	50
 REFERENCES.....	 50
 Appendix B.....	 52
 Separation Process Thermodynamics and Kinetics: Development of Microfluidic Devices for Solvent Extraction Studies and Radioanalytical Applications.....	 52
 SUMMARY	 53
 INTRODUCTION.....	 53
 Appendix C.....	 62
 Electrochemical Investigation of TALSPEAK Processes	 62
 INTRODUCTION.....	 63
 SIGNIFICANCE	 64
 APPROACH.....	 64
 SUMMARY OF RESULTS	 65
 CONCLUSIONS.....	 71
 REFERENCES.....	 71
 INDICATORS OF PROJECT QUALITY AND PRODUCTIVITY	 72
 Appendix D Distribution of Actinides between the Aqueous and Organic Phases in the TALSPEAK Process	 73
 SUMMARY	 74

Appendix DA.....	101
Solution Preparation for Valence Adjustment Study.....	101
Appendix DB.....	104
Solution Preparation for Distribution Coefficient Measurements.....	104
Appendix DC.....	106
Np and Pu Distribution Coefficients.....	106

FIGURES

Figure 1. Validation studies on the distribution of trivalent <i>f</i> -block elements in TALSPEAK-based liquid-liquid distribution system. (a) Characteristic TALSPEAK distribution trend for the extraction of 10 lanthanide mixture (La ³⁺ - Ho ³⁺) by 0.1 M HDEHP in <i>n</i> -dodecane from aqueous mixtures of 0.05 M DTPA and 1.0 M (H ⁺ , Na ⁺) lactate buffer at pH = 3.0. (b) Determination of the agreement between the ICPMS analyses and radiometric measurements of the distribution ratios for the extraction of cerium and europium. (c) Illustration of the expected suppression of the distribution ratios for lanthanides as the acidity of the aqueous phase is decreased. (d) Matching distribution results for the extraction of lanthanides from TALSPEAK aqueous solutions of varying preparation: recipe 1) 0.05 M Na ₅ DTPA, 1.0 M sodium lactate, recipe 2) 0.05 M Na ₅ DTPA, 1.0 M lactic acid, recipe 3) 0.05 M H ₅ DTPA, 1.0 M lactic acid.....	5
Figure 2. Effect of the total lanthanide concentration in solution on the distribution ratios investigated for the system: Organic – 0.1 M HDEHP in <i>n</i> -dodecane, Aqueous – 0.05 M Na ₅ DTPA, 1.0 M lactic acid, pH 3.0. (a) Overall TALSPEAK distribution curve. (b) Linear relationship on the extraction isotherm scale rule out HDEHP loading effects.....	6
Figure 3. Structural comparison of lactic acid and glycerine.....	7
Figure 4. Effect of increasing concentration of glycerine on the dissociation constant of lactic acid.....	9
Figure 5. Lactate dependency for the liquid-liquid distribution of Ce ³⁺ . Organic phase: HDEHP in <i>n</i> -dodecane. Aqueous phase: [Ln ³⁺] _{total} = 1 mM, p[H ⁺] = 3.5, [DTPA] = 0.05 M, varying [Lac ⁻] _{eq} , <i>I</i> = 1 - 2M.....	10
Figure 6. Comparison of the liquid-liquid distribution studies for Gd ³⁺ and Ho ³⁺ extraction. Organic phase: HDEHP in <i>n</i> -dodecane. Aqueous phase: [Ln ³⁺] _{total} = 1 mM, p[H ⁺] = 3.5, [DTPA] = 0.05 M, varying [Lac ⁻] _{eq} , <i>I</i> = 1 - 2 M.....	11
Figure 7. Extractant dependencies for the extraction of Eu ³⁺ from TALSPEAK mixtures containing 0, 0.5 and 1.0 M free lactate at equilibrium.....	12
Figure 8. Extraction of Eu from mineral acid solutions by HDEHP in toluene and <i>n</i> -dodecane. The distribution ratios collected for the aliphatic system are also plotted as a function of the activity of the HDEHP dimer.....	13
Figure 9. The comparison of the distribution ratios collected for the extraction of Eu from aqueous solution of 0.05 M DTPA, 0.05 M free lactate before and after correction for the non-ideal behavior of HDEHP dimer in <i>n</i> -dodecane.....	14

Figure 10. Increasing non-ideal behavior of HDEHP dimer..... 15

Figure 11. The comparison of the extraction of lanthanide mixture (La^{3+} - Ho^{3+}) by 0.2 M HDEHP in *n*-dodecane from pH 3.5 aqueous solutions containing 0.05 M DTPA, and either no lactate or 2.8 M total lactate..... 16

Figure 14. Influence of $[\text{DTPA}]_{(\text{aq})}$ on rate of extraction of Eu by 0.17 M HDEHP in dodecane using a vortex mixer to agitate the two phases. Aqueous phase composition 1 M lactic acid at pH 3.8, $[\text{DTPA}]$ 10-50mM..... 21

Figure 15. Influence of $[\text{DTPA}]_{(\text{aq})}$ on rate of extraction of (a) cerium and (b) americium by 0.17 M HDEHP in dodecane using a vortex mixer to agitate the two phases. Aqueous phase composition 1 M lactic acid at pH 3.8, $[\text{DTPA}]$ 10-50 mM..... 21

Figure 16. Influence of $[\text{DTPA}]_{(\text{aq})}$ on rate of extraction of Eu by 0.17 M HDEHP in dodecane using a rotary mixer to agitate the two phases. Aqueous phase composition 1.0 M lactic acid at pH 3.8, $[\text{DTPA}]$ 10-50 mM..... 23

Figure 17. Influence of $[\text{DTPA}]_{(\text{aq})}$ on rate of extraction of (a) cerium and (b) americium by 0.17 M HDEHP in dodecane using a rotary mixer to agitate the two phases. Aqueous phase composition 1 M lactic acid at pH 3.8, $[\text{DTPA}]$ 10-50 mM..... 23

Figure 18. a) structure of L-alanine, b) Structure of L-lactic acid..... 25

Figure 19. Distribution ratios of ^{154}Eu (●) and ^{241}Am (■) as a function of pH for an aqueous phase composition of 1.0 M L-alanine and 0.05 M DTPA, org. phase = 0.17 M HDEHP in dodecane..... 25

Figure 20. Distribution ratios of ^{154}Eu (●) and ^{241}Am (■) as a function of time for an aqueous phase composition of a) 1.0 M L-alanine and 0.05 M DTPA pH 1, org. phase = 0.17 M HDEHP in dodecane and b) 1.0 M L-alanine and 0.05 M DTPA pH 3.8, org. phase = 0.17 M HDEHP in dodecane. Experiments performed using a rotating bar. 26

Figure 21. Sample kinetics trace from the stopped flow spectrophotometer measuring the rate of reaction of Pr-AAIII complex with DTPA $[\text{Eu}] = 5 \times 10^{-5}$ M, $[\text{AAIII}] = 5 \times 10^{-5}$ M, 50 mM propionate buffer, $I = 0.1$ M (NaNO_3) $[\text{DTPA}] = 1 \times 10^{-3}$ M, pH 3.7. 27

Figure 22. Plot of average (a) k_1 and (b) k_2 vs. $[\text{AAIII}]$ in 50 mM propionate buffer, $I = 0.1$ M (NaNO_3). $[\text{Am}] = 5 \times 10^{-5}$ M : $[\text{AAIII}] = 1-5 \times 10^{-5}$ M, $[\text{DTPA}] = 1 \times 10^{-3}$ M pH 3.7..... 28

Figure 23. Plot of average k_1 for the reaction of DTPA with Pr, Eu, Er and Am as a function of ionic radii. $[\text{metal}] = 5 \times 10^{-5}$ M, $[\text{AAIII}] = 5 \times 10^{-5}$ M, 50 mM propionate buffer, $I = 0.1$ M (NaNO_3), $[\text{DTPA}] = 1 \times 10^{-3}$ M, pH 3.7..... 29

TABLES

Table I. Molar concentrations of all components chosen to reproduce TALSPEAK-related conditions at 4 different total lactate concentration..... 7

Table II. Comparison of the glass electrode calibration equations determined for the solutions of increasing concentration of glycerine. 8

Table III. Reversible rate constants for the extraction of 10 mM Eu from 1.0 M lactic acid at pH 3.8, $[\text{DTPA}]$ 10-50 mM, into 0.17 M HDEHP. 22

Table IV. Distribution coefficients and separation factors for Am, Eu and Ce from different amino acid buffer systems. Alanine buffer - $[\text{Alanine}] = 1.0$ M, pH 2.7, 35 mM DTPA,

7 mM Eu; Arginine buffer - [Arginine] = 1.0 M, pH 2.7, 35 mM DTPA, 7 mM Eu;
Methionine buffer - [Methionine] = 1.0 M, pH 1.7, 25 mM DTPA 10 mM Eu; Histidine
buffer - [Histidine] = 1.0 M, pH 1.7, 25 mM DTPA 10 mM Eu. 26

ACRONYMS

AAIII	Arsenazo III
ANL	Argonne National Laboratory
CV	Cyclic voltammetry
D	Distribution coefficient
DTPA	Di 2-ethylenetriamine-N,N,N',N'',N'''-pentaacetic acid
FCR&D	Fuel Cycle Research and Development
FS	Ferrous Sulfamate
HAN	Hydroxylamine Nitrate
HDEHP	Di ethyl hexyl phosphoric acid
ICPMS	Inductively Coupled Plasma Mass Spectrometry
INL	Idaho National Laboratory
LBNL	Lawrence Berkeley National Laboratory
NMR	Nuclear Magnetic Resonance
ORNL	Oak Ridge National Laboratory
SRNL	Savannah River National Laboratory
TALSPEAK	Trivalent Actinide Lanthanide Separations by Phosphorus-reagent Extraction from Aqueous Komplexes
UM	University of Manchester
UK	United Kingdom
US DOE	United States Department of Energy
UV-vis	Ultra Violet-visible

SEPARATIONS CAMPAIGN

THERMODYNAMICS AND KINETICS OF ADVANCED SEPARATIONS SYSTEMS – FY2010 SUMMARY REPORT

1. INTRODUCTION

To develop a sustainable closed nuclear fuel cycle, significant advances need to be made with respect to greater fuel utilization and a reduction in the long term heat loading and radiotoxicity in the final waste-forms. To simultaneously accomplish these goals some level of used fuel processing will be required. As such, there are two scenarios available for this; “Full Recycle” that will enable the long-lived actinide elements to be recycled/burned rather than disposed or “Modified Open” where some limited separations steps are performed to recover a reduced level of the actinides but substantially lowers proliferation risk of re-use. Solvent extraction processes are currently the primary methodology used worldwide to recover the actinides from used nuclear fuel. These chemical separations make use of *liquid-liquid distribution* techniques to separate the actinides from the remainder of the fission products.

The behavior of solutes in *liquid-liquid distributions* is influenced by many factors including their interactions with the aqueous phase electrolyte and organic reagents required to complete the separation.¹ As such, a thorough comprehension of the physicochemical properties of any separations system under study is essential to determine not only the final product but the mechanism via which the extraction takes place.² Studying the thermodynamic properties of a solvent extraction system (ΔG° , ΔH° and ΔS°) will provide an insight into the driving forces for the separation process, and possibly the end product. In addition, considering the effects of temperature on these fundamental parameters (below and above ambient) should lead to a more robust insight into process performance. Studying the kinetics of solvent extraction processes has two key components: the rates of the various chemical reactions occurring within the system of study and the rate of the phase transfer of the extracted species. Each of these components yields different but necessary information on describing the overall system. Understanding the rates at which the various chemical reactions within the system occur leads to comprehension of the molecular ordering between the solvent and solute that drive the process (*i.e.* mechanistic interpretation). Following on from this, understanding the phase transfer kinetics tells us how quickly the system reaches equilibrium. This becomes important in scale up and plant design so the correct equipment can be used depending on if the process is fast or slow. In summary, studying the thermodynamics of a system tells us where the end point is and studying the kinetics of a system tells us how we get there.

Having a complete understanding of any solvent extraction process from start to finish assists process chemists making corrective actions when the system enters “off normal” conditions. This becomes increasingly important when, as with used fuel separations systems, the equipment is in shielded cells with limited access. When embracing the necessity for some level of minor actinide recycle, we find that the solvent extraction processes available to us to perform this separation are significantly more complex than those currently deployed at industrial scale. This is due to the small chemical differences that have to be exploited to achieve a substantial separation between the trivalent actinides and lanthanides. As a result, although these processes are known to “work” under ideal conditions, a detailed molecular understanding of them has not yet been achieved. One obvious example of this is the TALSPEAK process (Trivalent Actinide Lanthanide Separations by Phosphorus-reagent Extraction from Aqueous Komplexes).

The TALSPEAK separation scheme was initially introduced by Weaver and Kappelmann at Oak Ridge National Laboratory (ORNL),³ who optimized the An/Ln separation factors by selecting a DTPA complexant in a mixture of 1.0 M H⁺/Na⁺ lactate buffer (pH = 3.6) as an operational platform of the process.³ Nilsson and Nash have recently reviewed the history of TALSPEAK characterization efforts, indicating many complex features of its chemistry.⁴ Although the inter-group separation has been demonstrated at both the bench and pilot plant scale, Nilsson and Nash have begun to move outside the operational envelope for TALSPEAK suggested by Weaver and Kappelmann, to focus on the predictive modeling of its chemistry.⁵ This approach targeted a more application-based set of criteria like the robustness of the process and the response to off-normal operating conditions by corrective actions. However, when attempting to theoretically reproduce this pH dependency for the lanthanide distribution, using the reported equilibrium constants for the chemical reactions expected for this process, a progressing discrepancy between the experiment and a calculation is observed.⁵

Although the work presented here primarily focuses on the TALSPEAK process, the aim of the program as a whole is to create a capability throughout the national laboratory complex that is able to take a separations system and understand it at a fundamental level. By concentrating on the thermodynamic and kinetic features of a chemical separations process it is envisaged that more accurate models for any process can be built. In addition, applying the knowledge gained should assist in corrective actions should a process end up in “off-normal” conditions. TALSPEAK provides an excellent platform for building such capability as mechanistically, after over 40 years of research into the process, it is still so ill defined.

This report summarizes the FCR&D research efforts for FY 2010. The major INL tasks this year were to continue work studying the behavior of the fundamental parameters ΔG , ΔH and ΔS in relation to the extraction TALSPEAK media and to continue investigations into the kinetics of the chemical processes associated with the TALSPEAK system. Increased scope tasks include work on ternary complexation within the TALSPEAK aqueous phase and the use of amino acids as a buffer for TALSPEAK. The synergistic research efforts at LBNL, ANL and SRNL in the Thermodynamics and Kinetics of Advanced Separations Systems program will also be summarized here.

2. APPROACH

Experimental efforts in FY10 mainly focused on the assembly of new thermodynamic data, which would enable us to expand on some of the possible reasoning behind the observed unpredictable behavior of TALSPEAK-type systems. To this end we have established new experimental capabilities to allow thorough investigation of liquid-liquid distribution equilibria for the entire series of lanthanide elements. It is illustrated in this report how studying the partitioning behavior of the entire family of lanthanides is crucial to inquisitive interpretation of TALSPEAK. In support of these thermodynamic measurements investigations have begun into the kinetics of phase transfer in the TALSPEAK separations system using metal loadings closer to that expected in a real process. Although some excellent work has been accomplished using tracers to study metal distribution behavior in this separations system, these types of studies may not adequately describe what will occur under process conditions.

The methodologies employed for our thermodynamic and kinetic studies are outlined below.

2.1 Thermodynamics

To establish a new experimental capability for extended constant temperature studies of liquid-liquid distribution of all 15 members of the lanthanide family, 0.1 M stock solutions were produced and characterized within our laboratories. A multitube vortexer capable to very long equilibration times was installed in a constant temperature chamber set at 25 °C, where all experimental activities were

performed. The organic-aqueous distribution of lanthanides was established using Inductively Coupled Plasma Mass Spectrometry (ICPMS). To validate this capability a series of initial tests we performed to reproduce literature data or reproduce the ICPMS results using radiometric techniques and establish some preliminary sets of data of value to the planned experimental activities.

The thermodynamic investigations of liquid-liquid distribution reactions continued using recently developed two-phase calorimetric methodology to study the thermochemical features of HDEHP-facilitated phase transfer of americium metal ion across a liquid-liquid boundary. In this report, the first account of a direct calorimetric measurement of the heat of liquid-liquid partitioning of any transuranic element reported to date is discussed. This methodology applies modern isothermal titration microcalorimetry, allowing accurate measurements of microjoule heat events inside a 1 mL reaction vessel. To follow the transfer of Am(III) from an aqueous solution into the organic diluent a simple, well-characterized liquid-liquid partitioning system was chosen. A cation-exchanging organophosphate phase transfer reagent – bis(2-ethylhexyl)phosphoric acid (HDEHP)– is a hard electron donor dissolved in *n*-dodecane.

2.2 Kinetics

The objective with these experiments was to perform some comparative studies with those conducted last year into europium and americium complexation kinetics in a propionate. In this evolution testing was broadened to include praseodymium and erbium in order to have a greater representation of the lanthanide series as a whole. These complexation kinetics tests were performed using arsenazo III (AAsIII) as an indicator for “free” metal ion in solution. To perform complexometric kinetic investigations stopped flow experiments were performed. The stopped flow experiments were performed on an OLIS Hummingbird DB 620 UV-vis-NIR spectrophotometer. The flow system was thermostated to ± 0.1 °C. The complexation kinetics of the metal-DTPA complex were monitored by the change in absorbance at 667 nm. Several replicate determinations were performed for each set of experimental conditions.

Liquid-liquid distribution studies have been performed to establish the effects of DTPA on the phase transfer kinetics in the TALSPEAK system. Small batch contact tests were performed under TALSPEAK relevant lactic acid/ lactate conditions and HDEHP concentrations. The aqueous phase consisted of 10 mM Eu in 1M lactic acid/ lactate buffer at pH 3.8 and this solution was spiked with tracer Ce, Eu and Am. Mixing was performed using a vortex mixer and a rotary bar.

3. SUMMARY OF RESULTS

3.1 Thermodynamics

3.1.1 Liquid-liquid Distribution of Lanthanides as Mediated by Lactate and HDEHP in Talspeak Solutions.

To investigate the effects of increasing complexity of the organic phase on the fundamental aspects of TALSPEAK chemistry, a series of liquid-liquid distribution studies were performed where free lactate concentration was varied in the aqueous phase and the concentration of HDEHP was varied in the organic phase. Each lactate dependency study was performed at constant pH to eliminate the effect of changing lactate:lactic acid ratio on the distribution ratios. Lactate dependencies were extended further into the more complex TALSPEAK-type conditions with an intent to span the entire range of lactate concentrations present in Danesi's and Nilsson's reports.^{5,6} Four independent lactate dependency studies were performed using 0.05, 0.10, 0.15 and 0.20 M HDEHP dissolved in *n*-dodecane. As a result, a 3 dimensional investigation could be developed, which correlated influencing effects of increasing concentrations of lactate and HDEHP on liquid-liquid distribution of lanthanides.

To establish a new experimental capability for extended studies of liquid-liquid distribution of lanthanides, oxides of all 15 members of this *f*-element family were fumed with either concentrated nitric acid or triflic acid to produce 0.1 M stock solutions to be used in all kinetic and thermodynamic studies of aqueous partitioning systems. A multitube vortexer capable to very long equilibration times was installed in a constant temperature chamber set at 25 °C, where all experimental activities were performed. The organic-aqueous distribution of lanthanides was established using Inductively Coupled Plasma Mass Spectrometry (ICPMS). In order to validate this newly established experimental capability at the INL, a series of initial tests were performed, which were designed to either reproduce targeted literature data, reproduce the ICPMS results using radiometric techniques or establish preliminary sets of data of value to the planned experimental activities. The assembled validation work is summarized here.

Initial work was performed to reproduce Danesi's results⁶ on the extraction of europium by 0.1 M HDEHP in *n*-dodecane from aqueous solution of 1.0 M sodium lactate, adjusted to pH of 3, where the concentration of total anion was controlled with NaCl, i.e. $[\text{Lac}^-] + [\text{Cl}^-] = 1 \text{ M}$. Figure 1a shows the assembled TALSPEAK distribution curve for the mixture of 10 lanthanides (La^{3+} - Ho^{3+}). For those conditions Danesi reported a distribution ratio of 3.6 for europium, which compared favorably to the experimentally determined value of 2.8. Considering that Danesi did not report exact recipes for the preparation of aqueous solutions in his study (it is unknown whether lactic acid or sodium lactate was used) the relative agreement of the results obtained here is acceptable. The characteristic TALSPEAK shape also agrees in its expected proportions with results reported in previous investigations.⁴ Figure 1b presents cerium, europium and americium distribution ratios at conditions described for the initial literature validation. The use of radiotracers – Ce-134, Eu-153 and Am-241 – allowed further validation of the data obtained by ICPMS. The evaluation of the americium behavior yielded the expected separation factor between the lanthanide elements and was representative of actinides. The lowest separation factor of 32 between neodymium and americium confirmed correct TALSPEAK conditions for our studies. This extent of the separation is expected when aqueous TALSPEAK solutions are adjusted to the pH of 3.0, which is slightly lower than the optimal setting (pH = 3.6) for maximized separation between actinides and lanthanides. Further initial assessment sought to confirm a proper pH response for our TALSPEAK investigations. Figure 1c shows the expected suppression of the distribution ratios for the investigated lanthanides due to the increased pH of aqueous solution to 3.5. The observed decrease agrees with previous investigations of pH dependencies of TALSPEAK systems reported by Weaver and Kappelmann,³ Nilsson and Nash,⁵ and represents perhaps the most significant unexplained feature of fundamental chemistry of TALSPEAK.

Aqueous solutions for TALSPEAK separations may be prepared using at least three different recipes which, depending on the starting reagent, may introduce varying amounts of sodium into the system. Aged lactic acid reagent may undergo a lactonization process, which could possibly affect the solution chemistry of the lactate buffer. As most literature reports do not specifically list the recipes for aqueous solution make up the extraction of lanthanides was tested using three types of aqueous mixtures that, when mixed, yield the same concentrations of lactate and DTPA, but contain between 1 – 2 M concentration of Na^+ ion. Figure 1d illustrates the characteristic TALSPEAK trends for the collected distribution ratio data. No dependence for the liquid-liquid distribution of lanthanides on the overall chemical form (acid or salt) of the major components of TALSPEAK aqueous phase was found. As a result all aqueous solutions for further studies of TALSPEAK chemistry were prepared using pentasodium salt solution (standardized using colorimetric titration with Arsenazo III) and lactic acid, thus eliminating the necessity of solid dissolution.

Fundamental studies of liquid-liquid distribution equilibria often rely on simplification of conditions to eliminate some possibly complicating aspects of solution chemistry. One of those factors is presence of macro amounts of metal in solution, which could introduce unexpected formation of polymeric metal complexes in the organic solution, excessive loading of extractant and possibly the formation of the third

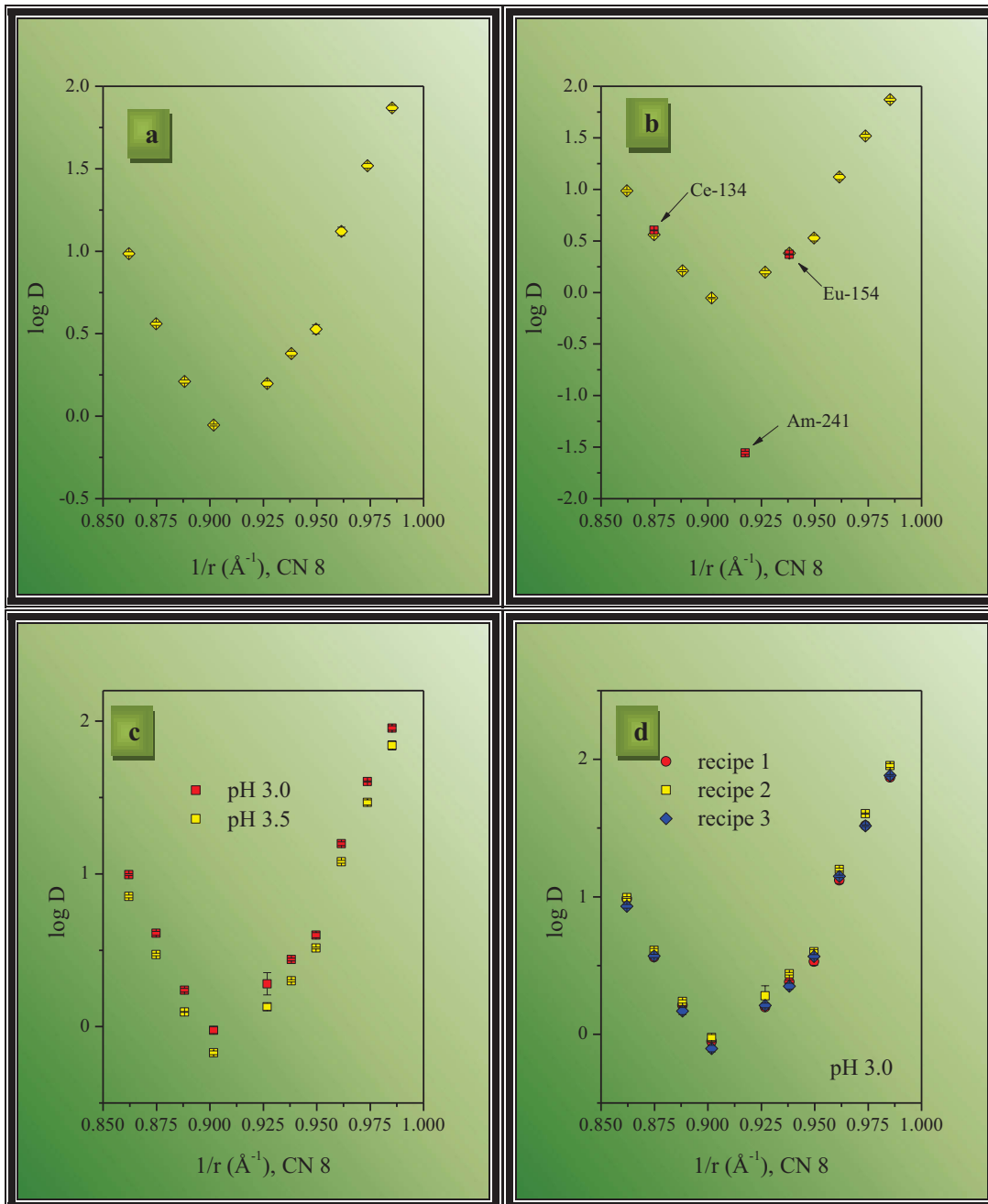


Figure 1. Validation studies on the distribution of trivalent *f*-block elements in TALSPEAK-based liquid-liquid distribution system. (a) Characteristic TALSPEAK distribution trend for the extraction of 10 lanthanide mixture (La^{3+} - Ho^{3+}) by 0.1 M HDEHP in n-dodecane from aqueous mixtures of 0.05 M DTPA and 1.0 M (H^+ , Na^+) lactate buffer at pH = 3.0. (b) Determination of the agreement between the ICPMS analyses and radiometric measurements of the distribution ratios for the extraction of cerium and europium. (c) Illustration of the expected suppression of the distribution ratios for lanthanides as the acidity of the aqueous phase is decreased. (d) Matching distribution results for the extraction of lanthanides from TALSPEAK aqueous solutions of varying preparation: recipe 1) 0.05 M Na_5DTPA , 1.0 M sodium lactate, recipe 2) 0.05 M Na_5DTPA , 1.0 M lactic acid, recipe 3) 0.05 M H_5DTPA , 1.0 M lactic acid.

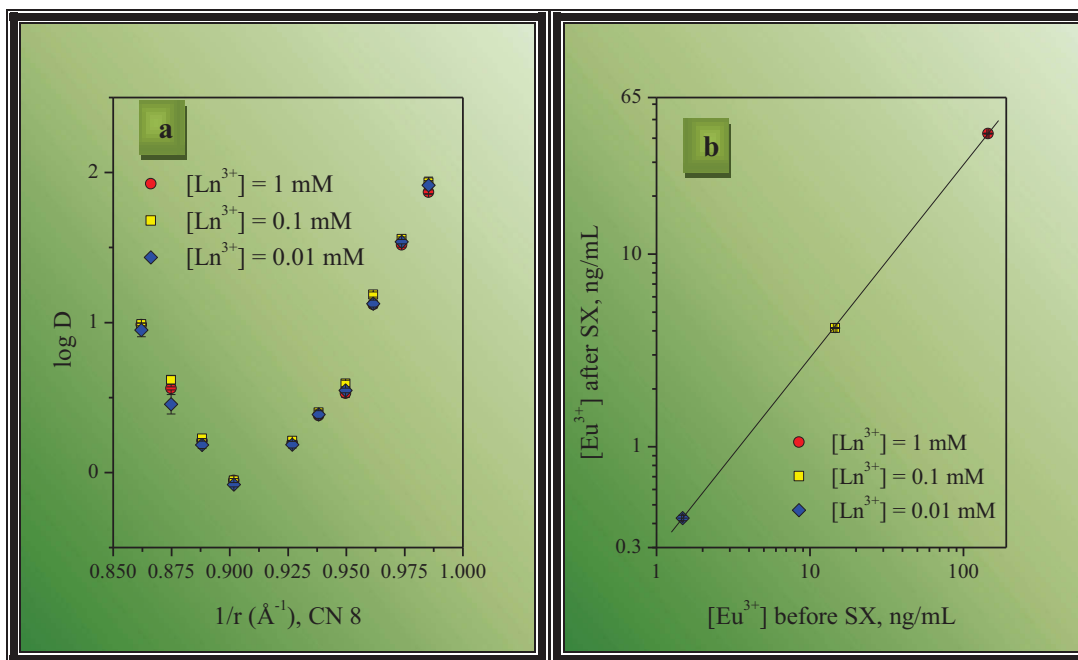


Figure 2. Effect of the total lanthanide concentration in solution on the distribution ratios investigated for the system: Organic – 0.1 M HDEHP in *n*-dodecane, Aqueous – 0.05 M Na_5DTPA , 1.0 M lactic acid, pH 3.0. (a) Overall TALSPEAK distribution curve. (b) Linear relationship on the extraction isotherm scale rule out HDEHP loading effects.

phase. Despite our decision to use 1 mM total lanthanide concentration in our studies, which should not result in any aforementioned complications, the effect of increasing concentration of metal in the system on the distribution ratios was studied. Figure 2a illustrates that no matter if the metal concentration in solution is 10 μM (nearly trace) or 1 mM the distribution ratios overlap, yielding the linear relationship (Figure 2b) that confirms lack of loading effects. Finally, the effects of the purity of HDEHP on the distribution ratios was investigated. The results of extraction for the extractant reagent purified by the method of copper salt precipitation (98.5 %) was compared with the commercially available HDEHP (97.1 %). The distribution ratios were slightly suppressed when the less-pure reagent was used, most likely due to the partitioning of the mono-2-ethylhexyl impurity of HDEHP into the aqueous phase.

The above listed preliminary studies of the TALSPEAK liquid-liquid distribution system supported proceeding with the main study, which targeted the effects of the increasing lactate concentrations on the distribution ratios of lanthanides. As discussed, the intent of the study attempts to combine the studies by Danesi⁶ and Nilsson⁵ to inspect lactate's influence at the operational conditions of TALSPEAK, while eliminating the uncertainty of changing pH throughout the study. To expand the lactate dependency study to those complex regions of high buffer concentrations an initial assessment of the non-ideal solution chemistry of such mixtures becomes necessary. Free lactate concentration at equilibrium may be calculated using a mass balance equation $[\text{Lac}]_{\text{eq}} = [\text{Lac}]_{\text{total}} / (1 + [\text{H}^+]/K_a)$ to illustrate the complexity of the solution. At pH 3.5, a 2.31 M total lactate concentration is needed ($\text{p}K_a = 3.64$) to produce a 1.0 M free lactate concentration. Under such conditions, a solution contains more than a molar concentration of neutral molecular carboxylic acid. This organic molecule most definitely affects the activity of water, which, in turn, may influence the thermodynamic equilibria in solution. For example, the dissociation of lactic acid may be affected as the acid / conjugate base balance shifts due to the high concentrations of carboxylic acid. A measurement of pH using a glass electrode may also experience deviations due to the differences between the solutions used in calibration and measurement. For pH measurements at high

ionic strength a strong acid / strong base titrations are normally performed to correlate the response of the electrode with the concentration of the hydrogen ion, i.e. $p[H^+]$. As such, an accepted method for this calibration usually employs a strong electrolyte – $NaNO_3$, $NaClO_4$ or $NaCl$ – to maintain the ionic strength. It is valid, however, to speculate on the appropriateness of such calibration, when a glass electrode will be utilized in measurements in complex buffer solutions containing 0.05 M (H^+ , Na^+)DTPA and up to 2 M (H^+ , Na^+)Lac. The electrode response may be skewed by changes in the liquid junction potential, asymmetry potential or directly by the medium effects.

Table I. Molar concentrations of all components chosen to reproduce TALSPEAK-related conditions at 4 different total lactate concentration.

Condition	[Lac] _{total} , M	Triflate, M	Glycerine, M	Nitrate, M
1	0.5	0.21	0.29	0.79
2	1.0	0.42	0.58	0.58
3	1.5	0.63	0.87	0.37
4	2.0	0.84	1.16	0.16

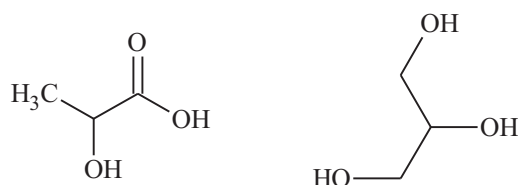


Figure 3. Structural comparison of lactic acid and glycerine.

It was decided to carefully examine this possible complication and investigate what deviations should be expected due to the presence of large concentrations of lactic acid in the solution. To mimic the effects of the lactic acid, glycerine was chosen as a similar organic molecule that should not complicate the analysis with acid/base equilibrium. Figure 3 compares the structures of lactic acid and glycerine. Sodium triflate was used to substitute for lactate anion as shown by our previous investigations.⁷ Using sodium nitrate as the ionic strength adjustor, a series of TALSPEAK-related solution mixtures was prepared to reproduce the conditions where high lactate concentrations exist. Mixing sodium triflate, glycerine and sodium nitrate mimicked the solution compositions at 4 different conditions, where 0.5, 1.0, 1.5 and 2.0M total lactate would be present. By choosing a pH of 3.5 and an arbitrary lactic acid pK_a of 3.64 the compositions of all the components could be calculated. Table I shows the concentrations of all participating species at 4 targeted conditions. For each reproduced condition, strong acid (HNO_3) and strong base ($NaOH$) were introduced into the solutions while adjusting the required amounts of sodium nitrate to keep the ionic strength at 1.0 M. Similarly, 10 mM sodium lactate concentration was prepared at each situation. A series of potentiometric investigations followed the standardization of each of 16 solutions prepared. Strong acid / strong base titrations were performed to study the response of the glass electrode when progressing through the systems of increasing complexity. Also, sodium lactate was titrated with nitric acid to observe the changes of the dissociation equilibrium due to the increasing concentrations of glycerine in solution.

Studying the strong acid / strong base equilibrium produced a series of electrode calibration equations, which illustrate the response of the glass electrode to the changing concentration of hydrogen

ion in solution. As the concentration of glycerine increased, a medium-inflicted deviation in the measured value of $p[H^+]$ was expected, which could introduce inaccurate final lactate buffer proportions. Table II summarizes the results of the potentiometric study, comparing the electrode calibration equations to that determined using a conventional strong electrolyte system – sodium nitrate. The glass electrode is clearly influenced by the changing characteristic of the aqueous solution; however, it appears that the observed changes in the slope and the intercept of the calibration equation are self-correcting. The slope and the intercept of the calibration equation appear to compensate the medium effects, so that the calibration returns very close values of $p[H^+]$ at the chosen electromotive force of 215.

Table II. Comparison of the glass electrode calibration equations determined for the solutions of increasing concentration of glycerine.

condition	Electrode calibration	mV	$p[H^+]$	error, $\pm 2\sigma$
0	$p[H^+] = -0.01670\text{mV} + 7.0924$	215	3.502	0.025
1	$p[H^+] = -0.01691\text{mV} + 7.1426$	215	3.507	0.027
2	$p[H^+] = -0.01709\text{mV} + 7.1814$	215	3.507	0.035
3	$p[H^+] = -0.01716\text{mV} + 7.1913$	215	3.502	0.042
4	$p[H^+] = -0.01727\text{mV} + 7.2152$	215	3.502	0.051

The performance of the glass electrode is compromised slightly as indicated by the increasing uncertainty in the pH measurement. However, it is clear that the effect of the growing concentration of glycerine in solution should not affect the glass electrode reading significantly. If our assumption of similar physico-chemical characteristics between glycerine and lactic acid is valid, it may be concluded that the medium effects due to a large presence of organic acid in the aqueous phase are minimal. This observation is reiterated by the small influence of the medium on the dissociation of lactic acid. Figure 4 illustrates the changes of the acid / base equilibrium of lactic acid as the aqueous environment becomes increasingly hydrophobic due to the presence of glycerine. The medium effect is small; however, even small changes in the pK_a of lactic acid are quite significant when working at very high total lactate concentrations. The observed correlation was used to adjust the recipes of the aqueous solutions for the lactate dependency studies.

As the medium effects imposed by the presence of lactic acid do not appear to significantly complicate the solution chemistry of TALSPEAK-type system, studies of liquid-liquid distribution ratios proceeded. The extraction of the lanthanide mixture (La^{3+} - Ho^{3+}) was monitored from aqueous solutions of 8 different concentrations of total lactate. The total concentration of the anion, $[Lac^-] + [NO_3^-]$, was adjusted to 1 M using sodium nitrate prior to the adjustment of pH. The acidity of the aqueous solutions was adjusted to 0.316 mM, i.e. $p[H^+]$ of 3.5. Such adjustment of $p[H^+]$ produced the working aqueous solutions for distribution study, where 0, 0.001, 0.005, 0.01, 0.05, 0.1, 0.5 and 1.0 M free lactate at equilibrium was present. All solutions contained 0.05 M DTPA and were pre-equilibrated prior to conducting the experiment. The liquid-liquid distribution equilibrium was established after 7 days of vortexing at 25.0 ± 0.1 °C. Following contacts, the solutions were centrifuged for 10 minutes to facilitate phase separation. The aqueous phase was separated, 100 μL was sampled for the ICPMS analysis, and the rest was used to check the $p[H^+]$ after equilibration. The glass electrode was calibrated prior to separations for each series of samples. Four lactate dependency studies were performed using different concentrations

of HDEHP in *n*-dodecane. The acidity of the aqueous solutions remained constant at $p[H^+] 3.50 \pm 0.05$ after the extraction.

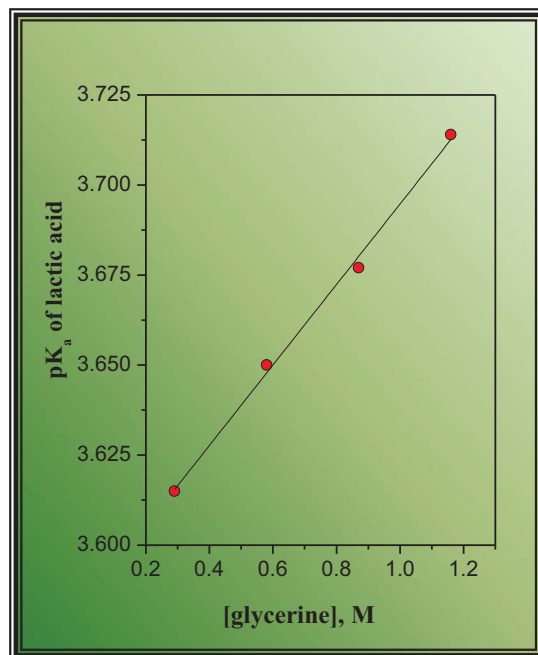


Figure 4. Effect of increasing concentration of glycerine on the dissociation constant of lactic acid.

Figure 5 summarizes the effect of increasing concentration of free lactate on the liquid-liquid distribution of Ce^{3+} for the studied concentrations of HDEHP. The observed trends, as expected, combine the features of the distribution studies reported by Danesi and Nilsson.^{5,6} The distribution ratios are independent of lactate up to 0.1 M concentration. This behavior is guided by strong complexation chemistry of DTPA, which does not allow lactate to participate in the coordination of trivalent lanthanides. As the concentration of free lactate enters those complex buffer regions, corresponding with the operational conditions of TALSPEAK, the distribution ratios fall drastically despite the pH of the aqueous solutions being constant. Interestingly, the decrease of the distribution ratios appears to be related to the changing complexity of the organic phase. The observed drop in the D values becomes more pronounced as the concentration of HDEHP changes from 0.10 to 0.15 M. The decreasing trend does not continue, however, for the largest investigated ligand concentration. Such “one-time” shift in the decreasing trend might be indicative of a specific transformation of either physico-chemical characteristics of the liquid phases or the mechanism of metal extraction as the concentration of HDEHP transitions from 0.10 M to 0.15 M. Such behavior may invoke an argument for the existence of a critical ligand concentration that, when attained, forces significant changes in the liquid-liquid distribution of the metal in such TALSPEAK-related systems.

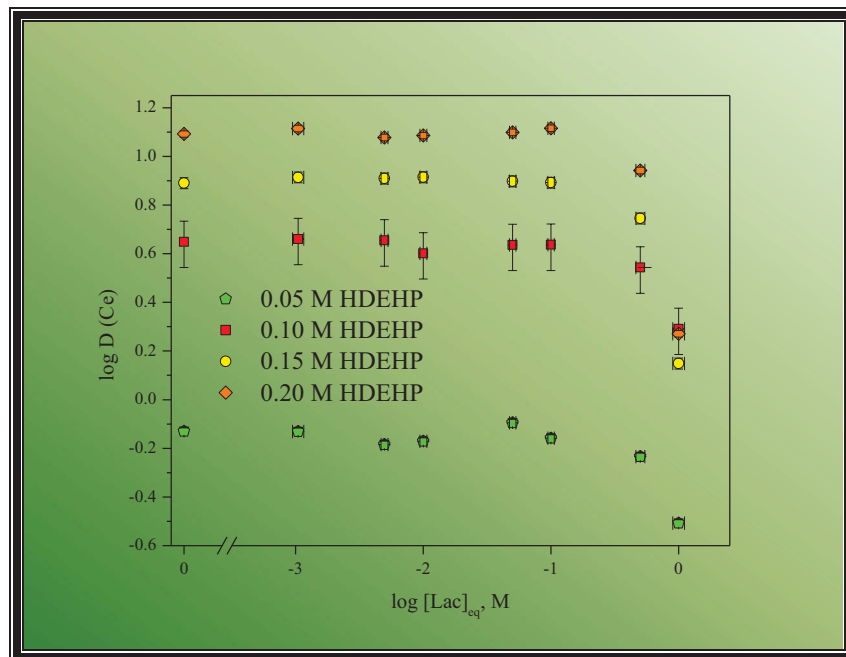


Figure 5. Lactate dependency for the liquid-liquid distribution of Ce^{3+} . Organic phase: HDEHP in *n*-dodecane. Aqueous phase: $[\text{Ln}^{3+}]_{\text{total}} = 1 \text{ mM}$, $\text{p}[\text{H}^+] = 3.5$, $[\text{DTPA}] = 0.05 \text{ M}$, varying $[\text{Lac}]_{\text{eq}}$, $I = 1 - 2\text{M}$.

The observed distribution ratio trends for the lactate / extractant dependency study were consistent for all investigated lanthanides. Figure 6 shows the results for the extraction of gadolinium and holmium for comparison. The observed *D* values follow the general extraction behavior based on the TALSPEAK curve, but the effect of lactate is similar to that presented for the extraction of cerium. The lack of differences in the distribution trend for the lactate dependency suggests that the decreasing extraction efficiency observed at high lactate concentration cannot be attributed to the formation of the metal:DTPA:lactate mixed complex in the aqueous phase. Such complexes are quite sensitive to the size and charge density of the metal ion, which is usually manifested in differences in the thermodynamic stability of such complexes across the lanthanide series.⁸ No such sensitivity has been observed in the trends of distribution ratios.

Shifting the focus onto another dimension of the distribution data, the information collected for each lactate concentration may be evaluated as a function of HDEHP concentration. Figure 7 shows the extractant dependencies at 0, 0.5 and 1.0 M positions along the lactate concentration range. The extractant dependency with no lactate in solution overlaps with those gathered up to 0.1 M free lactate in solution. The original slope of 2 for this HDEHP dependency starts to decrease when 0.5 M free lactate is present and is suppressed to 1 for the last condition along the lactate dependency.

The discussion of the observed trends in the presented three dimensional dependency study may be divided into two sections based on the possible origins of the distribution ratio behavior. The drastic decrease in the distribution ratios, when high lactate concentrations were present in solution, could be explained by changes in the physico-chemical characteristics of the fluid phases in the investigated system. Here, the large concentrations of the hydrophobic lactic acid could affect several solution equilibria, such as organic/aqueous partitioning or ionic hydration, which, in turn, directly influence the liquid-liquid distribution. The observed decreasing trend in the *D* values for the lactate dependency may also be analyzed from the mechanistic perspective, where changes in the stoichiometry of the metal phase transfer could be considered. To begin, the arguments are presented for the direct influence of solution properties on the distribution of lanthanides within the investigated TALSPEAK-related system.

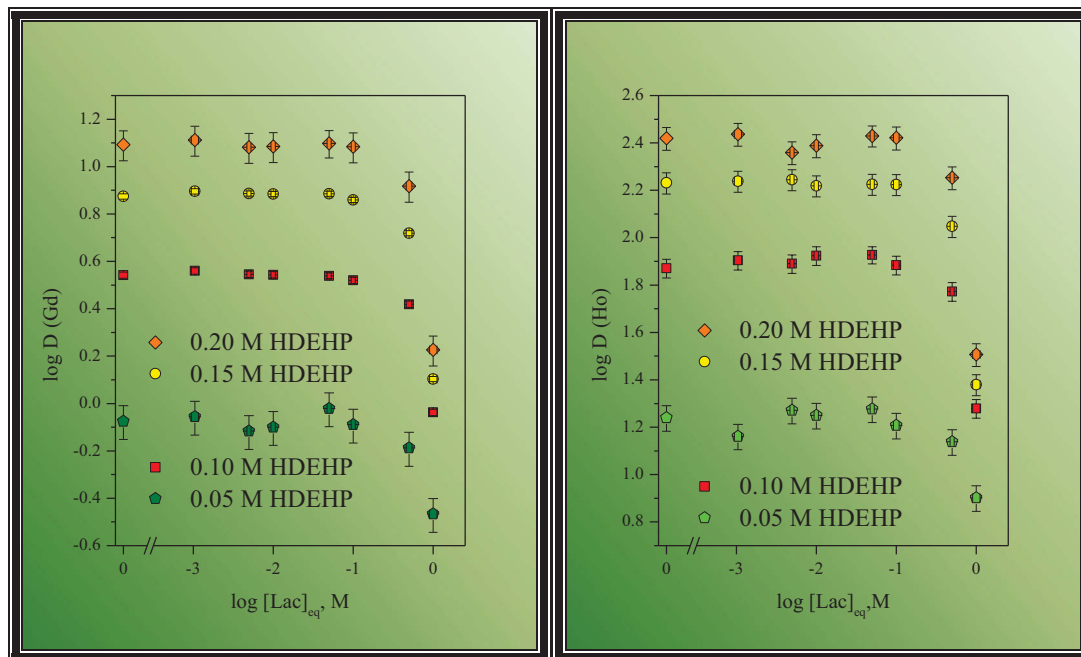


Figure 6. Comparison of the liquid-liquid distribution studies for Gd^{3+} and Ho^{3+} extraction. Organic phase: HDEHP in *n*-dodecane. Aqueous phase: $[\text{Ln}^{3+}]_{\text{total}} = 1 \text{ mM}$, $\text{p}[\text{H}^+] = 3.5$, $[\text{DTPA}] = 0.05 \text{ M}$, varying $[\text{Lac}]_{\text{eq}}$, $I = 1 - 2 \text{ M}$.

As argued previously, the presence of high concentrations of carboxylates may influence the activity of water in aqueous electrolyte mixture. The presence of organic molecules in solution may disrupt the structure of water and, in consequence, affect ionic hydration. Our glycerine study demonstrated a very limited influence of the increasing hydrophobic nature of aqueous environment on the dissociation equilibrium of lactic acid. The pK_a of lactic acid increases with the concentration of glycerine in solution. This indicates a weakening of acid dissociation equilibrium, most likely due to increasing difficulty of hydrating the free proton and lactate ion. The medium effect was small; however, the strongly hydrated trivalent lanthanides may be affected to a greater extent. An original TALSPEAK report assesses whether the liquid-liquid distribution of a trivalent metal ion could be affected as the concentration of lactic acid increases in solution.³ Weaver and Kappelman studied the extraction of trivalent americium in TALSPEAK-type systems, where the pH of the aqueous phase was as low as 0.2. At this acidity, lactic acid dominates the acid/conjugate base equilibrium. Since the distribution ratios for the extraction of Am from aqueous solutions containing 0.5 M and 1.0 M lactic acid overlap, it is reasonable to rule out this medium effect as a complicating factor in the interpretation of our results. A large presence of lactic acid may also alter the organic/aqueous partitioning of the phase transfer reagent, HDEHP. The enhanced hydrophobicity of the lactic acid-containing aqueous environment may enhance the solubility of HDEHP in that medium. The partitioning equilibrium constant is quite high ($\log K_D \sim 3.4$) for HDEHP in aliphatic diluents.⁹ Due to its strong tendency to aggregate in non-aqueous environment, the availability of the monomeric HDEHP for partitioning into the aqueous phase is minimal. However, it is feasible that large concentrations of lactic acid could promote the partitioning. To thoroughly test this hypothesis the aqueous solutions from the partitioning studies will also be analyzed for phosphorus using ICPMS. If phosphorus concentration (if detectable) will mimic the trend observed for the lanthanide distribution, the partitioning of HDEHP into the highly buffered solutions will have to be considered in detail.

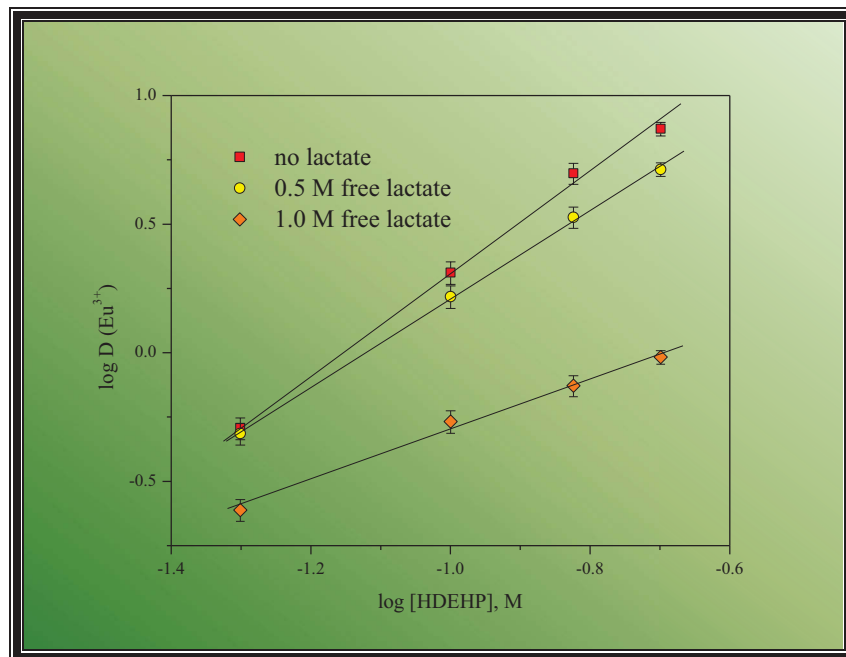
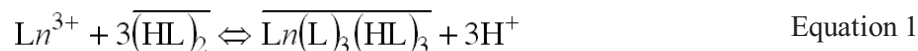


Figure 7. Extractant dependencies for the extraction of Eu^{3+} from TALSPEAK mixtures containing 0, 0.5 and 1.0 M free lactate at equilibrium.

A well-characterized, traditionally recognized mechanism of HDEHP-facilitated phase transfer of trivalent metal ion employs its extraction by 3 HDEHP dimers and a release of 3 hydrogen ions into the aqueous phase to balance the charge.¹⁰ The liquid-liquid distribution reaction involves the breaking of the extractant dimer and a replacement of the hydration sphere of the metal by a number of coordinating donor groups of HDEHP. This reaction occurs at the aqueous/organic interface, where the metal interacts with the phosphonate groups of HDEHP, and it crosses the phase boundary and enters the organic environment according to:



where HL is HDEHP and the horizontal bar represents species in the non-aqueous phase. Such stoichiometry of phase transfer, at idealized experimental conditions of slope analysis study, returns a slope of 3 when the liquid-liquid distribution of a trivalent metal is studied as a function of extractant concentration. As shown in figure 8, however, the distribution ratios collected at different concentrations of HDEHP are initially characterized by a 2nd power dependency. The slope of 2 is consistent for low lactate concentrations in solution, until its concentration reaches 0.1 M at equilibrium. Such extractant dependencies have been reported in the past by Kosyakov, who studied the stoichiometry of phase transfer in TALSPEAK-type solutions where the concentration of free lactate was constant at 0.22 M.¹¹ He observed a power of 2 relationships for both acid and extractant dependencies, studying the distribution of trivalent metals in systems with and without DTPA in solution.

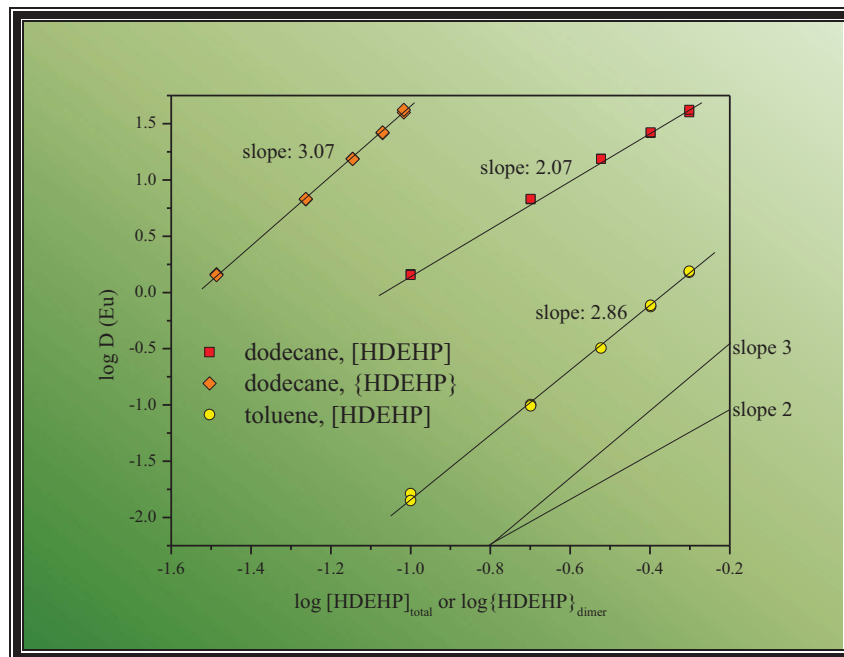
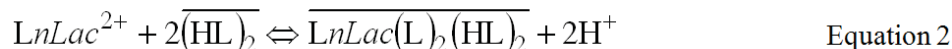


Figure 8. Extraction of Eu from mineral acid solutions by HDEHP in toluene and *n*-dodecane. The distribution ratios collected for the aliphatic system are also plotted as a function of the activity of the HDEHP dimer.

Based on the slope analyses, he proposed a different phase transfer mechanism where a monolactate metal complex is extracted as



where only 2 extractant dimers participate in metal coordination. The proposed mechanism of the partitioning of lactate into the organic phase matches very well with recent ¹⁴C-labeled lactate liquid-liquid distribution studies reported by Grimes.¹² Del Cul also observed the presence of lactate in the organic phase.¹³ The agreement between our data and the slopes reported by Kosyakov is striking; however, Figure 8 clearly shows that the extractant dependency for the extraction of europium from aqueous solutions without lactate is characterized by a slope of 2. Consequently, judging from our distribution studies with and without lactate, and Kosyakov studies with and without DTPA, the only remaining explanation of the observed slope suppression from the expected value of 3 must originate in the HDEHP-containing organic phase.

Several research groups observed similar slope suppression for the extractant dependency when HDEHP was dissolved in an aliphatic diluent.¹⁴⁻¹⁶ Danesi attributed this deviation from the expected slope to the non-ideal behavior of the HDEHP dimer in the aliphatic solvent, where weak dipole-dipole interactions between dimers take place.¹⁷ To account for this behavior, he developed an empirical correction, allowing to calculate the activity of the dimer in solution. To test this hypothesis we performed a series of extractions of europium from mineral acid solutions by different concentrations of HDEHP dissolved in aromatic and aliphatic diluent. Figure 8 summarizes the study. When HDEHP was diluted in toluene the slope for the extractant dependency was close to the expected value of 3. The slope of 2 describes the europium distribution relationship when HDEHP was dissolved in *n*-dodecane. When the distribution ratios were plotted as a function of the activity of the extractant dimer the slope returned to 3, still implying the metal extraction by a traditional mechanism. Following this line of reasoning, the same correction was applied to the TALSPEAK distribution data.

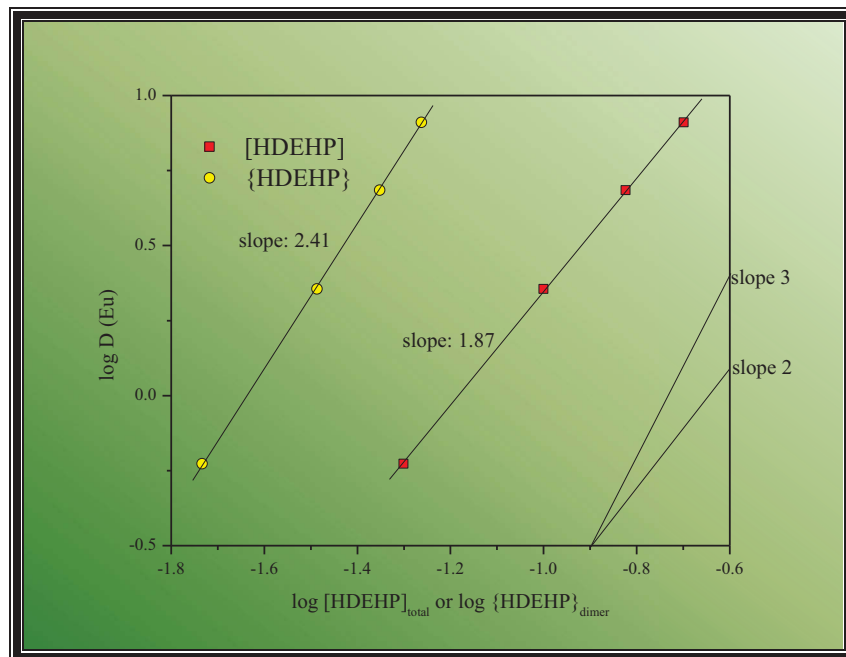


Figure 9. The comparison of the distribution ratios collected for the extraction of Eu from aqueous solution of 0.05 M DTPA, 0.05 M free lactate before and after correction for the non-ideal behavior of HDEHP dimer in *n*-dodecane.

Figure 9 clearly shows that the correction fails to return a meaningful result. A similar non-integer slope of 2.5 was calculated when Kosyakov's data was subjected to this treatment. This behavior of TALSPEAK distribution ratios excludes the argument of a non-ideal solution behavior of HDEHP dimer as a sole explanation of the observed slope suppression. At the investigated concentrations of HDEHP (0.1 – 0.2 M) smaller slope deviations are expected. A recent study by Zalupski reported the slope of 2.25 for the extraction dependency in this region of HDEHP concentrations.¹⁶ In this case the correction yielded expected results. Upon careful examination of the trend for the distribution ratios for the extraction of Eu by HDEHP in *n*-dodecane (figure 8) it is apparent that the D values are lowered to a greater extent for the highest ligand concentration. Figure 10 shows this deviation, together with some of the distribution ratios gathered by Zalupski. Despite this growing deviation, once plotted on the dimer activity scale, both studies converge very well reinforcing the validity of the correction. Our TALSPEAK data, collected using HDEHP concentrations where no curvature is expected based on Figure 10 arguments, do not allow the assignment a phase transfer mechanism described by equation 1 as the only liquid-liquid distribution reaction. Further investigation is necessary to explain the observed slope suppression.

Finally, shifting our attention to the distribution data collected for the solutions containing high concentrations of lactate (last 2 points for lactate dependency), the slope of the HDEHP dependency is further suppressed. It is tempting to explain this drastic slope decrease as the change in the mechanism of phase transfer to a micellar type of extraction. Those liquid-liquid distribution systems are usually characterized by the extractant dependency slope of 1, corresponding to the metal coordination by one micelle.¹⁸ However, inspecting the distribution ratio data presented in figure 7, it is clear that the increasing complexity of the organic phase, i.e. the HDEHP concentration, affects the correlation observed at 1.0 M free lactate. The D values appear to be suppressed to a greater extent at higher HDEHP content, deviating from the linear relationship.

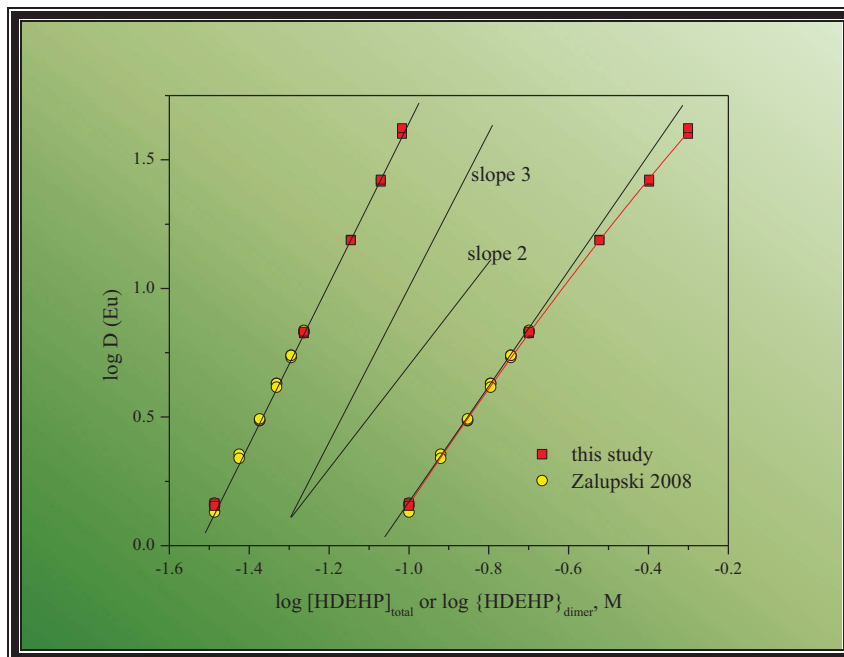


Figure 10. Increasing non-ideal behavior of HDEHP dimer.

This behavior is very similar to that observed for the extraction of Eu from mineral acid solutions at much higher ligand concentrations (0.3 – 0.5 M). It is evident that, while the application of the non-ideality correction could perhaps remove this curvature, the resulting slope of the extraction dependency will still return a number quite distant from an ideal behavior. Consequently, several mechanistic options remain when explaining the observed sharp decrease in the D values at the end of the lactate dependency trends:

Other aggregative and possibly micellar behavior of HDEHP in complex TALSPEAK systems

Extraction of LnLac^{2+}

Disruption of HDEHP dimer and formation of HDEHP \cdots HLac dimer

As efforts are continued to find a definite explanation for this behavior, one final important conclusion may be formulated. Figure 11 illustrates the characteristic trends in the distribution of lanthanide ions in TALSPEAK systems collected when no lactate and 2.8 M total lactate were present in the aqueous phase. It is essential to realize that the distribution trends remain the same across the lanthanide series at the start and an end of the investigated lactate concentration range. This lack of change in the ΔG trends across the lanthanide series suggests that, despite a significant change in the complexity of the aqueous phase, the phase transfer reaction is governed by similar electrostatic interactions. Consequently, the mechanism of lanthanide extraction is likely to proceed through the liquid-liquid cation exchange process and not the micellar type of phase transfer.

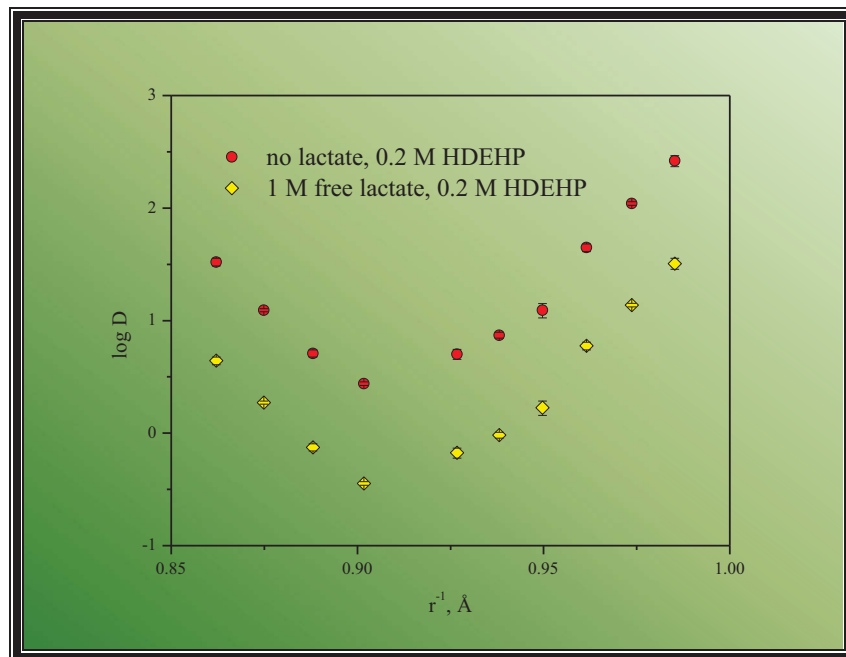


Figure 11. The comparison of the extraction of lanthanide mixture (La^{3+} - Ho^{3+}) by 0.2 M HDEHP in *n*-dodecane from pH 3.5 aqueous solutions containing 0.05 M DTPA, and either no lactate or 2.8 M total lactate.

3.1.2 Two-phase Calorimetric Investigation of HDEHP-facilitated Liquid-liquid Distribution of Trivalent Americium.

The thermochemistry of metal ion partitioning in a solvent extraction process can be considered as a balancing act between the endothermic heat associated with metal ion dehydration in the aqueous phase and the exothermic formation of lipophilic complexes in the organic phase. Marcus has noted that these processes dominate the enthalpy level diagrams for every liquid-liquid distribution process.¹⁹ Although the entropy can exert a significant influence on the net free energy of extraction, the final outcome of this enthalpic “tug of war” is often the driving force of a separation process. In any case, the change of the enthalpy of extraction, ΔH , for the liquid-liquid metal distribution reaction provides a quantitative description of the net change in bond strength associated with the phase transfer reaction. Furthermore, the enthalpy contribution to the free energy of phase transfer reactions is generally easier to manipulate to arrive at a desirable separation process. The change of the enthalpy of extraction is usually shaped by factors that affect the opposing forces of dehydration and complex formation including the structural features of the ligand, aqueous electrolyte or an organic diluent present in the system. Similar forces are balanced to drive complex formation in monophasic systems. Investigation of the thermochemistry of solvent extraction allows identification of the driving force of a separation process, building a solid foundation for improvements and the development of more challenging separation schemes.

To continue our thermodynamic investigations of liquid-liquid distribution reactions a recently developed two-phase calorimetric methodology was used to study the thermochemical features of HDEHP-facilitated phase transfer of americium metal ion across a liquid-liquid boundary. This is the first account of a direct calorimetric measurement of the heat of liquid-liquid partitioning of any transuranic element reported to date. This methodology applies modern isothermal titration microcalorimetry, allowing accurate measurements of microjoule heat events inside a 1 mL reaction vessel. To follow the transfer of Am(III) from an aqueous solution into the organic diluent a simple, well-characterized liquid-

liquid partitioning system was chosen. A cation-exchanging organophosphate phase transfer reagent – bis(2-ethylhexyl)phosphoric acid (HDEHP)– is a hard electron donor dissolved in *n*-dodecane. When aqueous mildly acidic (pH ~ 3) solutions containing metal ions of the oxidation states II, III, and IV are contacted with the organic mixtures of HDEHP the hydration sphere of the metal is replaced by a number of coordinating donor groups of HDEHP. This reaction occurs at the aqueous/organic interface, where the metal is coordinated by three HDEHP dimers, and it crosses the phase boundary and enters the organic environment according to equation 1.

The net heat balance of such transfer across the liquid-liquid boundary corresponds to the product of all change of enthalpy terms from the chemical processes involved in the partitioning, such as dehydration, electrostatic bonding and solvation. The overall change in the internal energy of the system resulting from a phase transfer may be detected calorimetrically. The change in the enthalpy of transfer across the liquid-liquid boundary – ΔH_{tr} – describes the process quantitatively according to $\Delta H_{tr} = q/\Delta m$, where q is the calorimetrically detected heat associated with the reaction and Δm is the molar amount of solute that crosses the liquid-liquid interface.

The design of the isothermal titration microcalorimeter (CSC 4200, TA Instruments) allowed the flexibility to adapt the conditions of the experiment to perform a 2-phase calorimetric study. The instrument transfers energy to or from the surroundings to compensate for any thermochemical process in the reaction vessel, thus maintaining its constant temperature. Semiconducting thermopile heat sensors, located between the reaction cup and the aluminum heat sink, monitor the heat flow based on the principle of the thermoelectric effect. Direct calorimetric measurement of ΔH_{tr} was afforded by careful design of experimental conditions to facilitate liquid-liquid partitioning process. The calorimetric vessel contained both aqueous (120 μ L) and non-aqueous (800 μ L) solutions. Aqueous phase consisted of 1 M sodium nitrate adjusted to a pH of 3.2. The organic phase was a 0.2 M solution of HDEHP in *n*-dodecane. Sequential 5 μ L additions of a titrant solution introduced americium (in 1 M NaNO₃) ion into the calorimetric reaction vessel.

When trivalent americium ions enter the cup they begin interacting with electron-donating polar groups of HDEHP, which are assembled at the interface and penetrate into the aqueous environment. As a result several phosphonate groups perturb the hydration layers of Am(III), replace the waters of hydration and transfer the coordinated ion into the organic solution. Such complex formation envelops the fully dehydrated metal ion inside the polar core, while extending the lipophilic hydrocarbon chains to allow for the solvation of the complex in non-aqueous environment. Figure 12 shows a power compensation trace for the HDEHP-mediated liquid-liquid distribution of Am(III) from mildly acidic aqueous sodium nitrate solution into the immiscible hydrocarbon phase. The experimental trace for the blank titration (titrant addition into a liquid-liquid system less HDEHP) is also included for comparison. Each peak corresponds to the increasing heat transfer rate (μ W/sec) as the calorimeter responds to the exothermic transfer of americium ions across the liquid-liquid interface. Previous 2-phase calorimetric investigations of liquid-liquid distribution of lanthanide ions in this system demonstrated that the observed power traces are solely responsible for the transfer of the metal ion across the phase boundary.¹⁶ The measured energy associated with the transfer is directly related to the concentration of the metal ion in titrant solution.

The integrated area under each peak of the power trace yields a net change of the internal energy of the system, q . The Am(III) titration experiments were investigated in duplicate and yielded an average integrated value of $-402 \pm 30 \mu$ J ($\pm 1\sigma$) as the observed heat of phase partitioning. This net energy is mainly a product of endothermic heat of metal ion dehydration and exothermic heat of complex formation in the organic phase. As the conditions of this phase transfer experiment ensure quantitative partitioning of Am(III) into the organic phase, the change in the enthalpy of transfer may be calculated.¹⁶ A ΔH_{tr} of -8.0 ± 1.2 kJ/mol ($\pm 2\sigma$) for the investigated liquid-liquid distribution equilibrium suggests favorable bonding interactions between Am(III) and HDEHP.

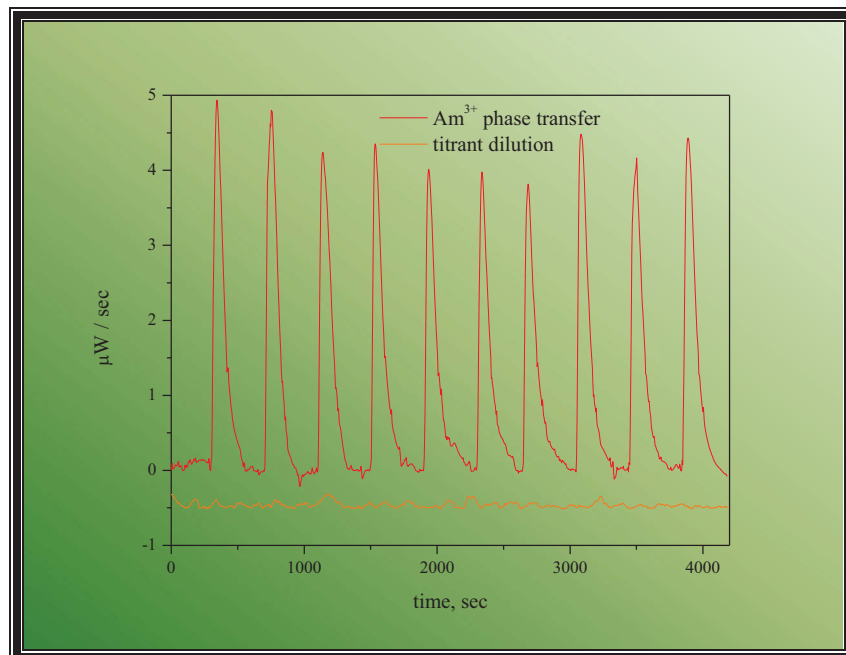


Figure 12. Calorimetric power compensation trace collected for the liquid-liquid distribution of americium ion. Aqueous phase: pH 3.2, 1.0 M NaNO₃. Organic phase: 0.2 M HDEHP in *n*-dodecane.

Figure 13 shows the thermodynamic parameters for the studied Am(III) partitioning, together with the previously determined values for lanthanide ions.¹⁶ The reported Gibbs free energy of Am(III) transfer represents an average value calculated from the extraction constants, $\log K_{\text{ex}}$, reported elsewhere for the extraction of Am³⁺ by HDEHP in aliphatic diluents.^{20,21} The entropy term was calculated from the experimentally obtained ΔH_{tr} value and the averaged ΔG_{tr} value as $\Delta S_{\text{tr}} = (\Delta H_{\text{tr}} - \Delta G_{\text{tr}})/T$.

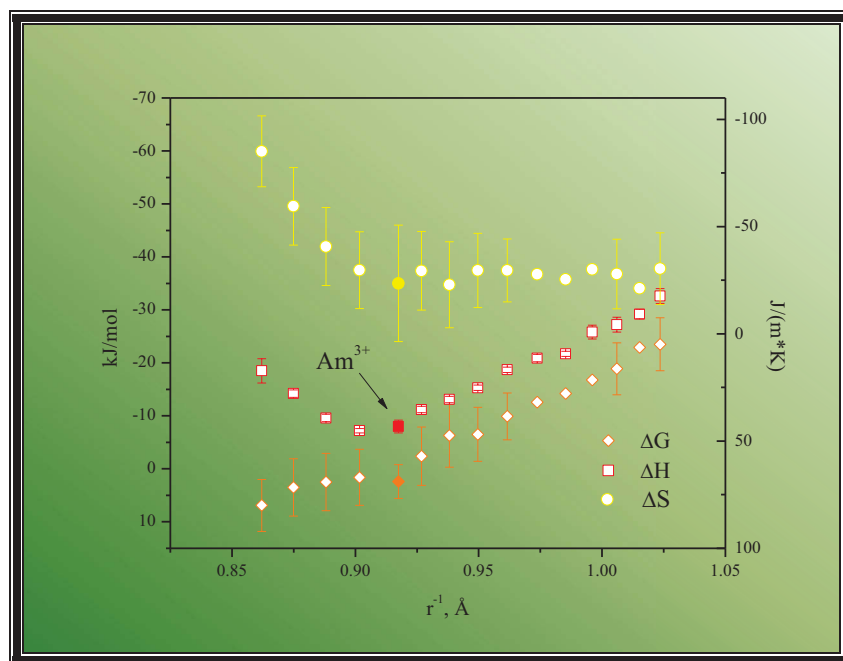


Figure 13. The comparison of the thermodynamic parameters for the HDEHP-facilitated liquid-liquid partitioning of Am(III) with those reported for the lanthanide series.

The reported thermodynamic parameters clearly illustrate the similarities of the solution chemistry of lanthanides and actinides. Trivalent *f*-elements are hard Lewis acids.²² As such, the complexation chemistry of actinides and lanthanides by hard oxygen-donating reagents is governed by electrostatic interactions.²³ The strength of an ionic bond is directly related to the charge density of the metal ion and, due to the *f*-element contraction, the complexation of Am(III) usually mimics that of Pm(III).²⁴ The thermodynamic parameters for the liquid-liquid distribution of trivalent americium illustrate this electrostatic dominance as HDEHP is a hard donor phase transfer reagent. The collected parameters for Am(III) correctly fit into the ΔG_{tr} , ΔH_{tr} and ΔS_{tr} trends at the expected position of Pm(III). The negative entropy term opposes the partitioning of the metal ion into the organic phase due to the ordering effect of complex formation as well as the hydration of three protons, which are exchanged back to the aqueous solution. A favorable exothermic heat of Am(III) / HDEHP compound formation opposes the unfavorable entropy term. The overall free energy of liquid-liquid distribution (ΔG_{tr}) of Am(III) is slightly endothermic, matching the light lanthanides characterized by lower charge density relative to the heavier and harder members of this series.

The reported thermochemical tracking of HDEHP-mediated transfer of trivalent americium ion across the liquid-liquid boundary illustrates the value of 2-phase calorimetric methodology. Similar thermodynamic inquiry is feasible for diverse chemical systems, where mass transport across the liquid-liquid interface occurs. Studying the thermochemical principles of such transformations reveal important properties of solvation, molecular interactions and progressive structural self-assembly in solution and may identify new thermodynamically-inexpensive channels for mass transfer. This methodology will remain an important characterization tool during the upcoming experimental efforts in FY11.

3.2 Kinetics

Mechanistically, the extraction behavior of metal ions in the TALSPEAK process is very ill defined; there is suggestion that metal:DTPA complex dissociation in the aqueous phase is the rate determining step.²⁵ It has also been demonstrated that the rate of phase transfer of lanthanide ions into HDEHP decreases across the series.^{3,26} For added complexity, decreasing the concentration of lactic acid in the TALSPEAK aqueous phase is also seen to significantly slow the metal ion phase transfer kinetics. In addition evidence has been provided that lactate is seen to partition into HDEHP only when metal ions are present.¹² Studies by Danesi²⁷ and Kolaric²⁵ both elude to the mechanism of phase transfer being assisted by the existence of ternary complexes of metal:DTPA:lactate in the aqueous phase. However, recent work by Jensen *et al.*²⁸ and work performed in this program in FY 2010 (see section 3.3) would seem to dispel the hypothesis that these species exist in the TALSPEAK media and hence, another mechanistic interpretation of the phase transfer process has to be formulated.

3.2.1 Solvent Extraction Phase Transfer Kinetics

Prior work has highlighted that up to 10 mins vigorous mixing is required to reach equilibrium for heavy lanthanides in TALSPEAK systems.²⁹ With this in mind, the initial experimental conditions for studying the kinetics of phase transfer of tracer Ce, macro Eu and tracer Am were as follows:

Aqueous phase

- 1 M total lactate pH adjusted to 3.8
- Varying DTPA concentration 10, 20, 40 50 mM
- 10 mM Eu, tracer Ce and ²⁴¹Am

Organic phase

- 0.17M HDEHP in n-dodecane

Mixing

- All organic phases were pre-equilibrated with appropriate aqueous phases
- Vortex mixing contact times of 1, 5 and 10 mins

Distribution ratios of europium, cerium and americium as a function of mixing time are presented in Figures 14 and 15. The data presented in Figure 14 show that at all DTPA concentrations, when using a vortex mixer for agitation, the extraction of europium reaches equilibrium between 5 and 10 mins mixing time. As the concentration of DTPA is increased, the distribution of europium significantly decreases, up to 40 mM DTPA in the aqueous phase. Interestingly, the data illustrates that under the conditions studied there is very little difference in using 40 mM DTPA and 50 mM DTPA. The decrease in distribution coefficient with increasing DTPA in the aqueous phase is not unexpected and is a result of the increased metal:DTPA complexation in the aqueous phase. When plotting $\log D$ vs $\log [DTPA]$ (at equilibrium), a slope of approximately 1 is obtained as previously observed by Tachimori.³⁰ The slope of 1 is indicative of one DTPA molecule complexing the europium ions in the aqueous phase.

Figure 15 shows that the extraction behavior of cerium and americium has some similarities to the extraction behavior of europium. That is to say the distribution coefficients decrease with increasing $[DTPA]$ in the aqueous phase and equilibrium is reached at somewhere between in the 5-10 min timeframe with vortex mixing. In addition, there is little difference in the distribution coefficient, of either cerium or americium when increasing the DTPA concentration from 40 mM to 50 mM in the aqueous phase. As with Eu, a plot of the equilibrium $\log D$ value vs $\log [DTPA]$ for both cerium and americium results in a slope of 1 indicating that the aqueous phase metal ion complex is 1:1. However, kinetically Figure 15 appears to show that there is a difference in the extraction behavior of both cerium and americium. For all concentrations of DTPA, one minute on the vortex mixer gives a higher distribution value than when the system has reached equilibrium.

For all of the metal ions studied, (Eu, Ce and Am) there is not enough data using the vortex mixer to develop rate constants for the extraction of these metal ions. To obtain reliable rate constants, further experimentation was performed on these systems by changing the method of mixing. By switching to a rotary bar, the mixing between the two phases becomes less vigorous and as such should significantly slow down the extraction kinetics.²⁵ All other experimental conditions were replicated from the initial vortex mixing tests apart from the mixing times now were extended to 15, 30, 60, 120 and 180 mins.

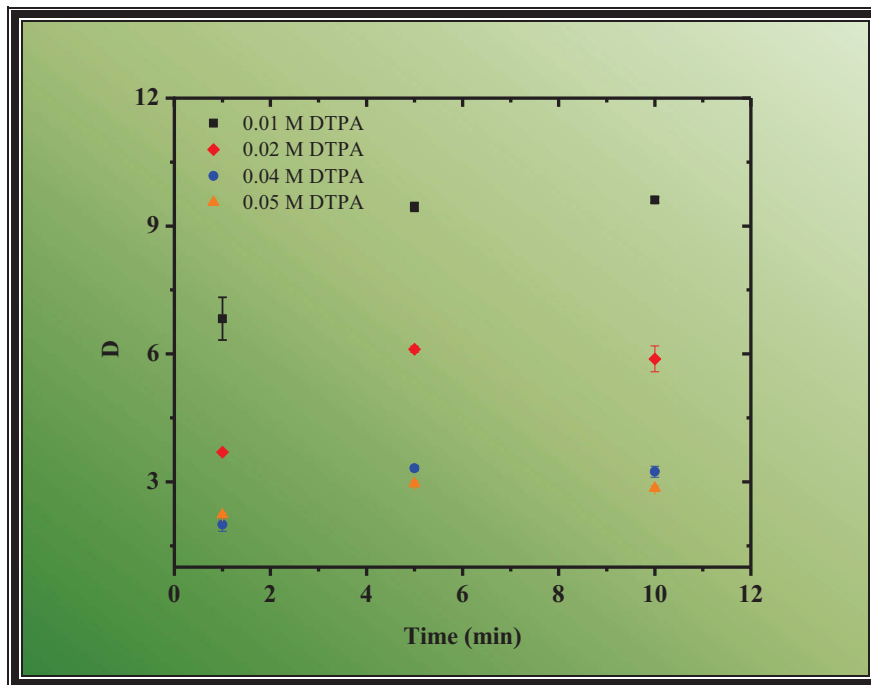


Figure 14. Influence of $[DTPA]_{(aq)}$ on rate of extraction of Eu by 0.17 M HDEHP in dodecane using a vortex mixer to agitate the two phases. Aqueous phase composition 1 M lactic acid at pH 3.8, $[DTPA]$ 10-50mM.

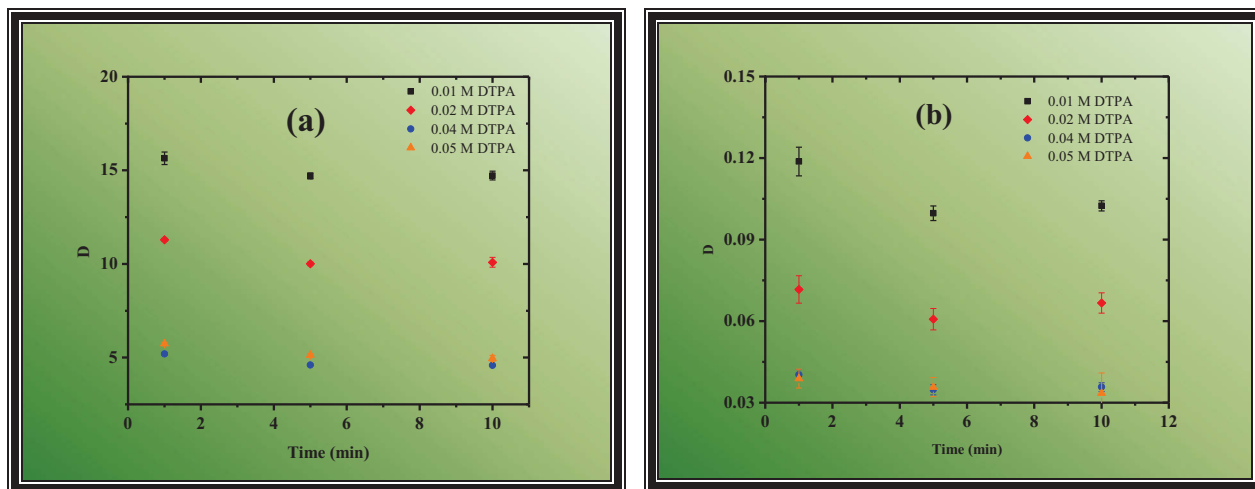


Figure 15. Influence of $[DTPA]_{(aq)}$ on rate of extraction of (a) cerium and (b) americium by 0.17 M HDEHP in dodecane using a vortex mixer to agitate the two phases. Aqueous phase composition 1 M lactic acid at pH 3.8, $[DTPA]$ 10-50 mM.

From the rotating bar experiments it can be seen that the extraction of Eu reaches equilibrium between 120 and 180 mins, (Figure 16). We see essentially a linear increase in the concentrations of the europium extracted into the organic phase over the first 120 mins for each DTPA concentration. It is also important to note that the equilibrium distribution values are almost identical to those obtained from the experiments where vortex mixing was used. As there is no significant change in the distribution coefficient when equilibrium is reached, it is reasonable to assume that the extraction mechanism is independent of the degree of agitation i.e. we do not see a kinetic product over thermodynamic product extracted. The reversible 1st order rate constant for the transfer of Eu from the aqueous phase to the organic phase at each DTPA concentration is derived from the slope of the plot of:

$$\log \left(\frac{D_f}{(1 + D_f) \left[\frac{D_f}{1 + D_f} - \frac{D_t}{1 + D_t} \right]} \right) \text{ vs. time} \quad \text{¶}$$

where D_f is distribution coefficient at equilibrium and D_t is the distribution coefficient at time t .²⁵ The rate of extraction of Eu for each DTPA concentration is given in Table III.

Table III. Reversible rate constants for the extraction of 10 mM Eu from 1.0 M lactic acid at pH 3.8, [DTPA] 10-50 mM, into 0.17 M HDEHP.

[DTPA]/ M	k (min ⁻¹)
0.01	0.070
0.02	0.049
0.04	0.047
0.05	0.026

It can be seen from these rate constants that the rate of extraction of Eu is inversely proportional to the DTPA concentration, clearly identifying that DTPA is involved in the mechanism of extraction of Eu into the HDEHP organic phase. When plotting $\log k$ vs $\log [\text{DTPA}]$ the slope of the line obtained is -0.5. This slope is somewhat different from that obtained by Kolarik (-0.3) when conducting similar experiments.²⁵ However, there are several differences in the experimental conditions of the present work that could play some part in obtaining a slightly different slope than that reported in the prior work. Here we not only have a significantly higher metal concentration but the HDEHP concentration is also lower than the work carried out by Kolarik.²⁵

When examining the results of the cerium extraction using the rotating bar, Figure 17a, it can be seen that there is a significantly different extraction profile with time than the more “classical” one observed with Eu. Indeed, the americium (Figure 17b) is seen to behave in a similar manner albeit with significantly lower distribution ratios. The trend is simpler for the aqueous phase that contains 10 mM DTPA with the distribution coefficient for both Ce and Am seen to decrease as the extraction time is increased until equilibrium appears to be reached by 180 mins. This situation is unusual as there appears to be a “fast” extraction of Ce, i.e. we initially observe a kinetic based extraction – something not usually associated with TALSPEAK. Previous work on TALSPEAK extraction kinetics highlights that the process is generally slow to reach equilibrium with decreasing rates across the lanthanide series.²⁶

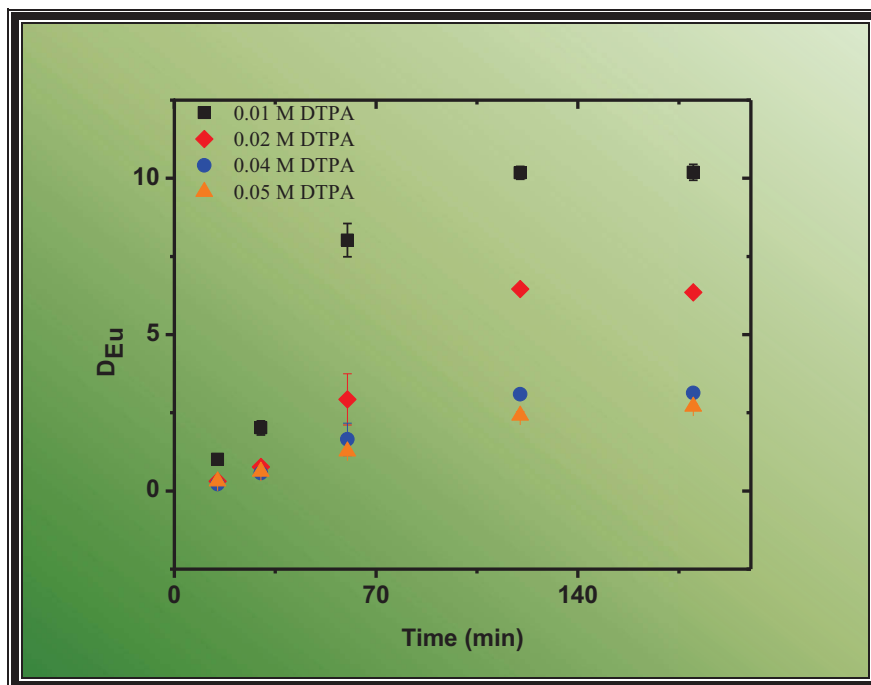


Figure 16. Influence of $[DTPA]_{(aq)}$ on rate of extraction of Eu by 0.17 M HDEHP in dodecane using a rotary mixer to agitate the two phases. Aqueous phase composition 1.0 M lactic acid at pH 3.8, $[DTPA]$ 10-50 mM.

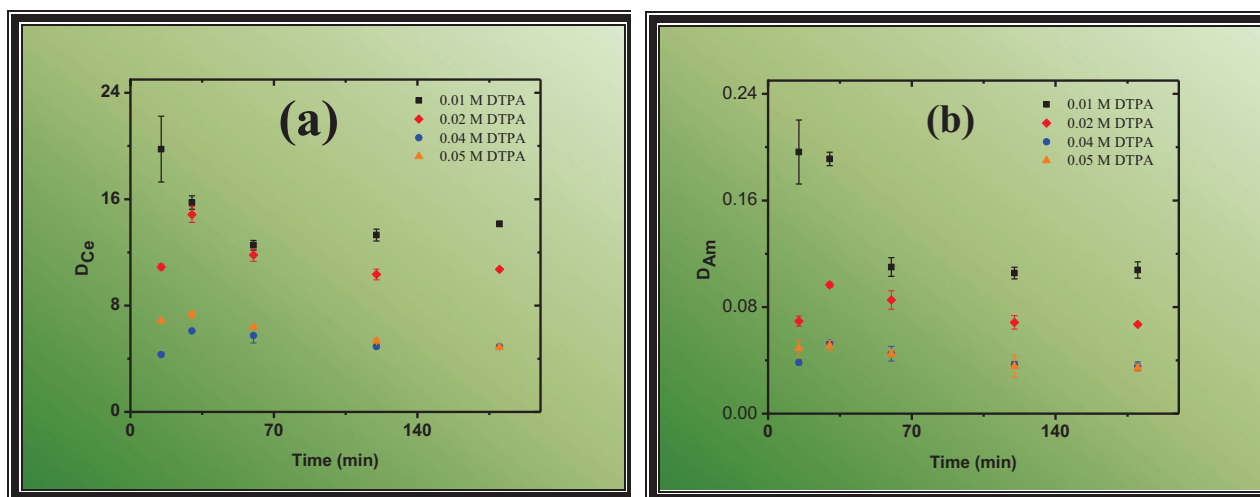


Figure 17. Influence of $[DTPA]_{(aq)}$ on rate of extraction of (a) cerium and (b) americium by 0.17 M HDEHP in dodecane using a rotary mixer to agitate the two phases. Aqueous phase composition 1 M lactic acid at pH 3.8, $[DTPA]$ 10-50 mM.

When the concentration of DTPA is increased in the aqueous phase the extraction profile (with time) is seen to initially increase and then decreases back to equilibrium by 180 mins. This type of extraction profile with cerium and americium has not previously been reported with respect to the TALSPEAK process. Due to these results, the data cannot be treated in the same manner as the Eu to develop rates of extraction. Instead, we have endeavored to explain these unusual extraction profiles and their relation to the extraction mechanism.

The light lanthanides are known to have kinetically less stable complexes with DTPA; in fact if increasing amounts of acetate are introduced into such a system then the rate of decomplexation is seen to increase.³¹ This is important in the TALSPEAK system, as the rate determining step for phase transfer is thought to be the decomplexation of the lanthanide ions from DTPA in the aqueous phase. To explain the results obtained here we first have to consider the (simplified) mechanistically important reactions:



At the beginning of the experiment of the initial test (10 mM DTPA), the aqueous phase experimental conditions were 1 M lactic acid at pH 3.8, [DTPA] 10 mM, tracer cerium, 10 mM Eu and tracer americium. It becomes obvious that the majority of the DTPA is complexed to Eu and most likely americium (Equations 3 and 5 lie mostly to the left). This is due to both the complexation constants of Eu and Am being larger than that of the DTPA:Ce complex but also the sheer quantity of Eu present in solution. These conditions would seem to suggest that most of the cerium is “free” in lactate solution. As the solutions begin to be mixed, cerium does not have to be decomplexed from DTPA to be extracted and hence HDEHP can extract cerium rapidly as though from a mineral acid solution.¹⁶ After a very short period of mixing, the equilibrium described by Equation 4 lies completely to the right. However, as the extraction experiment proceeds Eu begins to be extracted into the organic phase and releases some of the DTPA in to the aqueous phase, creating free DTPA in solution. With free DTPA now present in the aqueous phase, this begins to change the equilibrium of Equation 4 and so, with increasing free DTPA in the aqueous phase, this reaction begins to re-address itself to the left. This process continues until Eu has reached equilibrium and hence, stopped releasing DTPA into the aqueous phase, and as such the Ce does not reach equilibrium until after the Eu.

3.2.2 Solvent Extraction and Phase Transfer Kinetics from other Buffers

In the original work on TALSPEAK separations,^{3,26} Weaver and Kappleman investigated a wide range of buffers to perform this separation before settling on 1 M lactic acid buffer (pH ~3.6-3.8) and 50 mM DTPA. As has already been identified, the pH control is critical for efficient separations. If the pH increases above the value for optimum working conditions (3.6 – 3.8) the distribution coefficients of the lanthanides significantly decrease. On the other hand, if the pH falls below significantly below 3.6 DTPA can precipitate out of solution.⁴

As added scope to the original work package, investigations began into developing a modified TALSPEAK type process for the group actinide lanthanide separation that can operate at low pH (1-2) which would be more “process friendly” and, if possible, reduce or remove the requirement for a separate holdback reagent (e.g. DTPA). The hypothesis behind this work is that amino acids could be used as the aqueous phase buffer and “soft donor”. The carboxylic acid groups of amino acids have significantly lower pKa’s than lactic acid meaning that the aqueous phase can be buffered at pH’s closer to the 1-2 range (0.1-0.01 M H⁺). Ideally the amino acids will also preferentially complex the trivalent actinides

over the lanthanides so that an extractant such as HDEHP (as in TALSPEAK) can be used to extract the lanthanides into an organic phase, without the need for a separate holdback reagent.

Similar to the original TALSPEAK process, the lanthanide/ actinide separation factors for this proposed process will likely be reliant on the aqueous phase composition. Building on limited observations with glycine nitrate,³ preliminary investigations have been performed using L-alanine the simplest analogue for lactic acid where the α -hydroxy is replaced with an NH_2 group, Figure 18. The results from these initial tests using 1.0 M L-alanine at lower pH's and in the presence of DTPA have shown promise for this approach, with encouraging Eu/Am D values and separation factors, Figure 19.

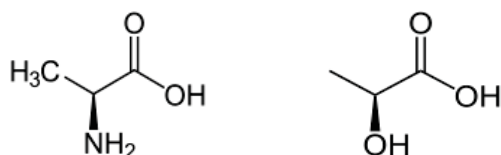


Figure 18. a) structure of L-alanine, b) Structure of L-lactic acid

The results obtained with the L-alanine system suggests that equilibrium in this system is reached at significantly shorter contact times than in a lactic acid system, Figure 20. As such, investigations continued into the extraction kinetics with different amino acids using (slow) rotary mixing and (fast) vortex mixing.

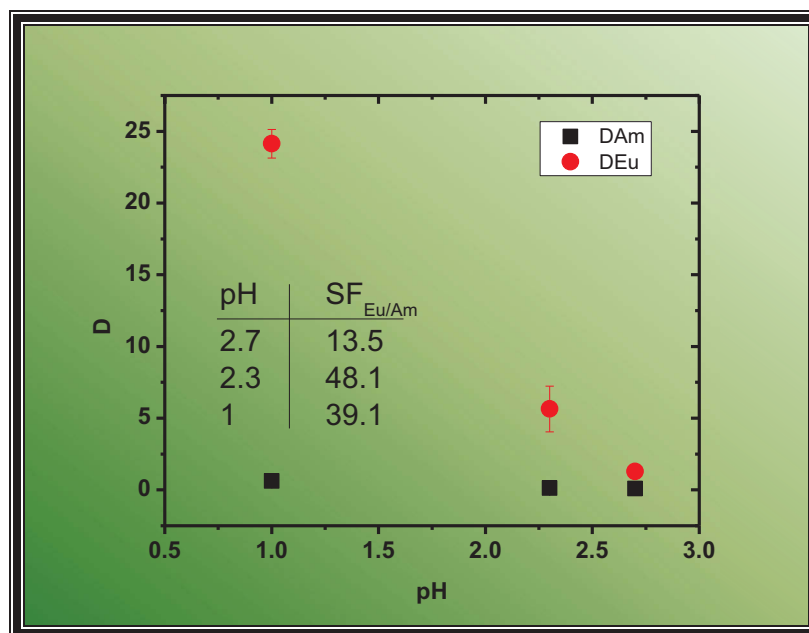


Figure 19. Distribution ratios of ¹⁵⁴Eu (●) and ²⁴¹Am (■) as a function of pH for an aqueous phase composition of 1.0 M L-alanine and 0.05 M DTPA, org. phase = 0.17 M HDEHP in dodecane.

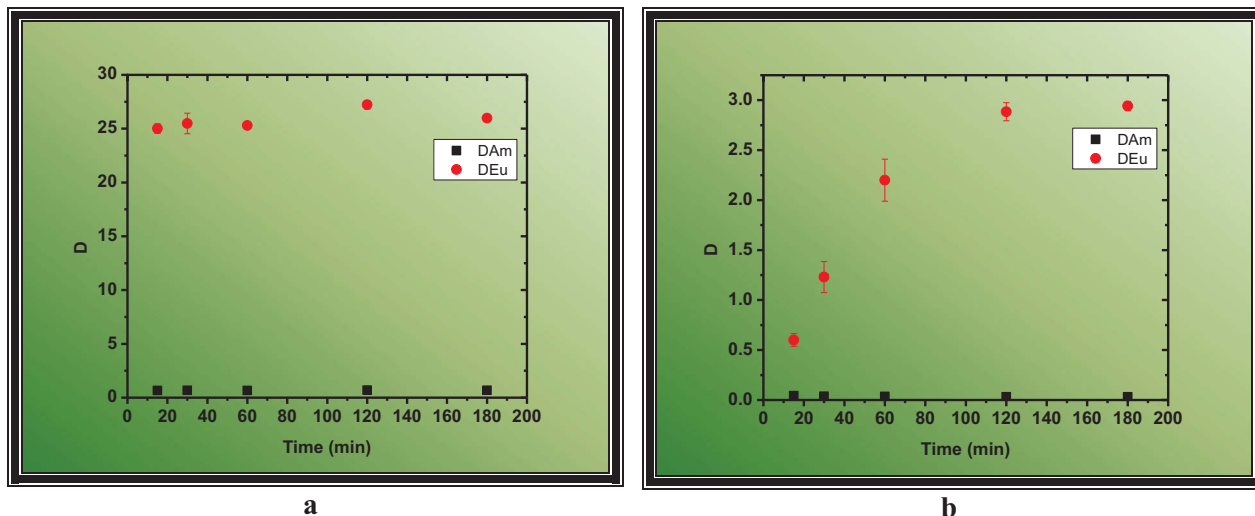


Figure 20. Distribution ratios of ^{154}Eu (●) and ^{241}Am (■) as a function of time for an aqueous phase composition of a) 1.0 M L-alanine and 0.05 M DTPA pH 1, org. phase = 0.17 M HDEHP in dodecane and b) 1.0 M L-alanine and 0.05 M DTPA pH 3.8, org. phase = 0.17 M HDEHP in dodecane. Experiments performed using a rotating bar.

Further to these tracer studies, solvent extraction experiments have also been performed with 10 mM Eu present in the aqueous phase. Although only preliminary results have been obtained from these studies, it appears that there are no significant differences in distribution coefficients with larger quantities of metal present. In addition, the fast phase transfer kinetics afforded by the alanine buffer results in equilibrium for each metal ion being reached in significantly shorter timescales than those observed in the TALSPEAK process.

Table IV shows the results of tests performed with additional amino acids. These tests were performed at different pH's and lower DTPA concentrations. It appears that changing the functionality of the amino acid has a significant effect on the distribution coefficient and separation factors that could be achieved using these types of molecules as buffers for actinide lanthanide separations. It is clear that there is perhaps great promise for the use of such reagents in further developing minor actinide/lanthanide separations especially given the advantages provided by the significant improvements seen with respect to phase transfer kinetics of the lanthanides.

Table IV. Distribution coefficients and separation factors for Am, Eu and Ce from different amino acid buffer systems. Alanine buffer - [Alanine] = 1.0 M, pH 2.7, 35 mM DTPA, 7 mM Eu; Arginine buffer - [Arginine] = 1.0 M, pH 2.7, 35 mM DTPA, 7 mM Eu; Methionine buffer - [Methionine] = 1.0 M, pH 1.7, 25 mM DTPA 10 mM Eu; Histidine buffer - [Histidine] = 1.0 M, pH 1.7, 25 mM DTPA 10 mM Eu.

Amino Acid	D_{Am}	D_{Eu}	D_{Ce}	$SF_{\text{Eu/Am}}$	$SF_{\text{Ce/Am}}$
DL-Alanine	0.14	0.91	10.82	6.29	74.71
L-Arginine	0.06	0.34	10.67	5.52	172.57
L-Methionine	0.93	55.92	23.59	60.08	25.34
L-Histidine	0.93	92.09	35.78	98.74	38.37

3.2.3 DTPA Complexation Kinetics

Following on from the work performed in FY '09,³² complexation kinetics experiments were performed to probe Pr, Eu, and Er complexation by DTPA in propionate media under stopped flow conditions. Propionate was chosen as the buffer due to its structural similarity with lactic acid but without the α -hydroxy group. The comparison of the collected kinetic data for both lactate and propionate systems should ascertain the actual effects of the α -hydroxy functionality on the complexation kinetics. Similarly to the studies performed in FY '09 in acetate media, the reaction between DTPA and the Ln-Arsenazo III (AAIII) complex exhibited slow complex formation kinetics i.e. the reaction had not reached completion after 60 seconds. This result is consistent with prior literature reports.³³ In addition to this, the first order rate equation (Equation 6) was not found to adequately describe the data generated in these experiments. As with the acetate system, the resultant kinetics trace is better described by a double exponential (Equation 7):

$$y = A_1 \times e^{-k_1x} + B \quad \text{Equation 6}$$

$$y = A_1 \times e^{-k_1x} + A_2 \times e^{-k_2x} + B \quad \text{Equation 7}$$

In fact, when the reaction is monitored over a one second time period there are two distinct processes occurring - one very fast (expected to be the free metal complexation reaction) and one unidentified reaction that occurs on a slower timescale. Unusually though, when the complexation reaction is monitored over a 30 second time period there are two distinct slow reactions occurring (Figure 21). Similar traces were observed for Am under the same conditions, albeit at slightly faster timescales. This infers that within the system under study there are 3 separate reactions occurring with rates k_1 , k_2 and k_3 . We were able to confirm this when processing the rate constants for the different experiments. The rate for the 2nd reaction, k_2 , in the short time scale experiment was (within error), identical to that of the first process in the longer timescale experiment.

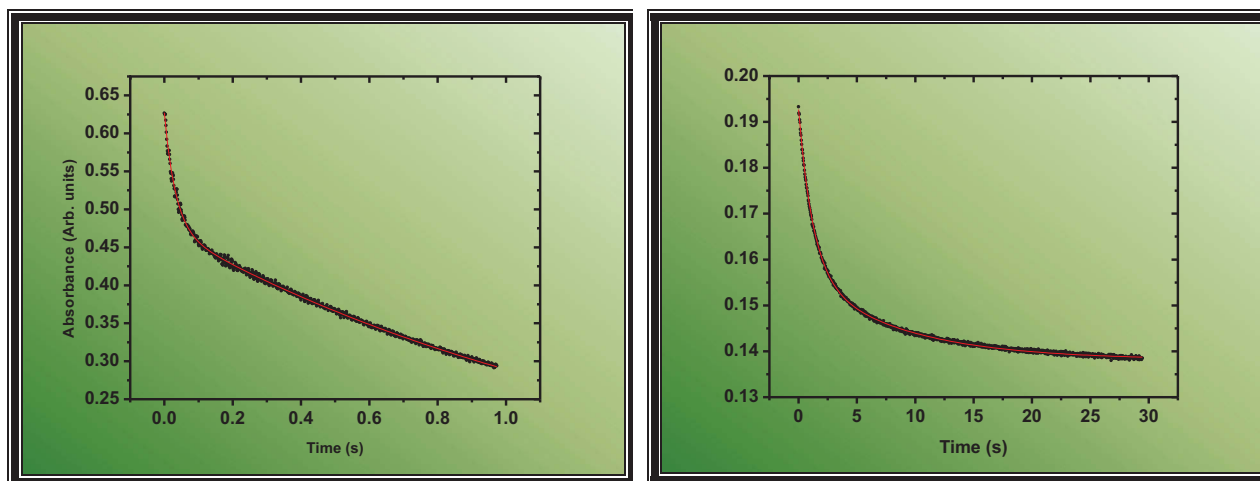


Figure 21. Sample kinetics trace from the stopped flow spectrophotometer measuring the rate of reaction of Pr-AAIII complex with DTPA $[Eu] = 5 \times 10^{-5} \text{ M}$, $[AAIII] = 5 \times 10^{-5} \text{ M}$, 50 mM propionate buffer, $I = 0.1 \text{ M}$ (NaNO_3) $[DTPA] = 1 \times 10^{-3} \text{ M}$, pH 3.7.

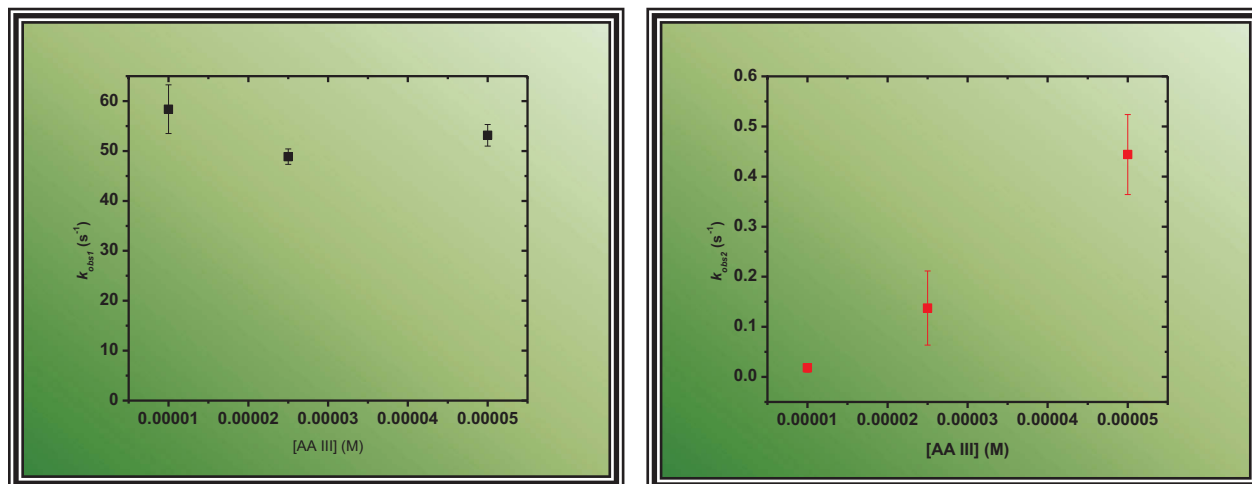


Figure 22. Plot of average (a) k_1 and (b) k_2 vs. [AAIII] in 50 mM propionate buffer, $I = 0.1$ M (NaNO_3). $[\text{Am}] = 5 \times 10^{-5}$ M : $[\text{AAIII}] = 1-5 \times 10^{-5}$ M, $[\text{DTPA}] = 1 \times 10^{-3}$ M pH 3.7.

To test if the AAIII was interfering in the systems under investigation, its effects on the reaction rates k_1 and k_2 were studied for the americium-DTPA complexation reaction. Figure 22 a&b show the results obtained. It can be seen that there was no effect of AAIII concentration on k_1 , confirming that k_1 is the rate of complexation for DTPA to the metal ion under study. However, the rate constant k_2 was seen to vary linearly with AAIII concentration indicating that AAIII is involved in the rate determining step for this process.

When comparing the assumed rate of reaction for DTPA binding to the lanthanides and americium (k_1), what is observed is that there is very little difference across the lanthanide series (Figure 23). However, the rate of reaction for DTPA binding to Am is seen to be significantly faster than any of the lanthanides studied. These results are similar to those measured for Eu and Am in an acetate buffer. The faster reaction of americium with DTPA over the lanthanides indicates that the mode of interaction has to be somewhat different between these ions. Interestingly though, this enhancement of the complexation kinetics could perhaps be attributed to something other than purely electrostatic interactions between Am and DTPA, because we see no difference in the rate of reaction across the lanthanide series where we only see changes in the physical properties of the ions (ionic radii/ m/z).

With confirmation that the AAIII is complicating the DTPA complexation studies with the lanthanides and actinides, further investigation is required into alternative colorimetric reagents to follow the complexation kinetics. In addition, temperature dependent kinetics to determine activation energies for the DTPA binding reaction will be performed. Determining the activation energies may assist in identifying the origin of the difference in behavior between the actinides and lanthanides with DTPA.

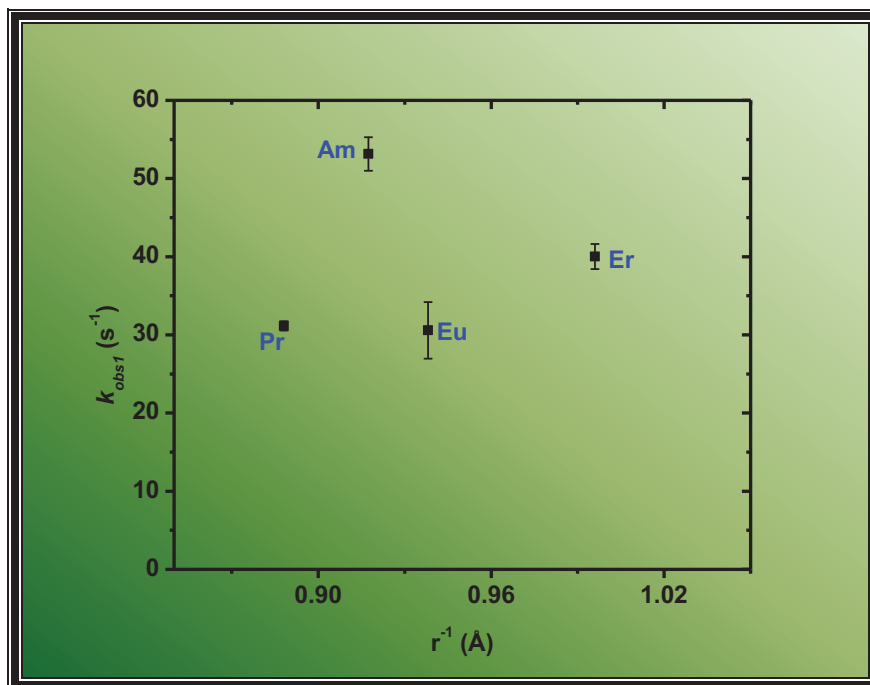


Figure 23. Plot of average k_1 for the reaction of DTPA with Pr, Eu, Er and Am as a function of ionic radii. $[\text{metal}] = 5 \times 10^{-5}$ M, $[\text{AAIII}] = 5 \times 10^{-5}$ M, 50 mM propionate buffer, $I = 0.1$ M (NaNO_3), $[\text{DTPA}] = 1 \times 10^{-3}$ M, pH 3.7.

3.3 Ternary Complexation

Since the inception of the TALSPEAK process there has been much discussion over the mechanism via which the interfacial transfer of the metal ions occur. From prior studies^{3,26,29} it is obvious that the lactate accelerates this process. The presence of yet to be identified metal:DTPA:lactate ternary complexes have been postulated to disrupt stable metal:DTPA coordination to ease HDEHP-facilitated phase transfer of the metal ion into the organic phase. In addition, Nilsson and Nash⁶ suggested that the existence of these complexes could be the part of the reason for the observed discrepancies between modeled extraction data experimental data obtained as a function of pH. With increased speculation over the existence of these complexes, a temperature dependant NMR study on some TALSPEAK-representative aqueous solutions was executed with the assistance of collaborators from the University of Manchester in the UK.

This study initially probed the complexation of La, Lu and Eu in binary mixtures with DTPA and lactate, respectively, at pD of 3.6 (pD is the deuterium equivalent of pH, this is due to the requirement for deuterated solvents in NMR studies). The use of La, Lu and Eu provided a comprehensive representation of the whole lanthanide series and could take into account any differences that might occur via the change in the ionic radii and charge density over the whole lanthanide series. When comparing the results of the proton NMR for free DTPA to the La-DTPA, Eu-DTPA and Lu-DTPA systems, it becomes clear that DTPA is bound to the metal ion in all systems in good agreement with the results of Choppin.³⁴ (Figure 24 and 25). In the binary La-lactate and Lu-lactate systems, it is difficult to tell that the lactate is bound in the inner sphere of the metal ion as there is virtually no difference in the lactate signal when La or Lu is present or absent. However, evidence that lactate is binding in the inner sphere of the lanthanides comes from the Eu-lactate binary system. As europium is a paramagnetic ion, when lactate binds the signals are shifted outside the normal ppm range. Therefore, the free lactate signals that are found at ~ 4.37 ppm (CH

proton) and ~ 1.40 ppm (CH_3 protons) shift to 0.90 ppm and 0.46 ppm respectively, when lactate is bound to the Eu ion. In addition, these signals are also seen to shift as temperature is decreased to 0.08 and -0.70 ppm, Figure 26 and 27.

As expected from the lactate-only systems, the collected proton NMR spectra for the La-DTPA-lactate and Lu-DTPA-lactate ternary systems match the lactate-only systems, indicating that there is no evidence for an inner sphere ternary complexation. The ^1H NMR spectra obtained suggest that the La-DTPA and Lu-DTPA complexes exist but lactate is unbound. Further evidence for no inner sphere ternary complexation comes from the Eu-DTPA-lactate system, where a paramagnetic shift of the magnitude observed in the binary Eu-lactate is not observed. Only slight shifts in the lactate signals in the Eu-DTPA-lactate system from 4.35 to 4.1 ppm for the CH proton and from 1.40 to 1.34 ppm for the CH_3 protons were seen Figure 28. This shift is most likely due to the lactate in presence of a paramagnetic ion rather than lactate being bound to it.

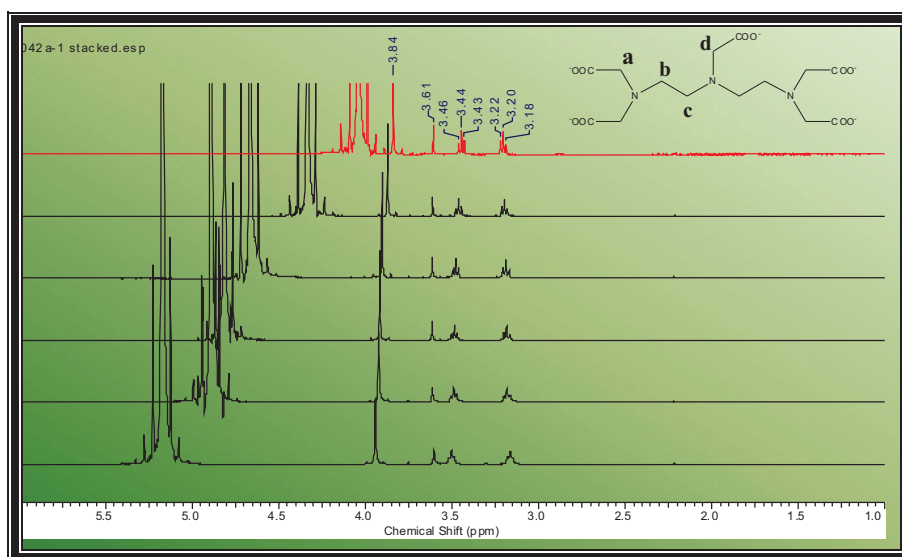


Figure 24. ^1H -NMR Spectra for free DTPA ($[\text{DTPA}] = 10$ mM, $\text{pD} = 3.6$). The peak at 3.84 ppm integrates to 8 (designated a), the peak at 3.61 ppm integrates to 2 (designated d), the peaks at 3.44 and 3.20 ppm both integrate to 4 (designated b and c, respectively).

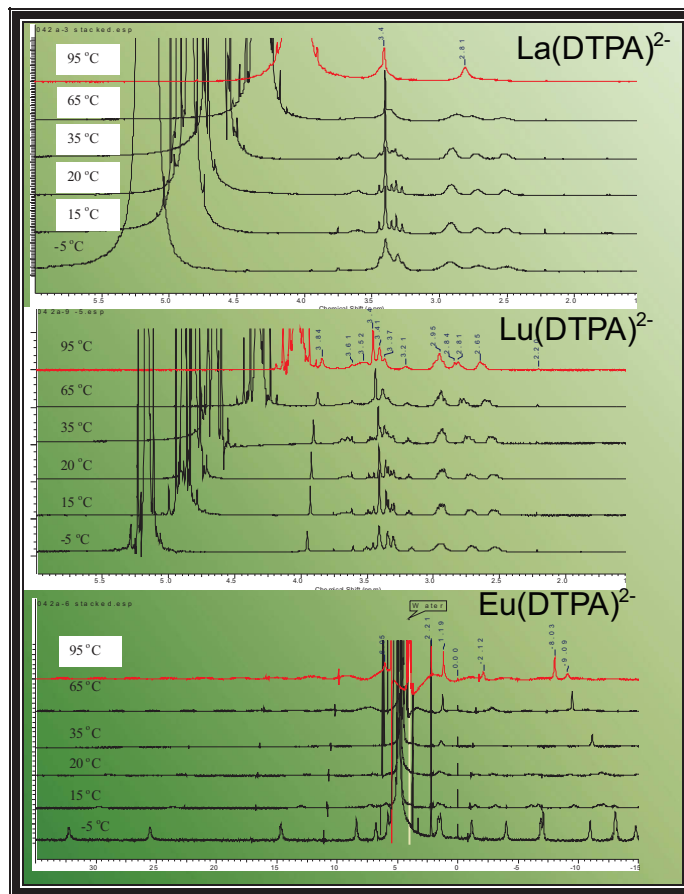


Figure 25. ¹H-NMR Spectra for solutions La-DTPA, Lu-DTPA and Eu-DTPA. [La³⁺] = [DTPA] = 10 mM, pD = 3.6, [Lu³⁺] = [DTPA] = 10 mM, pD = 3.5 and [Eu³⁺] = [DTPA] = 10 mM, pD = 3.5.

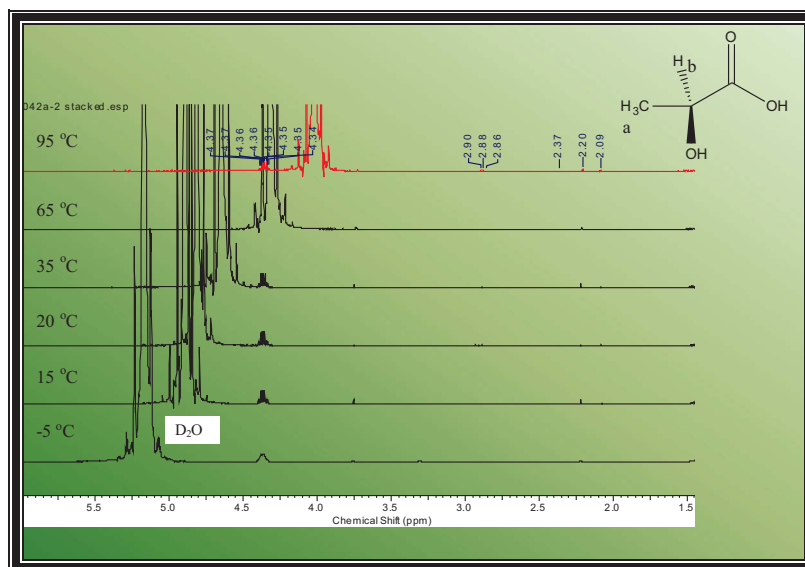


Figure 26. ¹H-NMR Spectra for lactate ([lactate] = 10 mM, pD = 3.4). The peak at 1.39 ppm integrates to 3 (designated a) and the peak at 4.35 ppm integrates to 1 (designated b).

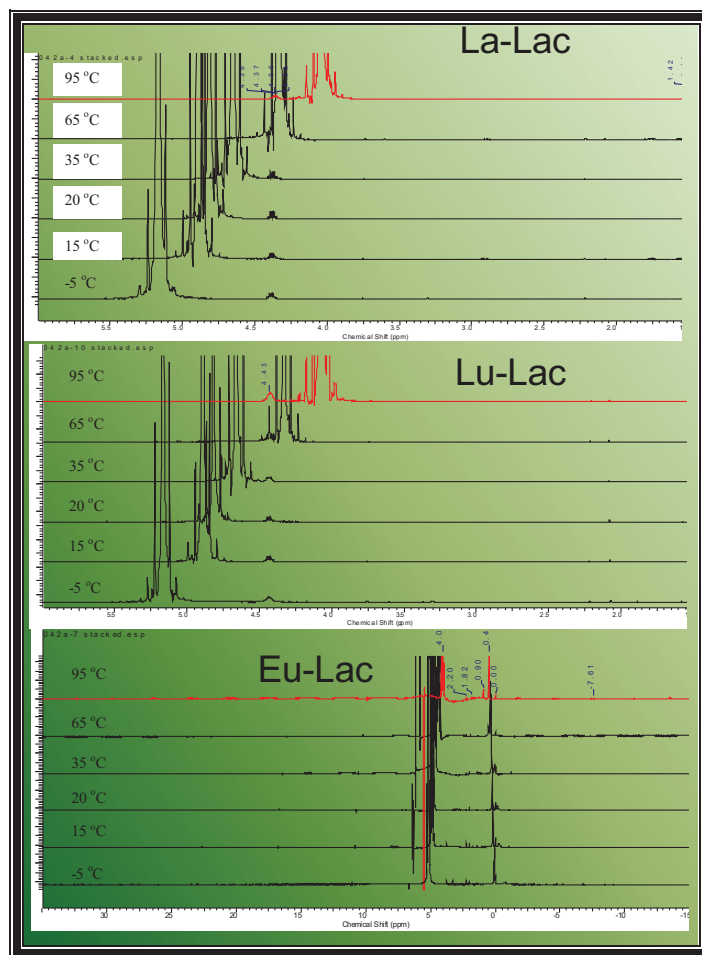


Figure 27. ¹H-NMR Spectra for solutions La-Lac, Lu-Lac and Eu-Lac. [La³⁺] = [lactate] = 10 mM, pD = 3.6, [Lu³⁺] = [lactate] = 10 mM, pD = 3.5 and [Eu³⁺] = [lactate] = 10 mM, pD = 3.5.

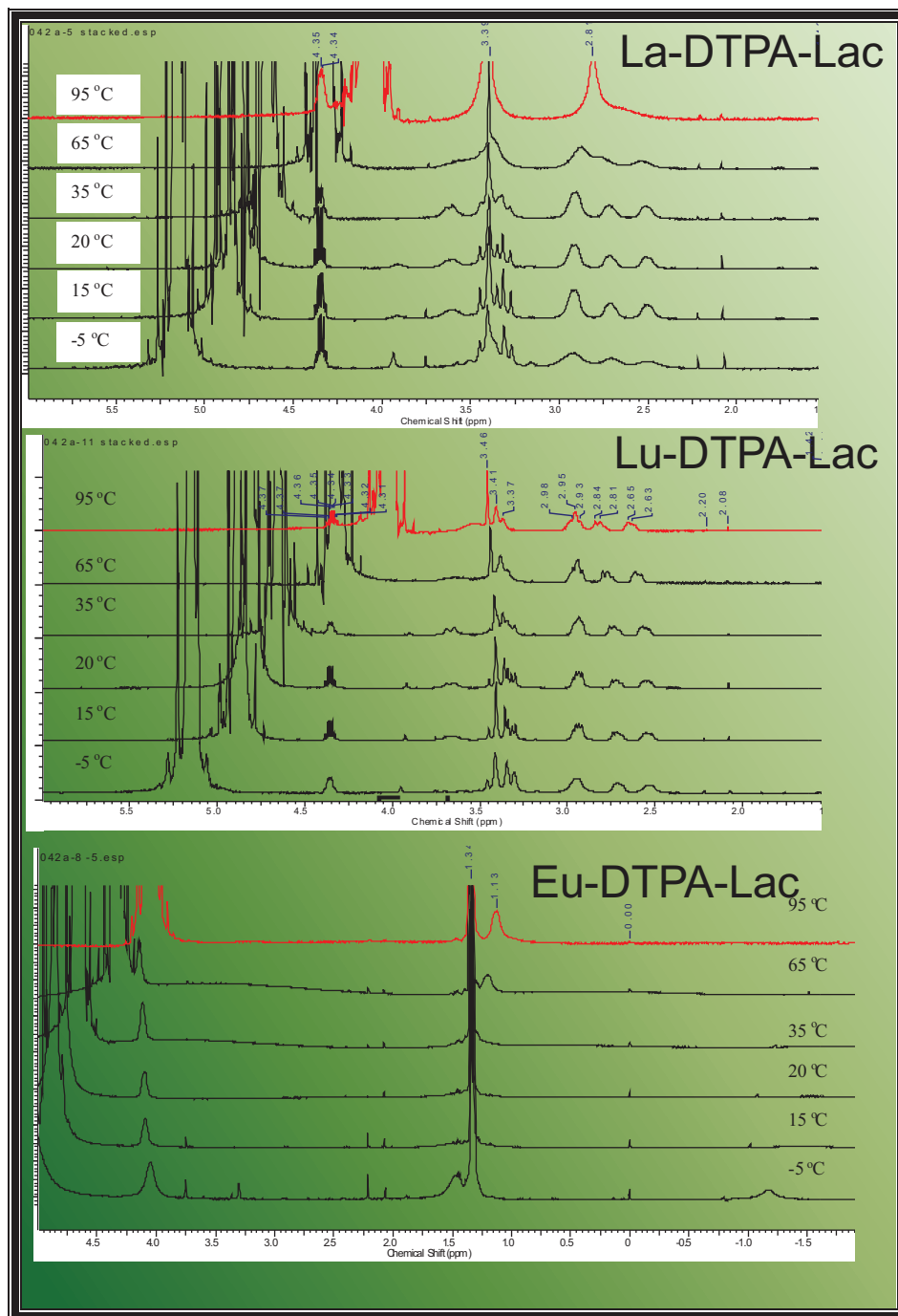


Figure 28. ¹H-NMR Spectra for solutions La-DTPA-Lac, Lu-DTPA-Lac and Eu-DTPA-Lac. [La³⁺] = [DTPA] = [lactate] = 10 mM, pD = 3.7, [Lu³⁺] = [DTPA] = [lactate] = 10 mM, pD = 3.5 and [Eu³⁺] = [DTPA] = [lactate] = 10 mM, pD = 3.6.

The results of this study suggest that there is no inner sphere complexation of lactate when DTPA is bound to a lanthanide ion and hence, no ternary complexation. These results support the work of Jensen et al.²⁸ showing that the observed trend of the metal distribution ratios in the TALSPEAK process cannot be accounted for by ternary complexation of the metal ions in the aqueous phase. Furthermore, these

results show that the phase transfer kinetics are not catalyzed by inner sphere ternary complexation as previously suggested. Hence, the mechanism by which metal partitioning occurs in the TALSPEAK system is still to be determined.

4. CONCLUSIONS AND FUTURE WORK

The ability to directly measure the heat of extraction of americium in biphasic systems has been demonstrated and was an important accomplishment for the FY 10 program of research. The application of this technique will provide new insights into the validity of the van't Hoff estimation of heats of extraction and into the phase transfer of metals across a liquid-liquid boundary for many different systems.

The dominant portion of this year's thermodynamic investigations of the TALSPEAK-type chemistry focused on the apparent shift from the idealized stoichiometric behavior expected from DTPA and HDEHP when lactate buffer is present in the system. Based on thermodynamic models lactate is not expected to be a contributing factor when determining the overall distribution of metal ion between an aqueous phase containing DTPA and an organic phase containing HDEHP. However, our metal distribution studies indicate a substantial deviation from this expected behavior at conditions that are typical of TALSPEAK process operation. Our strategically-designed studies of the liquid-liquid distribution of lanthanides produced several important conclusions:

- Medium effects of large lactic acid concentrations in the aqueous solutions on the glass electrode behavior, speciation of lactate, and metal distribution ratios appear to be minimal.
- No thermodynamically-stable mixed complexes exist in the aqueous solutions.
- The increasing complexity of the organic medium appears to influence the observed deviations.
- The mechanism of phase transfer is similar across the series of investigated conditions.

Although still quite general, these conclusions allow formulation of specific experimental tasks to continue the studies of TALSPEAK chemistry. We intend to focus our attention on the most complex aqueous regions and carefully study the critical HDEHP concentration, where the unpredictability gains strength.

The phase transfer kinetics studies have highlighted the difficulty of relying on tracer investigations alone to adequately describe the chemistry in liquid-liquid distributions. This research has highlighted how, in these complex extraction systems, attention to fundamental studies at applied conditions is essential to understand the process that is occurring. Without the studies presented here, we would still be under the assumption that the light lanthanides come to equilibrium first in the TALSPEAK process whereas, because of the interdependence of solution phase chemical equilibria, this is not the case and the light lanthanides only come to equilibrium in the system after the heavier lanthanides. Weight has been added to the argument that inner-sphere ternary complexes of the form metal:DTPA:lactate do not exist in TALSPEAK aqueous phases. However, it seems reasonable from the work presented here that lactate plays some role in the outer sphere dehydration of the metal ions.

In FY 2011 research will continue to develop thermodynamic and kinetic parameters that will assist in describing the TALSPEAK process. In particular investigations on the use of isothermal titration calorimetry to study the heat of extraction of curium will be performed and the use of microfluidic devices will be explored for studying extraction kinetics. Data collection on solution phase complexation kinetics of the actinides will also continue.

5. PRESENTATION AND PUBLICATION OF RESEARCH

1. Journal manuscript published: Zalupski, P.R., Nash, K.L., Martin, L.R.: **Thermodynamic features of the complexation of neodymium(III) and americium(III) by lactate in trifluoromethanesulfonate media.** J. Soln. Chem. 39, (2010) doi: 10.1007/s10953-010-9573-2.
2. P. Zalupski, K. Nash and L. R. Martin. **First Calorimetric Determination of the Enthalpy Change for Liquid-Liquid Distribution of Americium.** 34th Actinide Separations Conference, Argonne National Laboratory, IL, May 17th -20th 2010.
3. L. R. Martin, P. R. Zalupski, K. L. Nash. **Kinetic study of actinide (and lanthanide) interactions with DTPA.** Abstracts of Papers, 239th ACS National Meeting, San Francisco, CA, United States, March 21-25, 2010.
4. P. Zalupski, K. Nash and L. R. Martin. **Calorimetric studies of liquid-liquid distribution of actinides, lanthanides and other fission products.** Abstracts of Papers, 239th ACS National Meeting, San Francisco, CA, United States, March 21-25, 2010.
5. P. Zalupski, K. Nash and L. Martin. **Some thermodynamic considerations of TALSPEAK-based aqueous chemistry.** 16th Symposium on the Separation Science and Technology for Energy Applications. Gatlinburg, Tennessee, October 18 – 22, 2009.
6. L. R. Martin, P. R. Zalupski and Richard D. Tillotson. **Understanding the role of kinetics in f element separations systems.** Abstracts of Papers, 240th ACS National Meeting, Boston, MA, United States, August 22-26, 2010.
7. P. Zalupski and L. R. Martin. **Contributing to the recent discussions of the fundamentals of TALSPEAK chemistry.** Abstracts of Papers, 240th ACS National Meeting, Boston, MA, United States, August 22-26, 2010.
8. Guoxin Tian, Leigh R. Martin and Linfeng Rao, **Complexation of Lactate with Nd(III) and Eu(III) at Variable Temperatures: Studies by Potentiometry, Microcalorimetry, Optical Absorption and Luminescence Spectroscopy,** Accepted, Inorganic Chemistry.

6. COLLABORATORS AND PARTICIPANTS

1. Leigh R. Martin, Idaho National Laboratory (PI)
2. Peter R. Zalupski, Idaho National Laboratory, co-researcher
3. Richard D. Tillotson, Idaho National Laboratory, performs solvent extraction experiments.
4. Linfeng Rao, Lawrence Berkeley National Laboratory,
5. Guoxin Tian, Lawrence Berkeley National Laboratory,
6. Nicholas Bridges, Savannah River National Laboratory, Electrochemical investigations of TALSPEAK aqueous phase.
7. Tracy Rudisil, Savannah River National Laboratory,
8. Artem Guelis, Argonne National Laboratory, Microfluidic devices for kinetics.
9. Clint Sharrad, University of Manchester,
10. Louise Natrajan, University of Manchester
11. Tamara Griffiths, University of Manchester
12. Stephen P. Mezyk, Cal State Long Beach, kinetic analysis.

7. SUMMARY OF COLABORATORS EFFORTS IN FY 2010

The thermodynamics and kinetics program is a multi-lab effort to developing the necessary capabilities and expertise to study the these fundament properties that describe aqueous separations

systems. Although most of the work to date has focused on TALSPEAK chemistry, we are developing these capabilities and expertise in a manner such that it could be applied to any aqueous based separations technique that required study. Each lab has their own main focus area, with some overlap into the INL program for consistency in parameter measurements. Each laboratory produces its own end of year report for its focus area; however in this section the main highlights of the research from each contributor is summarized to show how this program is developing. Detailed reports from each contributor are presented in Appendix A-D.

7.1 LBNL

At Lawrence Berkeley National Laboratory (LBNL) the team lead by Dr. Linfeng Rao focuses on the determination of thermodynamic parameters of aqueous complexes between Ln(III)/ An(III) and TALSPEAK related ligands. These studies are designed to assist our understanding of the actual speciation in the complex aqueous phase of the TALSPEAK aqueous phase. The techniques applied for these studies are potentiometry, absorption spectrophotometry, luminescence spectrophotometry and calorimetry. In FY10, the focus has been on the temperature effect on the complexation of lanthanides (Nd and Eu) with lactate and DTPA, and the complexation of curium with nitrate.

7.1.1 Summary of LBNL results

The stability constants of Nd(III)/lactate and Eu(III)/lactate complexes were determined by two methods: potentiometry and spectrophotometry for Nd(III), and potentiometry and luminescence spectroscopy for Eu(III). It was identified that the stability constants of Nd(III)/lactate and Eu(III)/lactate complexes generally decrease as the temperature is increased. Such trends are consistent with the negative enthalpies of complexation obtained by calorimetry. This trend is in contrast with simple carboxylic acids such as acetate and propionate.

By comparing the experimentally determined $n_{\text{OH,exp}}$ (from luminescence lifetime measurements) with those predicted by speciation assuming different coordination modes for lactate in the Eu(III)/lactate complex, it is concluded that mode (c) in Figure 4 Appendix A, where the protonated α -hydroxyl group participates in the coordination, is the most probable coordination mode of lactate in the Eu(III)/lactate complexes.

The stability constants of Nd(III)/DTPA and Eu(III)/DTPA complexes were determined by two methods: potentiometry and spectrophotometry for Nd(III), and potentiometry and luminescence spectroscopy for Eu(III). The stability constants determined via each method agreed reasonably well. Unlike the lactate system, the effect of temperature is significant, the stability constants of both the ML and MHL complexes (with Nd and Eu) decreases by 1 – 2 orders of magnitude as the temperature is increased from 10°C to 70°C.

Investigations into the effect of temperature on the complexation of nitrate with Cm between 10-85°C, found that there was little effect of temperature on the equilibrium constants. However, from luminescence lifetime measurements of Cm(III) in nitrate solutions suggest that the nitrate ligand coordinates to Cm(III) in a bidentate mode, replacing two water molecules.

7.2 ANL

At Argonne National Laboratory (ANL) the team lead by Dr. Artem Guelis has focused on the use of microfluidic devices for the study of phase transfer kinetics. Kinetic data can be collected to allow for the calculation of metal diffusion coefficients since the surface area of the interface can be precisely

calculated. The samples can be analyzed for metal content using radiometric techniques or other analytical methods, e.g. ICP-MS. If successful these microfluidic devices will have a significant impact on the investigations of the solvent extraction kinetics and mechanism as they require only small amounts of solutions, they are cheap, reliable, and easy to operate.

7.2.1 Summary of ANL results

An all glass microfluidic chip, fabricated using photolithography, wet chemical etching, and glass bonding in a class 100 cleanroom at the University of Chicago, has been produced and used for the study of solvent extraction kinetics. A small fraction of the aqueous phase is siphoned away from the oil phase, at various stages along the capillary providing distribution data at these points of the extraction process. To our knowledge, this is the first microfluidic system that provides kinetic data for two-phase extraction, instead of simply providing an endpoint measurement. Preliminary tests on the extraction of orange-colored (0.1 M FeSCN^{2+} in $1.2 \text{ M Lactate} + 40 \text{ mM DTPA}$) into (1 M HDEHP in Dodecane), demonstrate the success of this technique (Appendix B Figure 3).

Despite these promising results, droplet formation and siphoning were not reproducible during testing with the TALSPEAK solutions for radioanalytical applications. It has been highlighted that there are two main reasons for this: 1) The presence of multiple surface-active compounds with different time-varying contact angles and 2) These solutions are considered “dirty” as they produce a residue in the glass channel that is difficult to remove. As such device design has been re-thought using a capillary network composed of Teflon tubing, with one piece of tubing specially modified using laser micromachining. These devices have an increased contact angle differential – increasing the range of permissible side channel geometries and main channel pressures that will still allow 100% separation of aqueous from organic phases. In addition, these systems can be completely disassembled and washed. Thorough washing of a glass microfluidic device is not always possible, as particles will tend to accumulate in channel corners.

In Figure 8 (Appendix B), the Teflon tubing device is shown to behave in a manner consistent with that necessary to achieve the project goals: at specific flow rates shown below, the complete siphoning of the oil phase is accomplished, leaving only the aqueous phase in the main channel for off-line analysis.

7.3 SRNL

At Savannah River National Laboratory (SRNL) there are two teams investigating slightly different aspects of TALSPEAK chemistry. The effort lead by Dr Nicholas Bridges uses electrochemistry to provide a new approach to understanding metal-ligand interactions between the actinides and TALSPEAK relevant ligands. Dr. Tracy Rudisill has been investigating the thermochemical behavior of other actinides within TALSPEAK separations.

7.3.1 Electrochemistry

Electrochemical investigations into the effects of DTPA and lactic acid on two actinides with significantly different oxidation potentials (Am and Pu) has provided insight into the systems control of the oxidation state. Initial testing highlighted in Figure 3 Appendix C, demonstrated that lactic acid is less stable to oxidation than DTPA. Interestingly though, oxidation of lactic acid does not occur by loss of the carboxylic acid as carbon dioxide,^(ref 4 Appendix C) but instead by oxidation of the α -hydroxyl group to a ketone. Oxidation of the α -hydroxyl group will form the α -ketone, pyruvic acid,^(ref 3 Appendix C) though the formation of pyruvic acid has not been confirmed through other techniques at this time. In addition, lactic acid is found to be less stable with regards to oxidation than its deprotonated congener lactate.

When Pu is added to the DTPA system we find that the Pu^{IV/V} couple is quasi-reversible but becomes more electrochemically reversible as the scan rate decreases (from a ΔE of 0.219 V at 1000 mV/s to ΔE of 0.121 V at 10 mV/s), Figure 5 Appendix C. Evidence has been presented that there are multiple coordination environments around the Pu metal ion in solution, indeed at high ratios of DTPA:Pu, the results of the electrochemical investigation suggests that nor complex coordination environments exist perhaps with multiple DTPA molecules per Pu ion. In lactate solution the Pu^{IV}/Pu^V couple exists at a higher potential than the Pu-DTPA, this is simply due to the change in coordination environment around the Pu ion in solution.

The aqueous electrochemical behavior of Am is much simpler than plutonium, due to americium due to the large redox couples required to perform the oxidation. The DTPA-Am system shows a significant decrease in the current associated with the oxidation of DTPA, Figure 8 Appendix C. The decrease in the redox potential of the DTPA is greater in the americium system, than the plutonium system. The implication of these results is not yet completely understood and is still under investigation. At the time this report was prepared the americium-lactic acid system has not been completed and thus is not reported here.

7.3.2 Solvent extraction

Plutonium was found to not be reduced by HAN once complexed by DTPA in the lactate solution. As such, oxidation state adjustments of Np and Pu were made using HAN and FS prior to combining with the lactic acid and DTPA. The UV-vis spectra were recorded following nominally 1, 2, 3, 7, and 8 days after preparation, the recoded spectra identified that the plutonium was not stable as the +3 ion under these conditions.

Distribution measurements of Np, Pu, Am, and Pa were made from an aqueous phase containing 1.5 M lactic acid, 0.05 M DTPA at a pH of 2.8 and 3.5. The organic phase consisted of 1.0M HDEHP in dodecane. These experiments were performed at ca. 20, 40 and 60°C. In the pH 2.8 experiments, Am was seen to have distribution coefficients greater than 1, when the pH was increased to 3.5 the Am seen to be retained in the aqueous phase as expected. Neptunium and protactinium were seen to extract into the organic phase more than any of the other actinides under study. As expected for the exothermic extraction of metal ions in TALSPEAK, distribution coefficients were seen to decrease as the temperature for the extraction was increased.

The actinide distribution coefficients measured at different temperatures were used to calculate conditional enthalpies (ΔH^0) and entropies (ΔS^0) of extraction. The thermodynamic properties calculated from the van't Hoff analysis are provided in Table 6, Appendix D. Inspection of the data at pH 3.5 on Figure 11 (Appendix D) and the correlation coefficients for the regression analysis (Appendix DC) show non-linearity in all studies performed. This non-linearity means that the conditional enthalpies (ΔH^0) and entropies (ΔS^0) of extraction determined in this study have to be treated with caution. There are several factors that may contribute to the non linearity; in the Pu and Np examples temperature changes may affect the rate of oxidation or reduction leading to a solution containing mixed oxidation states and hence different extraction behavior. However, a similar deviation is present in the redox stable Am and Pa examples. It has been suggested that the enthalpy of extraction may change as the temperature is increased causing the deviation. Alternately, this deviation may be due to the feed make up for the experiments. Further investigation is required into these results.

8. REFERENCES CITED

1. Marcus, Y. "Principles of Solubility and Solutins" in Solvent Extraction: Principles and Practice 2nd ed. Rydberg, J.; Cox, M.; Musikas, C. and Choppin, G.R. eds., Marcel Dekker: New York, p27 (2004).
2. Choppin, G.R.; Morgenstern, A. Solv. Extr. Ion Exch., 18, 1029, (2000).
3. Weaver, B; Kappelmann, F., TALSPEAK, A new method of separating americium and curium from the lanthanides by extraction from an aqueous solution of an aminopolyacetic acid complex with a monoacetic organophosphate or phosphonate. ORNL-3559, 1964.
4. Nilsson, M., Nash, K.L.: A review of the development and operational characteristics of the TALSPEAK process. Solvent Extr. Ion Exch. 25, 665-701 (2007).
5. Nilsson, M., Nash, K.L.: Trans-lanthanide extraction studies in the TALSPEAK system: Investigating the effect of acidity and temperature. Solvent Extr. Ion Exch. 27, 354-377 (2009).
6. Danesi, P.R., Cianetti, C., Horwitz, E.P.: Distribution equilibria of Eu(III) in the system: Bis(2-ethylhexyl)phosphoric acid, organic diluent – NaCl, lactic acid, polyaminocarboxylic acid, water. Sep. Sci. Technol. 17, 507-519 (1982).
7. Zalupski, P.R., Nash, K.L., Martin, L.R.: Thermodynamic features of the complexation of neodymium(III) and americium(III) by lactate in trifluoromethanesulfonate media. J. Soln. Chem. 39, (2010) doi: 10.1007/s10953-010-9573-2.
8. Marcus, Y.: The stability of mixed complexes in solution. Coord. Chem. Rev. 4, 273-322 (1969).
9. Kolarik, Z.: Interactions of acidic organophosphorus extractants in the organic phase. In Marcus, Y. (ed.) Solvent extraction reviews, pp. 1–62. Marcel Dekker, New York (1971) Vol. 1.
10. Kolarik, Z., Pankova, H.: Acidic organophosphorus extractants. I. Extraction of lanthanides by means of dialkyl phosphoric acids – effect of structure and size of alkyl group. J. Inorg. Nucl. Chem. 28, 2325-2333 (1966)
11. Kosyakov, V.N., Yerin, E.A.: On the mechanism of trivalent actinide extraction in the system HDEHP – lactic acid with DTPA. J. Radioanal. Chem. 56, 93-104 (1980).
12. Grimes, T., Nilsson, M., Nash, K.L.: Lactic acid partitioning in TALSPEAK. Sep. Sci. Technol. 45, 1725-1732 (2010).
13. Del Cul, G.D., Toth, L.M., Bond, W.D., Davis, G.D., Dai, S.: Citrate-based "Talspeak" Actinide-Lanthanide Separation Process. Sep. Sci. Technol. 32, 431-446 (1997).
14. Mason, G.W., Metta, D.N., Peppard, D.F.: The extraction of selected M(III) metals by bis 2-ethylhexyl phosphoric acid in *n*-heptane. J. Inorg. Nucl. Chem. 38, 2077-2079 (1976).
15. Danesi, P.R., Vandegrift, G.F.: Kinetics and mechanism of the interfacial mass transfer of Eu³⁺ and Am³⁺ in the system bis(2-ethylhexyl) phosphate-*n*-dodecane-NaCl-HCl-water. J. Phys. Chem. 85, 3646-3651 (1981).
16. Zalupski, P.R., Nash, K.L.: Two-phase calorimetry. I. Studies on the thermodynamics of lanthanide extraction by bis(2-ethyl(hexyl)) phosphoric acid. Solvent Extr. Ion Exch. 26, 514-533 (2008).
17. Danesi, P.R., Vandergrift, G.F.: Activity coefficients of bis(2-ethylhexyl)phosphoric acid in *n*-dodecane. Inorg. Nucl. Chem. Letters 17, 109-115 (1981).

18. Raieh, M.A., Aly, H.F.: Thermodynamics of dinonylnaphthalene sulfonic acid (HD). Extraction of trivalent americium, curium and californium. *J. Radioanal. Chem.* 57, 17-21 (1980).
19. Marcus, Y.: Thermodynamics of liquid-liquid distribution reactions. V. Enthalpy- and entropy-controlled extraction processes. In Lucas, B.H., Ritcey, G.M., Smith, H.W. (eds.) *Proceedings of the International Solvent Extraction Conference, ISEC1977*, pp. 154-158. Toronto, Canada (1977) Vol. 2.
20. Lundqvist, R., Lu, J.-F., Svantesson, I.: Hydrophilic complexes of the actinide. II. Comparison of TBP, HTTA and HDEHP liquid-liquid distribution systems. *Acta Chim. Scand.* A37, 743-753 (1983).
21. Mason, G.W., Schofer, N.L., Peppard, D.F. *J. Inorg. Nucl. Chem.* 32, 3911-3922 (1970).
22. Rizkalla, E.N., Choppin, G.R.: Hydration of actinides and lanthanides. In Gschneidner, K.A., Jr., Eyring, L., Choppin, G.R., Lander, G.H. (eds.) *Handbook on the physics and chemistry of rare earths*, pp. 529-557. Elsevier Science Publishers B.V., North-Holland, Amsterdam (1994) Vol. 18.
23. Choppin, G.R.: Comparative solution chemistry of the 4f and 5f elements. *J. Alloys Comp.* 223, 174-179 (1995).
24. Choppin, G.R., Jensen, M.P.: Thermodynamics and kinetics of actinide complexation. In Morss, L.R., Edelstein, N.M., Fuger, J. (eds.) *The chemistry of the actinide and transactinide elements*, pp. 2524-2621. Springer, Dordrecht, The Netherlands (2006) Vol. 4.
25. Kolarik, Z. and Kuhn, W., *Proc. Int. Solv. Extr. Conf.* 1974, Vol. 3, Society of Chemical Industry, London, 2593 (1974).
26. Weaver, B., Kappelmann, F.A.: Preferential extraction of lanthanides over trivalent actinides by monoacidic organophosphates from carboxylic acids and from mixtures of carboxylic and aminopolyacetic acids. *J. Inorg. Nucl. Chem.* 30, 263-272 (1968).
27. Danesi, P.R. and Cianetti, Kinetics and mechanism of the interfacial mass transfer of Eu(III) in the system: Bis(2-ethylhexyl)phosphoric acid, n-dodecane-NaCl, lactic acid, polyaminocarboxylic acid, water, *Sep. Sci. Technol.* 17, 969-989, (1982).
28. Leggett, C. J. Liu, Guokui and Jensen, M. P., Do Aqueous Ternary Complexes Influence the TALSPEAK Process?, *Solv. Extr. Ion Exch.*, 28, 313-334, (2010)
29. Nilsson, M., Nash, K.L., The Influence of lactic acid concentration on extraction equilibria and kinetics in talspeak chemistry, *Separation Science and Technology Conference*, Gatlinburg TN, October 2009.
30. Tachimori, S.; Nakamura, H. *J. Radioanal. Chem.*, 1979, 52, 343.
31. Glentworth, P., Wiseall, B., Wright, C.L. and Mahmood, A.J., *J. Inorg. Nucl. Chem.*, 30, 967 (1968).
32. Martin, L.R. and Zalupski, P.Z. Thermodynamics and Kinetics of Actinide Partitioning in Advanced Fuel Cycle Systems, AFCI-SEPA-PMO-MI-DV-2009-000191, (2009).
33. Försterová, M.; Svobodová, I.; Lubal, P.; Táborský, P.; Hermann, P. and Lukeš, I. *Dalton Trans.*, 535 (2007).
34. Choppin, G. R.; Thakur, P. and Mathur, J. N. *Comptes Rendus Chimie*, 10, 916-928 (2007).

Appendix A

Understanding Actinide/Lanthanide Speciation under TALSPEAK Conditions

Dr. Linfeng Rao

Lawrence Berkeley National Laboratory

SUMMARY

The TALSPEAK process (Trivalent Actinide Lanthanide Separations by Phosphorus-reagent Extraction from Aqueous Komplexes) has been shown to be a promising option for accomplishing one of the most challenging tasks in the Advanced Fuel Cycle – separation of the trivalent actinides (An(III)) from the trivalent fission product lanthanides (Ln(III)). Effective separations of An(III) from Ln(III) by TALSPEAK have been demonstrated in several pilot-scale operations. However, the fundamental chemistry underlying the separations remains unclear. Currently available thermodynamic data are not sufficient to interpret and/or predict the behavior of actinides and lanthanides in the process. Besides, the effects of operating conditions (e.g. temperature) on the thermodynamic parameters are unknown. Therefore, accurate prediction and precise control of the behavior of actinides and lanthanides in the TALSPEAK process are difficult if the operation “envelop” changes.

This is a collaborative project between Lawrence Berkeley National Laboratory (LBNL) and Idaho National Laboratory (INL), aiming at understanding the thermodynamics and kinetics of the chemical reactions involving An(III) and Ln(III) under TALSPEAK conditions. In FY10, complexation of lanthanides and actinides with key TALSPEAK ligands (lactate, DTPA and nitrate) was studied at elevated temperatures. The effect of temperature on the complexation and the coordination mode of An(III)/Ln(III) complexes were determined with multiple techniques including potentiometry, microcalorimetry, optical absorption and luminescence spectroscopy.

Fuel Cycle Research and Development Separations

UNDERSTANDING ACTINIDE/LANTHANIDE SPECIATION UNDER TALSPEAK CONDITIONS

INTRODUCTION

The TALSPEAK (Trivalent Actinide Lanthanide Separations by Phosphorus-reagent Extraction from Aqueous Komplexes) process has been shown to be effective in separations of trivalent actinides (An(III)) from trivalent lanthanides (Ln(III)), but the fundamental chemistry underlying the separations remains unclear. Currently available thermodynamic data are not sufficient for interpreting and/or predicting the behavior of actinides and lanthanides in the process. Besides, the effects of operating conditions (e.g. temperature) on the thermodynamic parameters are unknown. Therefore, accurate prediction and precise control of the behavior of actinides and lanthanides in the TALSPEAK process are difficult if the operation “envelop” changes.

To achieve accurate prediction and precise control of the behavior of actinides and lanthanides in the TALSPEAK process, we have started systematic studies to determine the thermodynamic parameters of the reactions in the TALSPEAK system, including the complexation of lanthanides and actinides with key TALSPEAK ligands, including lactate, DTPA and nitrate. The effect of operating conditions (e.g. temperature) on the thermodynamic parameters is evaluated. In FY10, the focus has been on the temperature effect on the complexation of lanthanides (Nd and Eu) with lactate and DTPA, and the complexation of curium with nitrate.

RESULTS

Complexation of Nd(III) and Eu(III) with Lactate (10-70°C)

Effect of Temperature on the Complexation

The stability constants of Nd(III)/lactate and Eu(III)/lactate complexes were determined by two methods: potentiometry and spectrophotometry for Nd(III), and potentiometry and luminescence spectroscopy for Eu(III). All data are summarized in Figure 1. For the Nd(III)/lactate system, the stability constants obtained by the two methods are in fair agreement within the 3σ uncertainties, except for the value of $\log \beta_3$ at 55°C. For the Eu(III)/lactate system, the stability constants of EuL^{2+} and $\text{EuL}_3(\text{aq})$ obtained by luminescence are in fairly good agreement with those by potentiometry, but the stability constants of EuL_2^+ by the two methods differ significantly. It is believed that the results by potentiometry is more reliable, because the emission spectra are analyzed based on the assumption that the emission intensities of all Eu(III) species are proportional to their concentrations. Such assumption may not be true for all systems. Therefore, the stability constants obtained from luminescence are not used for calculating the enthalpy and entropy of complexation for the Eu(III)/lactate complexes.

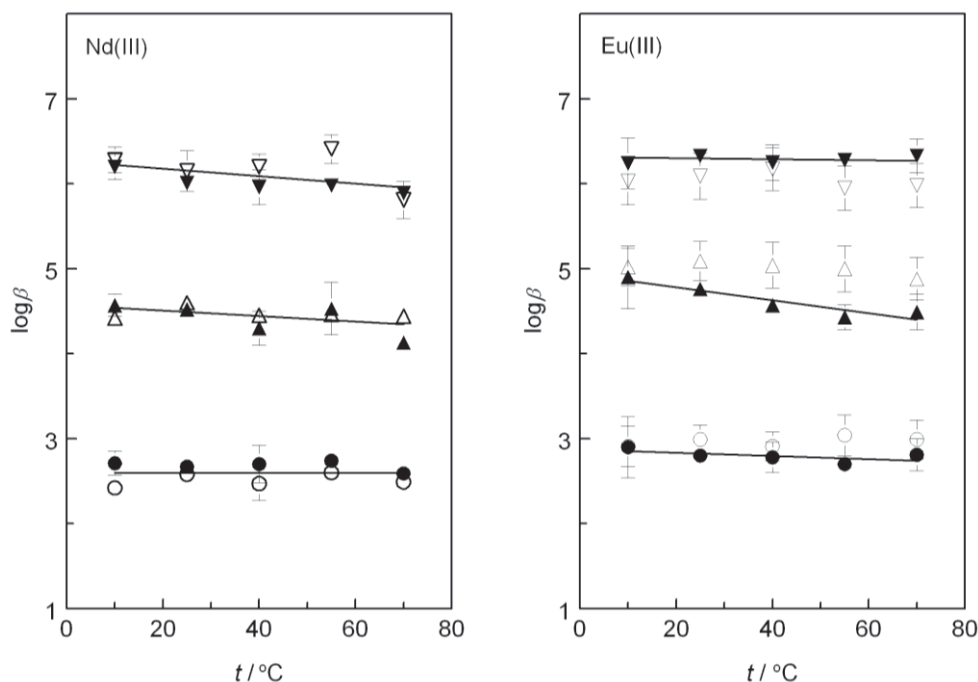


Figure 1. Effect of temperature on Nd(III)/lactate and Eu(III)/lactate complexation. $I = 1.05 \text{ mol}\cdot\text{kg}^{-1} \text{ NaClO}_4$. (●○) ML, (▲△) ML₂, (▼▽) ML₃. Solid symbols – data obtained by potentiometry; open symbols – data obtained by absorption spectroscopy (for Nd) or luminescence spectroscopy (for Eu).

Figure 1 shows that the stability constants of Nd(III)/lactate and Eu(III)/lactate complexes generally decrease as the temperature is increased. Such trends are consistent with the negative enthalpies of complexation obtained by calorimetry. On the contrary, the complexation of simple carboxylates (acetate, propionate, etc.) with lanthanides usually becomes stronger at higher temperatures and the enthalpy of

complexation is slightly endothermic ($\Delta H = 5 - 15$ kJ/M for lanthanide complexes with acetate or propanoate [1]). The complexation of lanthanides with lactate, and α -hydroxycarboxylates in general, is exothermic probably because the α -hydroxyl group is less hydrated than the carboxylate group so that less dehydration energy is required to form the coordination bond.

Direct determination of enthalpy of complexation for Nd(III)/lactate and Eu(III)/lactate complexes at 25°C by calorimetry

Figure 2 shows the data from calorimetric titrations, in the form of the accumulated reaction heat as a function of the volume of the titrant. Titrations with different concentrations of C_M^0 (M = Nd or Eu), C_L^0 and C_H^0 are shown. Using these data in conjunction with the stability constants obtained by potentiometry and spectrophotometry, the enthalpies of complexation at 25°C were calculated. The enthalpy values are all negative (-2 kJ/M for ML, -3 to -4 kJ/M for ML₂, and -11 to -12 kJ/M for ML₃), consistent with the trends of decreasing stability constants with the increase in temperature as shown in Figure 1.

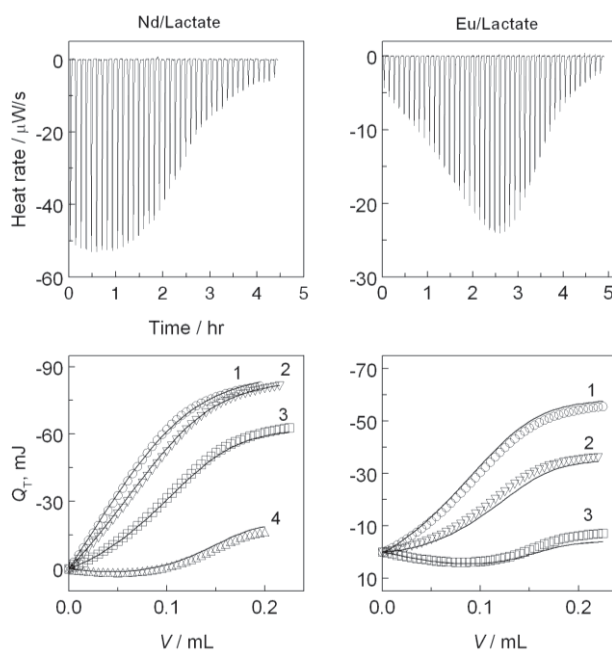


Figure 2. Calorimetric titrations of Nd(III)/lactate (left) and Eu(III)/lactate (right) complexation, $t = 25^\circ\text{C}$, $I = 1.00$ M NaClO₄. $V^0 = 0.900$ mL, titrant 0.300 M HClO₄. Initial concentrations ($C_H^0/C_M^0/C_L^0$ in mM): Lower left - (1) 17.60/24.80/66.70; (2) 13.20/18.60/66.70; (3) 8.80/12.40/66.70; (4) 4.40/6.20/66.70. Lower right - (1) 5.45/13.40/66.70; (2) 3.63/8.94/66.70 mM; (3) 1.82/4.47/66.70. The upper figures are the thermograms of the first titration for Nd(III) and Eu(III) systems.

Luminescence Data and the Coordination Modes in Ln(III)/Lactate Complexes

Figure 3 shows the luminescence emission spectra of Eu(III)/lactate solutions at 25°C. The spectra contains features originating from electronic transitions from the lowest excited state, ⁵D₀, to the ground state manifold, ⁷F_J (J = 0, 1, 2, 3,.....). As the concentration of lactate was increased from 0 to 0.072 M, the intensity of the hypersensitive ⁵D₀ → ⁷F₂ transition (around 615 - 620 nm) increased significantly. Figure 3 also shows the luminescence decay patterns of Eu(III)/lactate solutions. Single exponential functions are used to fit the data to obtain the luminescence lifetimes (τ). It is evident that τ becomes longer as C_{lactate} is increased, suggesting the number of water molecules (or, the number of O-H

oscillators) in the inner coordination sphere of Eu^{3+} is reduced due to the complexation with lactate. Using the previously established linear correlation between the luminescence lifetime and the number of water molecules ($n_{\text{H}_2\text{O}} = 1.05 \times \tau^{-1} - 0.7$, where τ is in milliseconds [2]) and based on the observation that one water molecule corresponds to two O-H oscillators in terms of luminescence quenching [3], the average number of O-H oscillators per Eu(III) in the solutions, $n_{\text{OH,exp}}$, were calculated. These data are compared with model-predicted values and help to understand the coordination mode of lactate in the Eu(III) complexes.

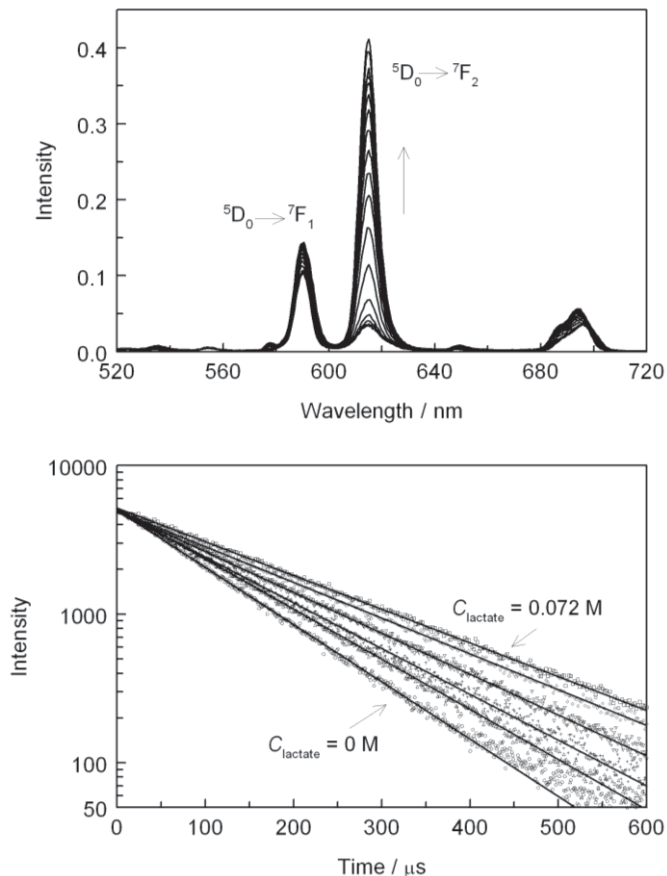


Figure 3. Luminescence emission spectra (upper) and luminescence decay (lower) of Eu(III)/lactate systems, $t = 25^\circ\text{C}$, $I = 1.00 \text{ M NaClO}_4$, $V^0 = 2.50 \text{ mL}$, $C_{\text{H}}^0 = 20.0 \text{ mM}$, $C_{\text{Eu}}^0 = 2.00 \text{ mM}$; titrant: 0.500 M sodium lactate; $[\text{lactate}]_{\text{total}}$ increased from 0 to 0.072 M during the titration. Excitation wavelength: 394 nm .

By comparing the experimentally determined $n_{\text{OH,exp}}$ with those predicted by speciation assuming different coordination modes for lactate in the Eu(III)/lactate complex, it is concluded that mode (c) in Figure 4, where the protonated α -hydroxyl group participates in the coordination, is the most probable coordination mode of lactate in the Eu(III)/lactate complexes.

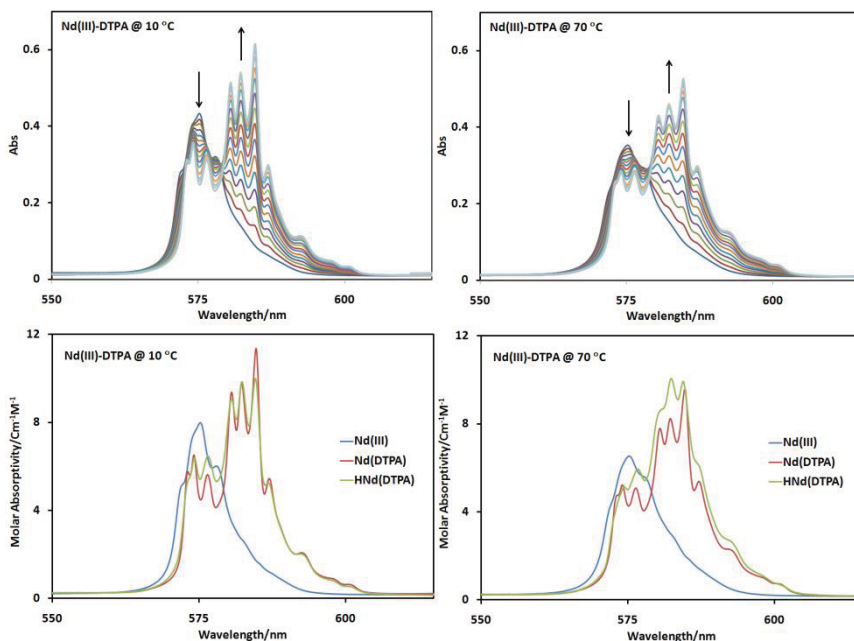


Figure 6. Spectrophotometric titrations of Nd(III)/DTPA complexation at 10°C (left) and 70°C (right) ($I = 1.0 \text{ M NaClO}_4$). Lower figures show the calculated molar absorptivities of the Nd(III) species.

Luminescence Spectroscopy for Eu(III)/DTPA (10 – 70°C)

The intensities of the luminescence bands of Eu(III) increased significantly as the concentration of DTPA was increased, as shown in Figure 7. The stability constants of two Eu(III)/DTPA complexes, EuDTPA and Eu(HDTPA), were calculated from the luminescence emission spectra.

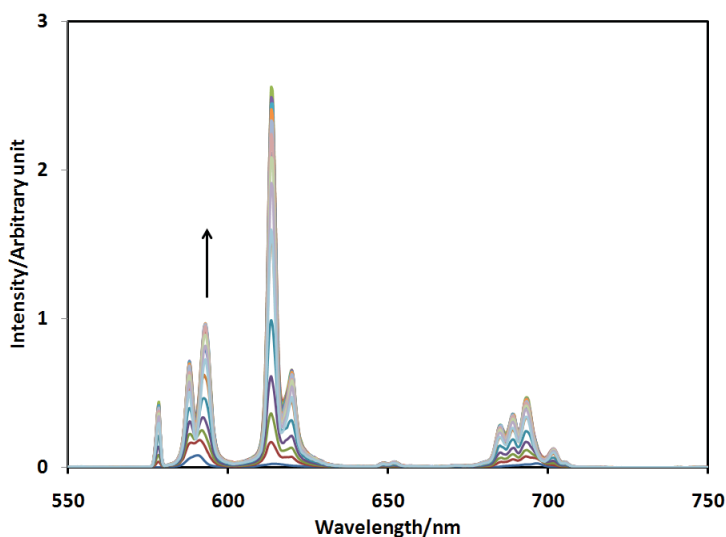


Figure 7. Luminescence emission spectra of Eu(III)/DTPA solutions at 25°C.

Effect of Temperature on the Complexation

Figure 8 summarizes the stability constants of Nd(III)/DTPA and Eu(III)/DTPA complexes in the temperature range of 10 to 70°C. As the data show, the effect of temperature is significant, the stability constants of both the ML and MHL complexes decreasing by 1 – 2 orders of magnitude as the temperature is increased from 10°C to 70°C.

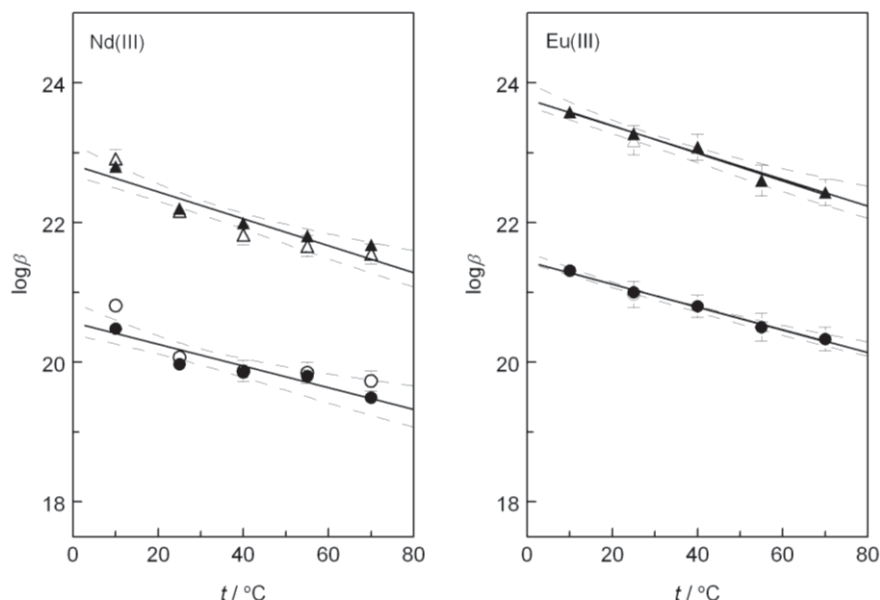


Figure 8. Effect of temperature on Nd(III)/DTPA and Eu(III)/DTPA complexation. $I = 1.05 \text{ mol}\cdot\text{kg}^{-1} \text{ NaClO}_4$. (●○) ML, (▲△) MHL. Solid symbols – data obtained by potentiometry; open symbols – data obtained by absorption spectroscopy (for Nd) or luminescence spectroscopy (for Eu).

Effect of Temperature on the Complexation of Cm(III) with Nitrate (10 – 85°C)

This study is conducted in a parallel mode to an earlier study on the complexation of lanthanides with nitrate at variable temperatures [4]. Stability constants of CmNO_3^{2+} at 10, 25, 40, 55, 70 and 85°C were determined and the coordination mode of nitrate in CmNO_3^{2+} was evaluated in comparison with that in the lanthanide nitrate complexes previously reported.

Figure 9 shows the luminescence emission spectra of Cm(III) in a titration with nitrate solutions. As the concentration of nitrate was increased, the luminescence intensity of the peak at 592 - 593 nm slightly decreased while the intensity of a new peak at a longer wavelength (around 595 - 596 nm) increased. An isobestic point, observed at about 594 nm, indicated there were two emitting Cm(III) species in the solutions being titrated. The emission peak at 592 - 593 nm is assigned to the free Cm^{3+} species, while the peak at 595 - 596 nm is assigned to the CmNO_3^{2+} complex. The equilibrium constants of the complexation at different temperatures were calculated and shown in Table 1. The stability constants at infinite dilution in Table 1 were obtained by using the Specific Ion Interaction approach (SIT) outlined in the literature [5].

Table 1 Equilibrium constants of Cm(III) complexation with nitrate at different temperatures ($\text{Cm}^{3+} + \text{NO}_3^- = \text{CmNO}_3^{2+}$) by luminescence spectroscopy.

T °C	I $\text{mol}\cdot\text{kg}^{-1}$ H_2O	$\log K_m$	$\Delta\varepsilon^*$ $\text{kg}\cdot\text{mol}^{-1}$	$\log K_m^0$	ΔH^0 $\text{kJ}\cdot\text{mol}^{-1}$	ΔS^0 $\text{J}\cdot\text{K}^{-1}\cdot\text{mol}^{-1}$	Ref.
10	1.05	-0.017 ± 0.03	-0.01 ± 0.02	1.18 ± 0.04			
25		-0.061 ± 0.03	-0.01 ± 0.02	1.16 ± 0.04	0 ± 1	22 ± 3	
40		-0.104 ± 0.03	-0.01 ± 0.02	1.16 ± 0.04			
55		-0.150 ± 0.03	-0.01 ± 0.02	1.15 ± 0.04			
70		-0.184 ± 0.03	-0.01 ± 0.02	1.16 ± 0.04			
85		-0.213 ± 0.03	-0.01 ± 0.02	1.17 ± 0.04			
5	0.1 – 4.6		0.03 ± 0.02	1.28 ± 0.07			[6]
15			0.03 ± 0.02	1.26 ± 0.06	1.8 ± 1.0	30.5 ± 3.5	
25			0.03 ± 0.02	1.29 ± 0.06			
50			0.02 ± 0.01	1.30 ± 0.03			
75			0.02 ± 0.02	1.38 ± 0.05			

* ε is the specific ion interaction parameter defined in the SIT approach [5]. Values of $\Delta\varepsilon$ for the present work are the average of the $\Delta\varepsilon$ for the perchlorate medium [5] and the $\Delta\varepsilon$ for the nitrate medium [6] at 25°C.

Data from this work indicate that there is little effect of temperature on the complexation of Cm(III) with nitrate in the temperature range up to 85°C. The enthalpy of complexation at infinite dilution, ΔH^0 , for this temperature range was determined by the Van't Hoff equation to be essentially zero.

Representative patterns of the Cm(III) luminescence decay are shown in Figure 10 by two sets of data for solutions with $C_{\text{nitrate}} = 0$ and $0.90 \text{ mol}\cdot\text{dm}^{-3}$ at 25°C. The decay patterns are fitted with a single exponential function and the lifetime ($\tau_{\text{H}_2\text{O}}$) is thus calculated.

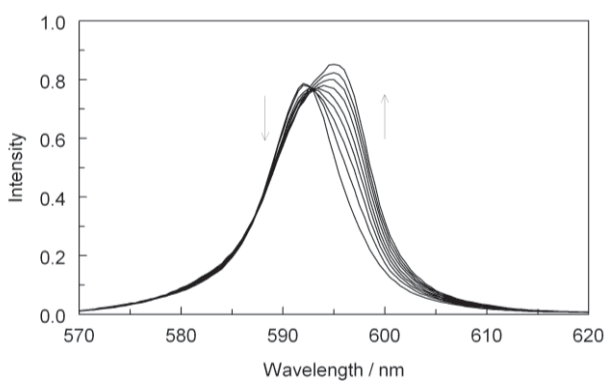


Figure 9. Luminescence emission spectra of Cm(III)/nitrate systems. $I = 1.0 \text{ mol}\cdot\text{dm}^{-3}$ $\text{Na}(\text{ClO}_4/\text{NO}_3)$, $t = 25^\circ\text{C}$. $[\text{Cm}(\text{III})]_{\text{total}} = 0.4 \text{ mmol}\cdot\text{dm}^{-3}$, $[\text{H}^+] = 0.100 \text{ mol}\cdot\text{dm}^{-3}$, $[\text{nitrate}]_{\text{total}}$ from 0 to $0.900 \text{ mol}\cdot\text{dm}^{-3}$. $\lambda_{\text{ex}} = 396 \text{ nm}$

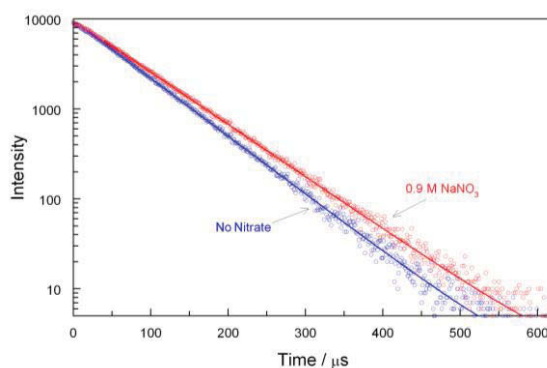


Figure 10. Decay of Cm(III) luminescence (at 592 - 596 nm) in aqueous solutions. $I = 1.0 \text{ mol}\cdot\text{dm}^{-3}$ $\text{Na}(\text{ClO}_4/\text{NO}_3)$, $t = 25^\circ\text{C}$. $[\text{Cm}(\text{III})]_{\text{total}} = 0.4 \text{ mmol}\cdot\text{dm}^{-3}$, $[\text{H}^+] = 0.10 \text{ mol}\cdot\text{dm}^{-3}$, $[\text{nitrate}]_{\text{total}} = 0$ (blue) and $0.90 \text{ mol}\cdot\text{dm}^{-3}$ (red). $\lambda_{\text{ex}} = 396 \text{ nm}$.

It has been shown that, due to the efficient coupling of the energy level of the excited state (${}^6D_{7/2}$) with the overtones of high-frequency OH vibrations of the water molecules, the luminescence lifetime of Cm^{3+} decreases as the number of water molecules in the inner coordination sphere increases [7-9]. A linear relationship between the luminescence lifetime of Cm^{3+} and the number of water molecules at 25°C has been determined to be $n_{\text{H}_2\text{O}} = 0.65 \times \tau_{\text{H}_2\text{O}}^{-1} - 0.88$, where $\tau_{\text{H}_2\text{O}}$ is in milliseconds [9]. The luminescence lifetimes of $\text{Cm}(\text{III})$ in nitrate solutions suggest that the nitrate ligand coordinates to $\text{Cm}(\text{III})$ in a bidentate mode, replacing two water molecules.

PUBLICATIONS

Four manuscripts have been submitted or in preparation for publication:

- G. Tian, L. Rao, Effect of Temperature on the Protonation of the TALSPEAK Ligands: Lactic and Diethylenetrinitropentaacetic Acids, *Separation Science and Technology*, in press.
- L. Rao, G. Tian, Effect of Temperature on the Complexation of $\text{Cm}(\text{III})$ with Nitrate in Aqueous Solutions, *J. Chem. Thermodynamics*, submitted (this work is jointly supported by the FCRD and the BES programs).
- G. Tian, L. R. Martin, L. Rao, Complexation of Lactate with $\text{Nd}(\text{III})$ and $\text{Eu}(\text{III})$ at Variable Temperatures: Studies by Potentiometry, Microcalorimetry, Optical Absorption and Luminescence Spectroscopy, *Inorg Chem.*, submitted.
- G. Tian, L. R. Martin, L. Rao, Complexation of Diethylenetrinitropentaacetic Acid with $\text{Nd}(\text{III})$ and $\text{Eu}(\text{III})$ at Variable Temperatures, manuscript in preparation.

FUTURE PLAN

Complexation of $\text{Cm}(\text{III})$ with lactate and DTPA at variable temperatures

Luminescence spectroscopy is a very useful technique for this study. In FY09 and FY10, a considerable amount of time was spent on investigating the hydration state of $\text{Cm}(\text{III})$ and its complexation with the background ligand (nitrate) at variable temperatures. On the basis of these results, the complexation of $\text{Cm}(\text{III})$ with the TALSPEAK ligands (lactate and DTPA) at variable temperatures will be studied next. The thermodynamic data on $\text{Cm}(\text{III})$, together with those on the lanthanides, will provide more accurate prediction of the behavior of actinides/lanthanides in TALSPEAK as the operation temperature changes.

The complexation of $\text{Ln}(\text{III})/\text{An}(\text{III})$ with propanoic acid at variable temperatures, in comparison with lactic acid

Lactic acid and propanoic acid differ by the α -hydroxyl group in the former. Suggested by Dr. L. R. Martin of Idaho National Laboratory, such a comparative study could help to understand the role(s) that lactic acid plays in the TALSPEAK process. In addition, based on our recent results on the coordination mode(s) of lactate in the $\text{Eu}(\text{III})$ complexes, the study of $\text{Eu}(\text{III})$ /propanoate by luminescence spectroscopy could provide further insight into the coordination modes and the correlation between the luminescence lifetime and the O-H oscillators in the inner coordination sphere of $\text{Eu}(\text{III})$.

REFERENCES

1. NIST Standard Reference Database 46: *NIST Critically Selected Stability Constants of Metal Complexes Database*, Version 8.0, U.S. Department of Commerce, 2004.
2. Barthelemy, P. P.; Choppin, G. R. *Inorg. Chem.* **1989**, 28, 3354.
3. Kimura, T.; Nagaishi, R.; Kato, Y.; Yoshida, Z. *Radiochim. Acta* **2001**, 89, 125.

4. Rao, L.; Tian, G. *Inorg. Chem.* **2009**, 48, 964.
5. Hummel, W.; Anderegg, G.; Puigdomènech, I.; Rao, L.; Tochiyama, O. “*Chemical Thermodynamics of Compounds and Complexes of: U, Np, Pu, Am, Tc, Zr, Ni and Se with Selected Organic Ligands*”, (Mompean, F. J.; Illemassene, M.; Perrone, J. eds.), Amsterdam: Elsevier B.V. 2005.
6. Skerencak, A.; Panak, P. J.; Hauser, W.; Neck, V.; Klenze, R.; Lindqvist-Reis, P.; Fanghänel, Th. *Radiochim. Acta* **97**, 385–393 (2009).
7. Beitz, J. V. *Radiochim. Acta* **52/53**, 35–39 (1991).
8. Kim, J. I.; Klenze, R.; Wimmer, H.; Runde, W.; Hauser, W. *J. Alloys Compd.* **213–214**, 333 (1994).
9. Kimura, T.; Choppin, G. R.; Kato, Y.; Yoshida, Z. *Radiochim. Acta* **72**, 61–64 (1996).

Appendix B

Separation Process Thermodynamics and Kinetics: Development of Microfluidic Devices for Solvent Extraction Studies and Radioanalytical Applications

Dr. Artem Guelis

Argonne National Laboratory

SUMMARY

The project proposes studying the extraction of radioactive species from an aqueous phase into an organic phase using a microfluidic platform. The fundamental components of the microfluidic device proposed are:

- 1) A system for generating nL scale droplets: specifically, a “T-junction” to predictably produce a monodisperse emulsion of the solutions of interest.
- 2) A system for controlling the motion of these nL scale droplets: specifically, a capillary network, with a diameter on the order of 100’s of μm ; small enough to enable rapid diffusion and mixing.
- 3) A side channel, perpendicular to the main capillary channel, with significantly smaller dimensions, through which one phase is selectively siphoned away from the main channel. Separation is achieved by designing the system to balance capillary forces vs. flow pressure. This side channel serves to “quench” the extraction of the species of interest between phases by physically isolating the two phases.

The collection of the kinetic data will allow for calculating the diffusion coefficients of the metals since the surface area of the interface can be precisely calculated. The primary focus of the investigation is the TALSPEAK kinetics and mechanism. The samples can be analyzed for metal content using radiometric techniques or other analytical methods, e.g. ICP-MS. The microfluidic devices will have a significant impact on the investigations of the solvent extraction kinetics and mechanism as they require only small amounts of solutions, they are cheap, reliable, and easy to operate. Many tests can be run automatically in one day, which makes it a very attractive technique for monitoring the solvent extractions processes remotely.

Fuel Cycle Research and Development Separations

SEPARATION PROCESS THERMODYNAMICS AND KINETICS: DEVELOPMENT OF MICROFLUIDIC DEVICES FOR SOLVENT EXTRACTION STUDIES AND RADIOANALYTICAL APPLICATIONS

INTRODUCTION

Metal solvent extraction has been a subject of wide fundamental, analytical and technological investigations; however, the kinetics of the solvent extraction has been left without sufficient attention. Using a kinetics study, the extraction mechanism can be revealed allowing modifications and better control of the process parameters. For example, recent studies at ANL [1] showed that due to slow extraction kinetics, TALSPEAK process performs the An/Ln separation effectively only if centrifugal contactors with high mixing intensity are used. The same separation goals may not be achievable if the process is conducted using mixer-settlers. Despite the many years since the discovery of TALSPEAK, its extraction mechanism is not clear and kinetic studies could be particularly beneficial for this problem.

The reasons for the lack of the extraction kinetics studies could be a) the interdisciplinary character of the subject which deals with closely related engineering and chemical concepts and b) the difficulty to find suitable criteria to compare the mass-transfer studies with physico-chemical, reaction mechanism investigations. The current experimental methods to study liquid-liquid systems from the separation science point of view were developed more than 30 years ago and they do not utilize the state-of-the-art techniques. All the reported techniques suffer from one or a few experimental drawbacks [2]. For example, Highly Stirred Tanks require relatively large amounts of phases and the interface surface area is difficult to calculate. Constant Interfacial Area Stirred Cells are limited to studying fast and medium fast reactions because the surface area available for the extraction is quite limited.

For investigating solvent extraction mechanism and the kinetics, we propose to develop microfluidic devices in collaboration with the Ismagilov group at the University of Chicago. The Ismagilov group has previously demonstrated a microfluidic platform for performing kinetic measurements with better than millisecond resolution [3]. They have measured both fast ($k = 1000 \text{ s}^{-1}$) and slow ($k=1 \text{ s}^{-1}$) kinetics in this microfluidic platform by taking advantage of rapid on-chip dilution, multiple time range access, and explicit treatment of mixing for improving time resolution of the system. They have a great deal of experience in this arena across a wide range of model systems [4,5,6].

These microfluidic systems function by defining a microfluidic channel through which both an aqueous and an organic phase flow (Fig). By carefully defining the channel geometry and surface chemistry, droplets of either phase can be generated. Performing kinetic experiments in droplets has as primary benefits rapid mixing and minimal dispersion, which allows for high resolution, and therefore high speed, measurements.

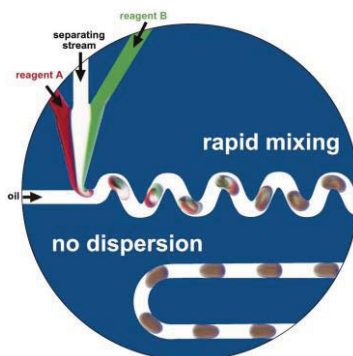


Figure 1 - Aqueous droplets of 250 pL formed in a microfluidic channel in a continuous flow of a water-immiscible fluid act as microreactors that mix the reagents rapidly and transport them with no dispersion. These droplets may also be used to control chemical reaction networks on millisecond time scale.

Such microfluidic devices have not been used for the separation science investigations previously. The validation of the developed devices will be done as follows. Solvent extraction studies will be conducted via mixing an organic phase containing the extractant and a metal-containing aqueous phase. One of the great advantages of these devices is the ability to monitor the reactions via optical and/or fluorescence microphotographs; each position in space in the microreactor always corresponds to the exact same time in the reaction. The appropriate metal-specific fluorescent dyes will be added to the phases and the kinetics of the chemical reaction either in the aqueous phase, the interface phenomena or the organic phase reactions will be observed. The images are collected using a microscope and a high speed digital camera and then image-processing software is applied to obtain intensity profiles of the channels. Knowing the surface area of the droplets, their velocity, the channel cross-section and other

parameters, one could calculate the rates of the observed reactions. Varying the flow rates and the concentrations of the reagents will allow investigating the separation processes with unprecedented precision, reliability, and an ease of operation. Besides microscopy, the monitoring of the reaction progress can be conducted using several other well-established techniques developed by the Ismagilov group. The organic and the aqueous streams from the device can be also separated and analyzed independently using conventional analytical methods such as ICP-MS, gamma counting, pH and conductivity measurements and so on.

Besides the research of the solvent extraction mechanism, microfluidic devices can be designed for analytical purposes when generating a small volume of the sample is vital for the analysis. For example, if a spent fuel solution needs to be analyzed for the actinide content, the uranium can be extracted with TBP/dodecane stream remotely using this device, while Pu, reduced to Pu(+3), resides in the aqueous phase. A small-size sample can be generated and submitted for ICP-MS analysis and so on.

EXPERIMENTAL RESULTS

GLASS-BASED MICROFLUIDIC DEVICES

The device allows for the determination of solvent extraction kinetics by creating a segmented organic/aqueous flow, rapidly mixing the contents, and siphoning off a small fraction of the aqueous phase away from the oil phase, thus preventing further extraction from the siphoned aqueous fraction. To our knowledge, this is the first microfluidic system that provides kinetic data for two-phase extraction, instead of simply providing an endpoint measurement. The device is an all glass microfluidic chip, fabricated using photolithography, wet chemical etching, and glass bonding in a class 100 cleanroom at the University of Chicago. The system utilizes the inherent differences in wettability of glass between the aqueous and organic phases in order to isolate the aqueous phase for off-chip analysis by standardized, validated methods. A series of small capillary channels (20 μm depth x 90 μm width in the current design) stem from the side of a larger channel (170 μm x 600 μm) that contains both the oil and the aqueous phases. All channels are hydrophilic. In order to prevent droplets of the organic phase from being pushed into the small capillary channel, the device is designed carefully so that the pressure in the larger channel is less than the capillary pressure, or the pressure due to surface tension of the oil on the hydrophilic glass.

A schematic of the device, and a photograph to show the scale, are shown in Fig 2:

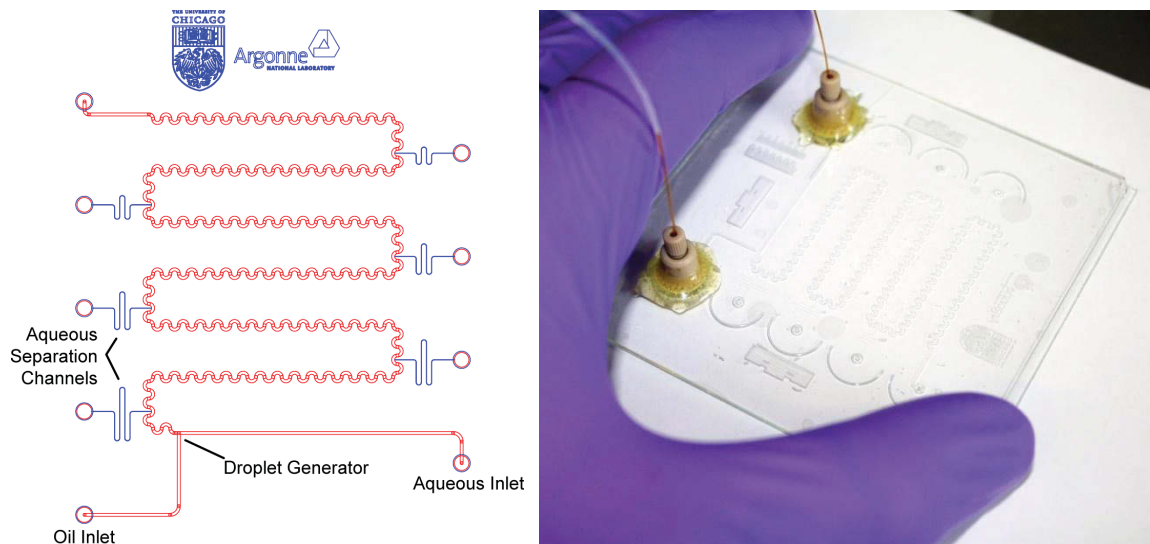


Figure 2. The schematic and a photograph of the glass microfluidic device.

Preliminary tests have been performed to verify the uniform segmentation of the flow, the speed of mixing, and the basic functioning of the device in terms of siphoning off the aqueous phase. In Figure 3 droplets are generated, and extraction of a model compound appears uniform. The image shows the extraction of orange-colored (0.1 M FeSCN^{2+} in $1.2 \text{ M Lactate} + 40 \text{ mM DTPA}$) into (1 M HDEHP in Dodecane), which is visible as the aqueous segments grow paler in color as the flow from left to right across the image.

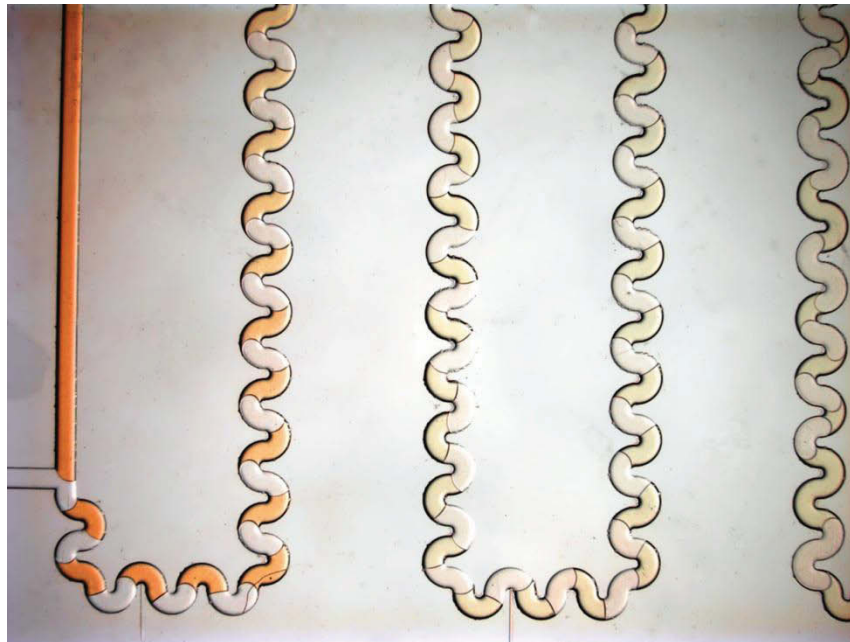


Figure 3. Extraction of FeSCN^{2+} (orange) from aqueous phase into 1 M HDEHP/ddn

Current development involves tuning the device dimensions and flow parameters to account for minor differences in the actual device operation and the physical model we utilized to design it. For example, Figures 4 and 5 below show differing siphon behaviors at two points along the device. In Fig 4, both oil

and water enter the capillary, indicating the actual pressure in the main channel is unexpectedly higher than the capillary pressure. In Fig 5, which is a capillary from farther downstream in the device, only a single (aqueous) phase is visible, indicating the capillary pressure is within operating conditions. Iteratively refining the physical model and adjusting the device dimensions will allow us to shift the pressures towards the appropriate points. We anticipate that we can obtain single-phase aqueous flow in the capillaries within a few generations of the model and device, at which point the device will be ready to use for collection of kinetic data. The images of the capillaries below are shown with enhanced contrast to show the two capillary behaviors currently observed: segmented organic / aqueous flow (undesired) on Figure 4 and single phase aqueous flow (desired) on Figure 5.

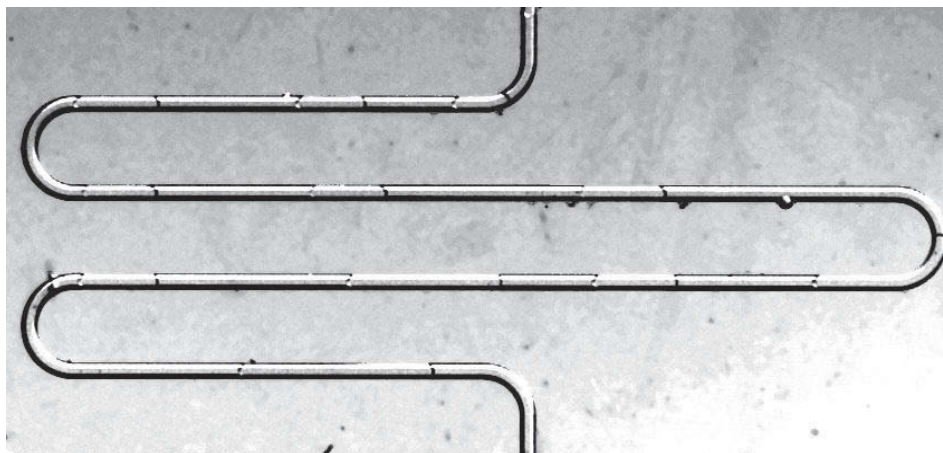


Figure 4 (see text for details)

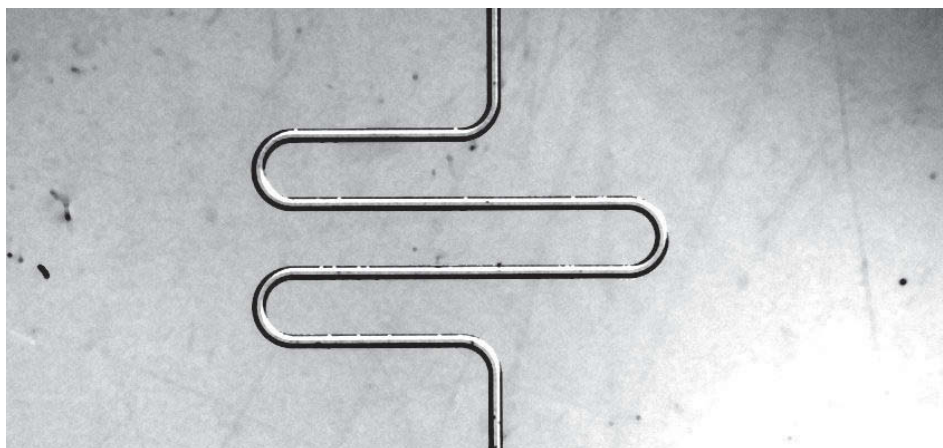


Figure 5 (see text for details)

TEFLON-BASED MICROFLUIDIC DEVICES

Our initial design envisioned lithographically patterned, bonded glass microfluidic devices to meet the stated requirements. These glass devices performed well during testing with model solutions that were not capable of extraction, specifically dodecane and an aqueous FeSCN^{2+} solution. However, it was found that droplet formation and siphoning were not reproducible during testing with the TALSPEAK solutions for radioanalytical applications. There were apparently two primary reasons for this result. First, these solutions are complex, with multiple surface-active compounds time-varying contact angles in

which the wetting phase easily switches from organic to aqueous, which complicates design of these devices. Second, these solutions are quite “dirty”, and produced a residue in the glass channels which may be either a polymerized substance or a difficult to remove double emulsion. Unless a method is found to remove this residue, the glass devices cannot be re-used and must be disposable; this is problematic because they require several days of manually intensive work to produce. It may still be possible to overcome these problems in a glass device. Furthermore, the glass devices will likely work just fine if neutral extractants (e.g. TBP, CMPO) and mineral acids (e.g. HNO₃) are used as the organic and aqueous media, respectively. Neutral extractants and nitric acid do not contain surfactants that likely caused the problem in the TALSPEAK system. Further testing of the glass devices is planned.

However, to move the project forward, we have rethought the device design, and have currently settled on a device fabricated from commercially available chromatography components, with the capillary network composed of Teflon tubing, with one piece of tubing specially modified using laser micromachining.

The Teflon tubing based device has two primary advantages over a glass microfluidic device:

1) Increased contact angle differential: the contact angle for the oil / aqueous phases in teflon vs. glass increases from 95/85 to 155/25, significantly increasing the range of permissible side channel geometries and main channel pressures that will still allow 100% separation of aqueous from organic phases. It contains a single phase (oil) always wetting, unlike in the glass devices where the wetting phase was sometimes one phase, sometimes the other.

2) Ease of cleaning: the system can be completely disassembled and washed. Thorough washing of a glass microfluidic device is not always possible, as particles will tend to accumulate in channel corners. Particle accumulation alters the pressure drops in the system and can change the surface chemistry and contact angles of the glass, which usually renders the siphoning capillaries ineffective. Teflon tubing, with its round cross-section and smooth interior surface, is easier to wash thoroughly.

3) Rapidity of fabrication: the tubing-based device requires one laser-machining step and can be assembled from otherwise off-the-shelf components in a few hours. The glass etched and bonded devices require approximately two days of fabrication time.

The primary disadvantages of a Teflon tubing based device vs. a glass microfluidic device are:

1) Slightly increased dead volume.

2) Decreased integration, which may make the device appear more complex to an end-user.

Overview of Teflon Tubing Based System Components

An overview of the tubing based system is shown in Figure 6:

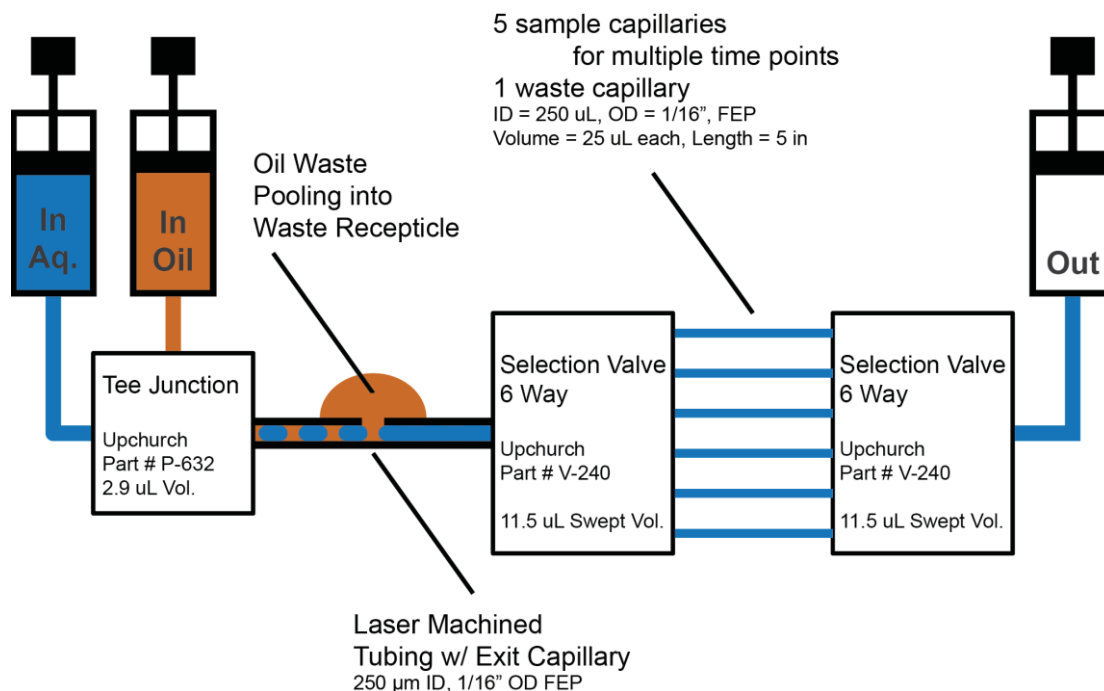


Figure 6. Schematic of the Teflon device

This system utilizes entirely off the shelf components. One piece of capillary tubing must be laser machined using an excimer laser system operating at 193 nm. Such a system is currently available in the Ismagilov Laboratory. Further, Resonetics LLC, a New Hampshire based laser micromachining supplier who designed the laser micromachining workstation currently deployed in the Ismagilov Laboratory, is capable of contract machining of tubing on a piece by piece basis.

One of the great advantages of microfluidic systems is the low dead volume and waste inherent in such highly integrated systems. The tubing based system shown above does have slightly higher waste volumes, calculated below:

Sample tubing: $25 \mu\text{L} * 5 = 125 \mu\text{L}$

Swept volume waste: $2.9 \mu\text{L} + 11.5 \mu\text{L} * 2 = 25.9 \mu\text{L}$ per time point = $129.5 \mu\text{L}$ total

Estimated waste volume while awaiting equilibration: $25 \mu\text{L}$

An additional $25 \mu\text{L}$ will be required in the connection tubing between the syringes and the tee junction, though this can be recovered and reused;

Siphoning System in Teflon Tubing Based Device

A microphotograph of the “Exit” capillary hole, through which the oil phase is preferentially siphoned away from the aqueous phase, is shown below, along with a cross-section of the feature.

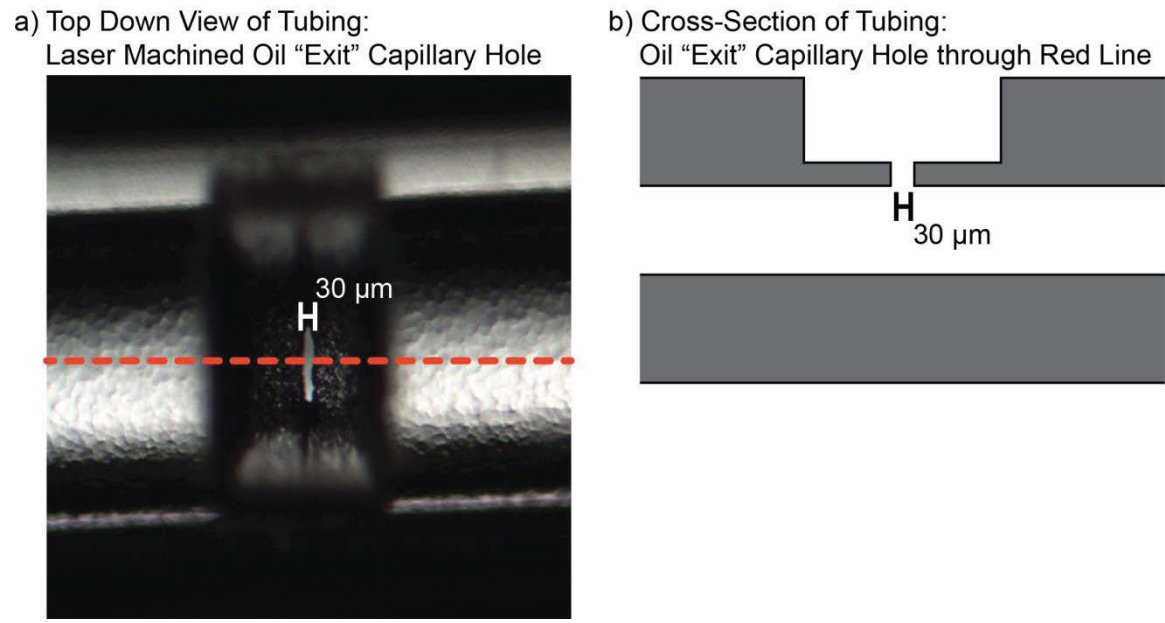


Figure 7. Tubing Arrangement for siphoning of the organic phase.

While it proved difficult to repeatedly utilize solutions other than our model system in the glass microfluidic device, Figure 8 shows the solutions of interest for radioanalytical applications with a small amount of iron thiocyanate dye added to ease visualization of the aqueous phase. The colorless phase is 1M HDEHP in dodecane, and the yellow-tinted phase is an aqueous solution of 45 mM DPTA, 1.35 M lactic acid, and 0.05 M FeSCN²⁺.

As can be seen in Figure 8, the Teflon tubing device behaves in a manner consistent with that necessary to achieve the project goals: at specific flow rates shown below, the complete siphoning of the oil phase is accomplished, leaving only the aqueous phase in the main channel for off-line analysis.

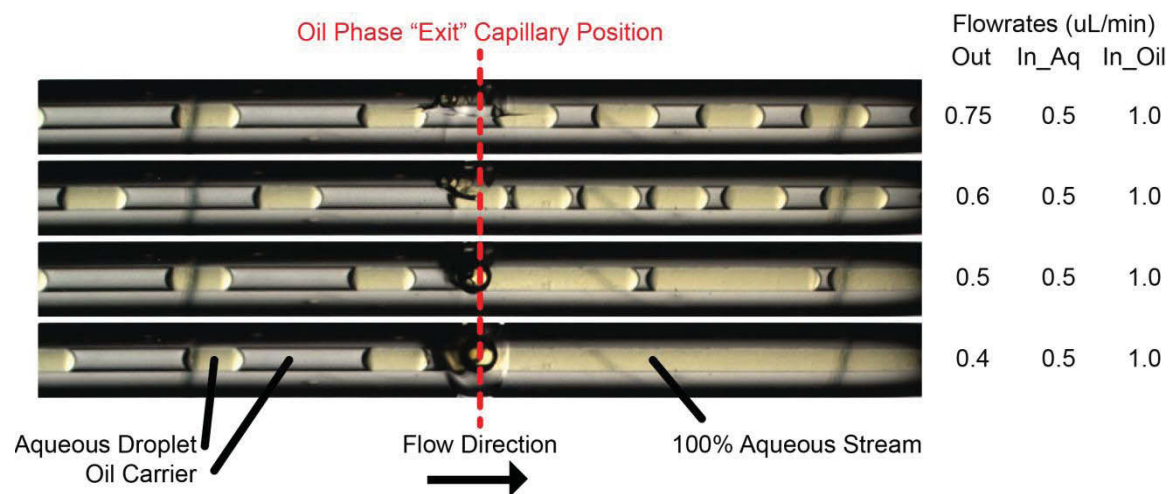


Figure 8. Exit of the organic phase at different flowrates

In summary, we propose to use the Teflon tubing device to measure the kinetics of metal extraction from solutions of interest, such as in the TALSPEAK process. This device should enable more rapid advancement of this project than the glass devices previously described. The kinetic datapoints will be collected by changing the flowrates of both phases, while the surface area remains constant. The devices will be tested on the TALSPEAK system in the nearest future.

Collaborators and Participants:

Kevin Paul Nichols (Ph.D.), Rebecca Pompano (Ph.D.) and Prof. Rustem Ismagilov; all University of Chicago.

4. Reference:

- 1 *A.V. Gelis, G. F. Vandegrift, A. Bakel, D. L. Bowers, A. S. Hebden, C. Pereira, and M. Regalbuto Extraction behaviour of actinides and lanthanides in TALSPEAK, TRUEX and NPEX processes of UREX+, Radiochim. Acta 97, 4, 2009*
- 2 *P.R Danesi, R. Chiarizia The kinetics of metal solvent EXTRACTION, CRC critical reviews in Analytical chemistry, crc Press, 1980.*
- 3 *Helen Song and Rustem F. Ismagilov, "Millisecond Kinetics on a Microfluidic Chip Using Nanoliters of Reagents", J. Am. Chem. Soc. 2003 125: 14613-14619*
- 4 *Bo Zheng, Joshua D. Tice, L. Spencer Roach, and Rustem F. Ismagilov, "A Droplet-Based, Composite PDMS/Glass Capillary Microfluidic System for Evaluating Protein Crystallization Conditions by Microbatch and Vapor-Diffusion Methods with On-Chip X-Ray Diffraction", Angew. Chem. Int. Edit. 2004 43: 2508-2511*
- 5 *Michelle R. Bringer, Cory J. Gerdtz, Helen Song, Joshua D. Tice, and Rustem F. Ismagilov, "Microfluidic Systems for Chemical Kinetics that Rely on Chaotic Mixing in Droplets", Philos. T. Roy. Soc. A 2004 362: 1087-1104*
- 6 *Helen Song, Delai L. Chen, and Rustem F. Ismagilov, "Reactions in droplets in microfluidic channels", Angew. Chem. Int. Ed. 2006 45:7336-7356.*

Appendix C

Electrochemical Investigation of TALSPEAK Processes

Dr. Nicholas Bridges

Savannah River National Laboratory

SUMMARY

As a viable scheme to separate the trivalent actinide from the lanthanides, the TALSPEAK process (trivalent actinide-lanthanide separation by phosphorous-reagent extraction from aqueous complexes) is the most promising, yet still not fully understood. Recently, Oak Ridge National Laboratory conducted a complete separation of used fuel, ending with a demonstration of the TALSPEAK process. In the demonstration of the TALSPEAK processes, carryover of uranium, neptunium and plutonium was observed. To better understand the effects of plutonium and compare it to americium, electroanalytical techniques were used to probe the aqueous phase of the TALSPEAK process.

The investigation of aqueous-based solution with either diethylenetriamine-N,N,N',N'',N'''-pentaacetic acid (DTPA) or lactic acid with plutonium and americium revealed interesting results related to the chemical stability of the organic ligands, and the coordination environment associated with the actinide. Lactic acid is prone to oxidation yielding pyruvic acid, a carboxylic acid α -ketone. The oxidation of Pu^{IV} to $\text{Pu}^{\text{V}}\text{O}_2^+$ causes a change in the coordination environment with DTPA, which is electrochemical reversible. Additional evidence indicates the possibility of multiple coordination environments of Pu^{IV} -DTPA complexes, and further studies will be needed to better understand and confirm these findings.

Fuel Cycle Research and Development Separations

ELECTROCHEMICAL INVESTIGATION OF TALSPEAK PROCESSES

INTRODUCTION

The separation of transplutonium elements from the lanthanide series may be accomplished with the trivalent actinide-lanthanide separations by phosphorous-reagent extraction from aqueous complexes (TALSPEAK) processes.^{1,2} Separation of transplutonium elements from lanthanides is complicated by the similar liquid extraction behavior of americium, curium, and the lanthanides, due to their similar size and predominance in the +3 oxidation state. For the TALSPEAK process to become viable on a production scale, a stronger fundamental understanding of all the components and how they interact is needed.

From the pilot scale demonstration of the TALSPEAK process in a closed fuel cycle conducted at Oak Ridge National Laboratory (ORNL) an unexpected result was reported. In the TALSPEAK processes run at ORNL, significant amounts of early actinides (i.e., uranium, 4.3g; neptunium, 0.23g; and plutonium, 0.91g) were present in the feed stream, and thus were carried through the TALSPEAK process.³

In this study, electrochemical techniques were used to investigate the aqueous phases of diethylenetriamine-N,N,N',N'',N'''-pentaacetic acid (DTPA) or lactic acid with plutonium and americium, to better understand the TALSPEAK process's interactions with the actinides.

SIGNIFICANCE

Today, most of the chemistry studies performed on the TALSPEAK processes has centered on the separation of transplutonium and lanthanide elements. The most recent pilot process of a closed fuel cycle was successful, but not without some interesting results. One of these results was the presence of uranium, neptunium, and plutonium carryover into the TALSPEAK processes. Though neptunium and plutonium followed the americium and curium, their interactions with the TALSPEAK processes is not as well studied as americium. Uranium was extracted by the organic phase and was unable to be stripped due to the strong interactions of uranium with bis-(2-ethylhexyl) phosphoric acid. It is well known that the transplutonium elements are not easily oxidized/reduced, and thus are found in solution in the +3 oxidation state. However, plutonium has a wide range of oxidation potentials in aqueous systems. Understanding the chemical and oxidation stabilities of the TALSPEAK process will benefit further research and operation of the TALSPEAK process.

APPROACH

The TALSPEAK process is based on a selective extraction of lanthanides, into an organic feed of bis-(2-ethylhexyl) phosphoric acid in a hydrocarbon diluent from an aqueous solution of normally 1.0 M lactic acid and 50 mM DPTA at a pH window of ~3.5-4.0. Though these concentrations and pH are not finalized, the majority of the research community uses these values. This work will use the most common operating conditions but with each component separated to understand the individual effects on the overall system.

Each of the organic species present can have an effect on the oxidation state and chemical potentials of the early actinides, especially for plutonium and neptunium, due to the strength of interactions with actinides. The high oxidation potential of americium, curium, and the lanthanides will prevent their oxidation to higher states under the investigated conditions. To probe the interaction of americium and plutonium with select ligands, cyclic voltammetry (CV) was used, as it has the ability to measure the oxidation/reduction potentials and kinetics of the inner coordination sphere interactions upon reduction/oxidation of Am or Pu.

Stock solution of 25, 50, and 75 mM DTPA were prepared in 1.0 M NaClO₄ (a non-complexing electrolyte needed for the electrochemical experiments) and pH adjusted to 3.50, 3.75, and 4.00 ± 0.02 using either NaOH or HClO₄. Lactic acid solutions of 0.85, 1.00, and 1.15 M, were prepared in 1.0 M NaClO₄ and pH adjusted to 3.50, 3.75, and 4.00 ± 0.02. Electrochemical experiments were performed in a once-through air radiological glovebox with an electrical feed-through connecting a BASi Epsilon potentiostat to the electrochemical cell located within the glovebox. The electrodes were electrochemically polished before use in ~1M HNO₃. Three milliliters of the aqueous solution were placed in a disposable polyethylene-terephthalate cup followed by the platinum working and auxiliary electrodes and a silver/silver chloride reference electrode. Background CV scans were collected at 1000, 500, 250, 100, 50, 25, and 10 mV/s. An aliquot of 60 µL of 404 mM ²³⁹⁻²⁴¹Pu or 163 mM ²⁴¹Am solution was added and pH adjusted to within ± 0.05 pH units of the desired pH with either NaOH or HClO₄. (Plutonium stock was purified twice using an anion exchange column before being concentrated and anion exchanged to the perchlorate salt.) The plutonium's isotopic distribution is weapons grade, >94% ²³⁹Pu, and had less than 600 ppm americium contaminant. Americium stock was removed from aged reactor-grade plutonium, originally ~9% ²⁴¹Pu, with two elutions through an anion exchange column to remove the bulk plutonium. The eluant was then purified on an Eichrom DGA

column to remove iron, as ferrous sulfamate that was added to ensure all plutonium was present in the +4 oxidation state before the anion exchange column, and any other impurities that were present in the americium stock. The final product has less than detectable amounts of plutonium by gamma analysis. The americium stock was transferred to the perchlorate salt.

SUMMARY OF RESULTS

The methodical approach to investigating the individual effects of DTPA and lactic acid on two different actinides with significantly different oxidation potentials has provided insight into the systems control of the oxidation state. The results will be discussed for each actinide.

DTPA:

Due to the multiple carboxylic acid and amine functionalities present in DTPA, the cyclic voltammetry revealed an electrochemical potential within the range of investigation, limited by the electrochemical window of water. The time span of these electrochemical experiments is not fast enough to prevent intra-molecule proton exchange. This prevents multiple DTPA oxidation/reductions from being observed. If the proton exchanges were slow enough, then one should expect the separation of multiple oxidation/reduction peaks to be present due to the slight chemical differences between the carboxylate or amine functional groups being oxidized or reduced. Figure 1 illustrates the speciation of 50 mM DTPA in 1.0 M ionic strength at 25 °C. As the pH increases from 3.50 to 4.00, there is significant increase in the $[DTPA-H_2]^{3-}$ concentration while decreasing the $[DTPA-H_3]^{2-}$ and $[DTPA-H_4]^-$ concentrations which is observed in the shift of the oxidation potential to lower potential (more stable) and a less electrochemically reversible reaction, Figure 2.

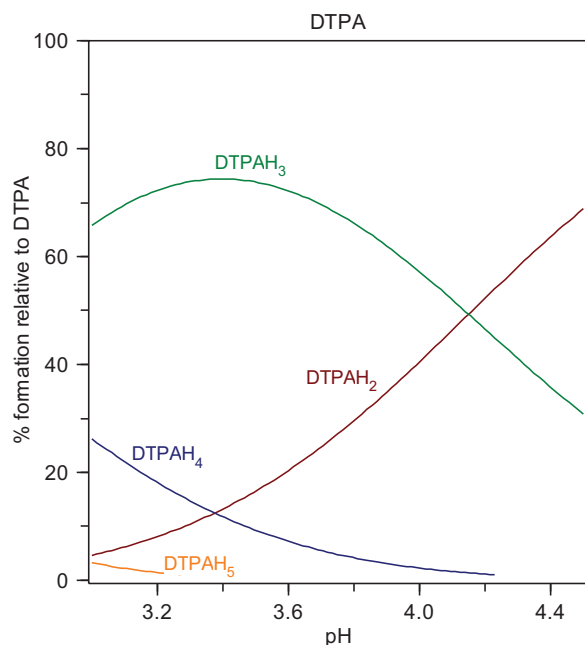


Figure 1 Speciation of DTPA in investigated pH range. Carboxylic acid pK_A (DTPA) = 1.68, 2.1, 2.6, 4.15, 8.2, 9.9.

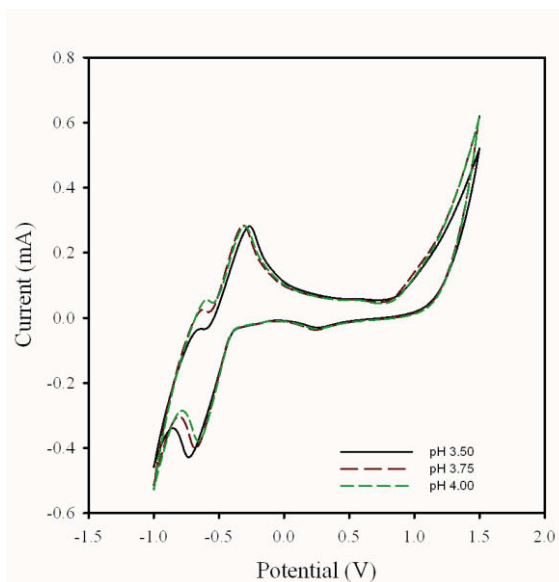


Figure 2 Cyclic voltammetry of 50mM DTPA in 1.0 M $NaClO_4$ at variable pH. 1000 mV/s, Pt//Pt//Ag/AgCl.

Chemical oxidation of carboxylic acids is mechanistically preferred when the carboxylic acid functionality is protonated as seen in the Hunsdiecker and Kochi oxidation reactions of carboxylic acids.⁴ The by-product is usually carbon dioxide which is released from the system during oxidation. This general trend is also observed in the small shift to lower potential (increased stability to oxidation) as the pH increases (increasing the amount of $[\text{DTPA-H}_2]^{3-}$ while decreasing the $[\text{DTPA-H}_3]^{2-}$ and $[\text{DTPA-H}_4]^{-}$).

Lactic Acid:

Over the tested pH range, the system crosses over the pK_A (3.86) of lactic acid, thus the presence of both the protonated lactic acid and unprotonated lactate is expected. The ratio of lactic acid to lactate will change significantly over the studied range, at lower pHs favoring the lactic acid and higher pH the lactate. In Figure 3, it was observed that lactic acid is less stable to oxidation than DTPA. Oxidation of lactic acid does not occur by loss of the carboxylic acid, but instead by oxidation of the α -hydroxyl group to a ketone. Oxidation of the α -hydroxyl group will form the α -ketone, pyruvic acid,³ though the formation of pyruvic acid has not been confirmed through other techniques at this time. The pK_A of pyruvic acid is 2.45, thus at pH 3.5 – 4.0 it would predominately be present as pyruvate, in the pH range investigated here. The significant shift in the oxidation potential of lactic acid/lactate at elevated pH could be due to changes in the distribution of the electronic density of molecule as it changes from lactic acid to lactate.

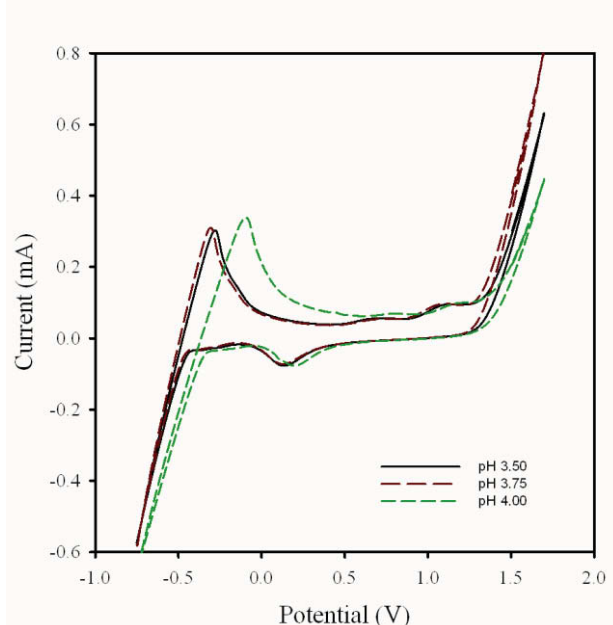


Figure 3 Cyclic voltammery of 1.0 M lactic acid in 1.0 M NaClO_4 at variable pH. 1000 mV/s, Pt//Pt//Ag/AgCl.

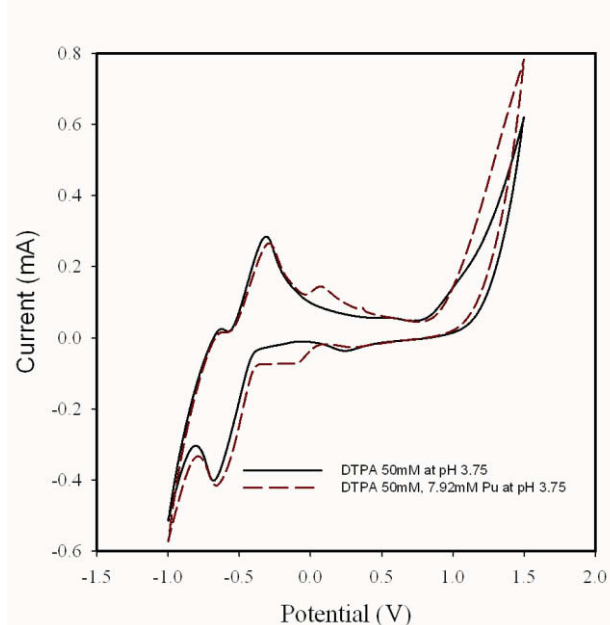


Figure 4 Cyclic voltammery of 50 mM DTPA in 1.0 M NaClO_4 at 3.75 with 7.92 mM Pu. 1000 mV/s, Pt//Pt//Ag/AgCl.

Plutonium systems:

In the presence of plutonium, the DTPA system has two significant changes in comparison to systems that contain simply DTPA. The most significant is the introduction of a plutonium redox potential, Figure 4. Due to the relatively long time-span of the electrochemical experiments in comparison to the time span of proton exchange, it is impossible to establish the species of free DTPA or complexed. The $\text{Pu}^{\text{IV/V}}$ is quasi-reversible but becomes more

electrochemically reversible as the scan rate decreases (from a ΔE of 0.219 V at 1000 mV/s to ΔE of 0.121 V at 10 mV/s), Figure 5. In Table 1 evidence of multiple coordination environments around the Pu is observed by the change in the electrochemical reversibility of the Pu^{IV/V}. At lower ratios of DTPA:Pu, the system is more reversible and at the lowest scan rate, 10 mV/s, approaches the ideal reversibility of 58 mV, the difference in the anodic and cathodic potentials. (In a diffusion controlled system, the ratio of oxidized to reduced species in the boundary layer is on the order of 1/10. Using Nernst's equation, Equation 1, the ΔE for a completely reversible, one electron transfer reaction becomes 58 mV. A reversible electrochemical reaction means that the coordination environment of the metal center is the same before and after the oxidation and reduction reaction.⁶) At high ratios of DTPA:Pu, the system become more irreversible possibly due to a more complex coordination environment associated with multiple DTPA per plutonium atom, Figure 6.

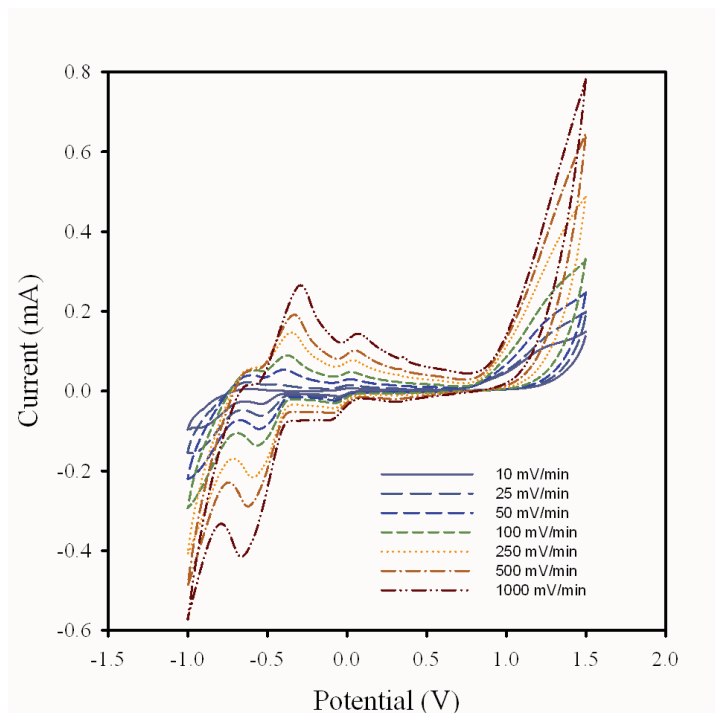
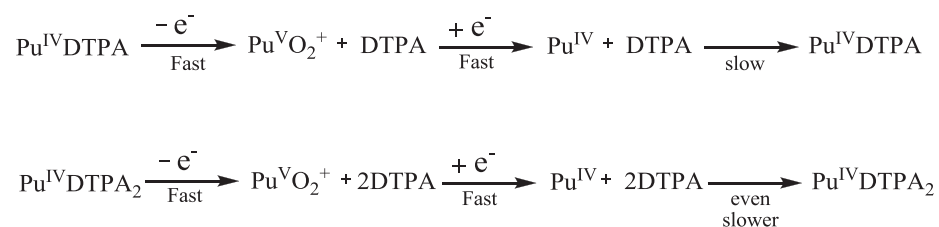


Figure 5 Cyclic voltametry of 50 mM DTPA in 1.0 M NaClO₄ with variable scan rates with 7.92 mM Pu. pH 3.75, Pt//Pt//Ag/AgCl.

Table 1 Compare reversibility as a function of variable concentrations of DTPA to Pu at pH 3.75.

Scan Rate (mV/s)	25 mM DTPA (DTPA:Pu, 3.2:1)			50 mM DTPA (DTPA:Pu, 6.3:1)			75 mM DTPA (DTPA:Pu, 9.5:1)		
	Reduction (mV)	Oxidation (mV)	ΔE (mV)	Reduction (mV)	Oxidation (mV)	ΔE (mV)	Reduction (mV)	Oxidation (mV)	ΔE (mV)
10	37	-46	83	45	-76	121	52	-76	126
25	39	-82	121	51	-76	127	43	-81	124
50	36	-85	121	58	-86	144	51	-81	132
100	55	-100	155	55	-85	140	55	-78	133
250	61	-103	164	68	-103	171	69	-73	142
500	78	-103	181	86	-119	205	97	-96	193
1000	87	-117	204	102	-117	219	124	-117	241

**Figure 6** Possible reaction mechanism of for the change in reversibility of Pu^{IV/V} in various concentrations of DTPA.

$$E = E^o - \frac{RT}{\eta F} \ln \frac{\alpha_{\text{Red}}}{\alpha_{\text{Ox}}}$$

Equation 1: Nernst Equation. E – chemical potential; E^o – standard cell potential; R – universal gas constant; T – temperature; η - number of electrons transferred; F – Faraday's constant; α - chemical activity of reduced/oxidized species

The oxidation peak associated with the free DTPA ligand has a small decrease in the amplitude after the addition of plutonium. This decrease is due to complexation with plutonium, thus decreasing the amount of free DTPA. Due to the excess of DTPA and pH control, there is no change in the oxidation potential or reversibility, Figure 4

In the lactic acid system, the Pu^{IV}/Pu^V couple is at a higher potential than the Pu-DTPA, Figure 7. This is due to the difference in the coordination environment around the plutonium in the lactic system, compared to the DTPA system. (Through rearrangement of the Nernst equation, a relationship between the equilibrium constant and the chemical potentials can be established. The larger equilibrium constant of DTPA is observed in the lower chemical potential of the Pu^{IV/V} couple, Equations 2-4.)⁷ As the pH changes (effecting the ratio of lactic acid to lactate) a significant change in redox window of lactic acid is seen. At pH 4.00, the significant shift to higher potentials for electrochemical window of lactic acid is shifted back to what is observed in lower pH systems. It is unclear if plutonium causes this shift, and further experiments are needed to confirm this phenomenon and better understand these results.

$$E = E^o - \frac{RT}{nF} \ln(\alpha_i) = \left(\frac{\partial G}{\partial \eta} \right)_{p,T,\eta}$$

Equation 2: Simplified Nernst equation and related to Gibbs free energy; constant pressure, temperature and number of electrons transferred.

$$-nFE^o = \Delta G_{p,T}$$

Equation 3: Gibbs free energy relation; constant pressure, and temperature.

$$\Delta G_{p,T} = -RT \ln K$$

Equation 4: Gibbs free energy; K – equilibrium constant.

Americium:

At the time this report was prepared the americium-lactic acid system has not been completed and thus is not reported in the year review. The experiments are on-going and the results will be included in next year's progress report.

The electrochemistry of americium is much simpler than plutonium, due to americium only forming higher oxidation states under strong oxidizing conditions in the presence of a strong complexing agent (e.g., carbonate media) or in the solid state. The DTPA-Am system has a significant decrease in the current associated with the oxidation of DTPA, Figure 8. The decrease in the redox potential of the DTPA is greater in the americium system, than the plutonium system. In the TALSPEAK processes, americium is more selectively bound to the DTPA than the lanthanides, which are extracted into the organic phase by bis-(2-ethylhexyl) phosphoric acid. As the americium is loaded into the aqueous phase as the perchlorate salt, with a perchlorate electrolyte, the DTPA-Am complexation will dominate, thus decreasing the 'free' DTPA.

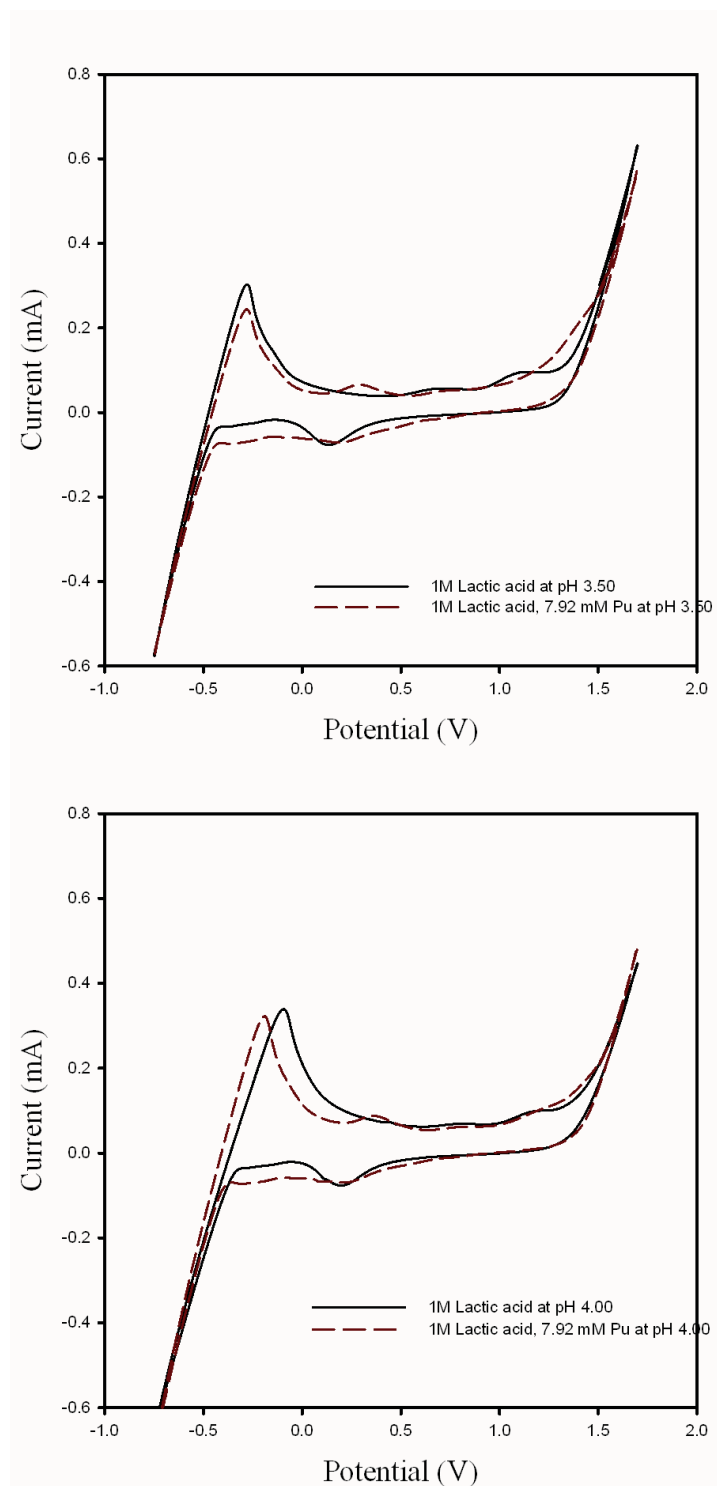


Figure 7 Cyclic voltammetry of 1.0 M lactic acid in 1.0 M NaClO₄ at variable pH with 7.92 mM Pu. A) pH = 3.50; B) pH = 4.00. 1000 mV/s, Pt//Pt//Ag/AgCl.

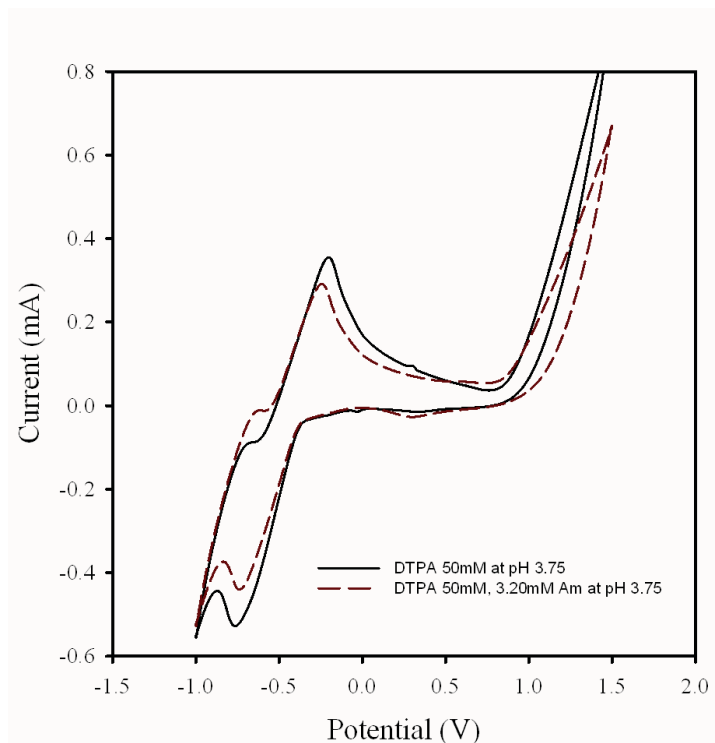


Figure 8 Cyclic voltammetry of 50 mM DTPA in 1.0 M NaClO₄ at variable pH with 3.20 mM Am. 1000 mV/s, Pt//Pt//Ag/AgCl.

CONCLUSIONS

Through electrochemical means, an initial investigation into the aqueous phase of the TALSPEAK processes has revealed some interesting results. Though on the surface, DTPA and lactic acid seem similar with both having carboxylic acid functionalities, their interactions with plutonium and americium are very different. The addition of the α -hydroxyl in lactic acid allows for the oxidation to an α -ketone, yielding pyruvic acid. The impact of pyruvic acid to the TALSPEAK process is unknown, and the formation of the acid depends on the presence of a strong oxidizer. The fact that it is a carboxylic acid α -ketone will cause a different coordination environment with a metal center than lactic acid.

Lactic acid has the lowest oxidation potential in the tested systems, and could be the balancing half-cell reaction if a reduction of an elevated oxidation state occurs, such as Pu^{V/VI} to Pu^{IV}. As the stronger chelator, DTPA did offer some insight into the coordination of plutonium. Though not completely understood yet, there is evidence of different coordination environments as the ratio of plutonium:DTPA changed, as seen in Table 1. Further investigation into the phenomena will be conducted next fiscal year.

REFERENCES

- 1 Weaver, B.; Kappelmann, F. A. *Talspeak: A new method of separating americium and curium from the lanthanides by extraction from an aqueous solution of an aminopolyacetic acid complex with a monoacidic organophosphate or phosphonate*; ORNL-3559; Union Carbide Corporation, Orak Ridges, TN, August 1964.

- 2 Nilsson, M.; Nash, K. L. *Solvent Extr. Ion Exch.* **2007**, *25*, 665.
- 3 Felker, L.K.; Bnder, J. L.; Benker, D. E.; Collins, E.D.; Bailey, P. D.; Bell, G. L.; Judin, R. T.; Spencer, B.B.; Del Cul, G. D.; Vedder, R. J.; Wlaker, E. A.; Voit, S. L. “Results, Evaluation, and Lessons Learned from the Coupled End-to-End Project Campaign 1 Using Dresden BWR Used Fuel,” ORNL/GNEP/LTR-2008-044, June 2008.
- 4 Boger, Dale L. *Modern Organic Synthesis*, TSRI Press: La Jolla, CA, 1999; p. 319.
- 5 Izawa, S.; Tsukamoto, A. *J. Electrochem.* **1951**, *11*, 187.
- 6 Heineman, W.R.; Kissinger, P. T. *Laboratory Techniques in Electroanalytical Chemistry*, Kissinger, P. T.; Heineman, W. R., Ed., Marcel Dekker, Inc. New York, 2007, pp. 57-196.
- 7 Scholz, F. *Electroanalytical Methods: Guide to Experiments and Application*, Scholtz, F., Ed. Springer, New York, 2007, pp. 11-31.

INDICATORS OF PROJECT QUALITY AND PRODUCTIVITY

N. J. Bridges, A. E. Visser “Understanding the Electrochemical Behavior of Actinides to aid in their Separation,” Presented by A. E. Visser, before 240th ACS National Meeting (2010), Boston, MA, Abstract I&EC-51.

Appendix D

Distribution of Actinides between the Aqueous and Organic Phases in the TALSPEAK Process

Dr. Tracy Rudisill

Savannah River National Laboratory

SUMMARY

One objective of the US Department of Energy's Office of Nuclear Energy (DOE-NE) is the development of sustainable nuclear fuel cycles which improve uranium resource utilization, maximize energy generation, minimize waste generation, improve safety, and complement institutional measures limiting proliferation risks.[1] Activities in progress which support this objective include the development of advanced separation technologies to recover the actinides from used nuclear fuels. With the increased interest in the development of technology to allow closure of the nuclear fuel cycle, the TALSPEAK process is being considered for the separation of Am and Cm from the lanthanide fission products in a next generation reprocessing plant. However, at this time, the level of understanding associated with the chemistry and the control of the process variables is not acceptable for deployment of the process on an industrial scale. To address this issue, DOE-NE is supporting basic scientific studies focused on the TALSPEAK process through its Fuel Cycle Research and Development (R&D) program. One aspect of these studies is an experimental program at the Savannah River National Laboratory (SRNL) in which temperature-dependent distribution coefficients for the extraction of actinide elements in the TALSPEAK process were measured. The data were subsequently used to calculate conditional enthalpies and entropies of extraction by van't Hoff analysis to better understand the thermodynamic driving forces for the TALSPEAK process.

In the SRNL studies, the distribution of Pu(III) in the TALSPEAK process was of particular interest. A small amount of Pu(III) would be present in the feed due to process losses and valence adjustment in prior recovery operations. Actinide elements such as Np and Pu have multiple stable oxidation states in aqueous solutions; therefore the oxidation state for these elements must be controlled in the TALSPEAK process, as the extraction chemistry is dependent upon the actinide's valence. Since our plans included the measurement of Pu(III) distribution coefficients using a Np(V) solution containing small amounts of ^{238}Pu , it was necessary to demonstrate that the desired oxidation states of Np and Pu are produced and could be stabilized in a buffered lactate solution containing diethylenetriaminepentaacetic (DTPA). The stability of Np(V) and Pu(III) in lactic acid/DTPA solutions was evaluated by ultraviolet-visible (UV-vis) spectroscopy. To perform the evaluation, Np and Pu were added to solutions containing either hydroxylamine nitrate (HAN) or ferrous sulfamate (FS) as the reductant and nominally 1.5 M lactic acid/0.05 M DTPA. The pH of the solution was subsequently adjusted to nominally 2.8 as would be performed in the TALSPEAK process.

In the valence adjustment study, we found that it was necessary to reduce Pu to Pu(III) prior to combining with the lactic acid and DTPA. The Pu reduction was performed using either HAN or FS. When FS was used, Np was reduced to Np(IV). The spectroscopic studies showed that Np(V) and Pu(III) are not stable in lactic acid/DTPA solutions. The stability of Np(IV)- and Pu(IV)-DTPA complexes are much greater than the stability of the Np(V)- and Pu(III)-DTPA complexes, and as a result, Np is slowly reduced to Np(IV) and Pu is slowly oxidized to Pu(IV) due to the reduced activity of the more stable complexes. When Np(V) was added to a solution containing a 1.5 M lactic acid/ammonium lactate buffer and 0.05 M DTPA, approximately 50% of the Np was reduced to Np(IV) in the first day. The fraction of Np(V) in the solution continued to diminish with time and was essentially reduced to Np(IV) after one week. When Pu(III) was added to a lactic acid/DTPA solution of the same composition, the spectrum recorded following at least two days after preparation of the solution continued to show some sign of Pu(III). The Pu(III) was completely oxidized to Pu(IV) after 3-4 days.

The UV-vis spectroscopy demonstrated that Np(V) and Pu(III) were the predominate valences in the lactic acid/DTPA solution for the better part of a day following solution preparation. Based on these results, we chose to initially add HAN to the actinide tracer solution prepared for the distribution coefficient measurements (to produce Pu(III)) prior to combining with lactic acid and DTPA. The distribution coefficient measurements were expected to be complete in 2-3 h; therefore, Np(V) and Pu(III) valences would predominate in the solution during this time. Prior to adding the HAN to the actinide

tracers, we added sufficient Am(III) activity to allow the measurement of distribution coefficients during the extraction experiments. Protactinium (V) distribution coefficients were also measured using the activity which was in secular equilibrium with the ²³⁷Np. The actinide distribution coefficients were measured at pH 2.8 and 3.5 and covered a range of temperatures from nominally 20 to 60 °C.

The actinide distribution coefficient measurements showed that Np(V) and Pa(V) were more strongly extracted into the bis-(2-ethylhexyl)phosphoric acid (HDEHP) solvent than Pu(III) and Am(III). The increased extraction of the Np and Pa was due to the increased stability of the Pu(III)- and Am(III)-DTPA complexes compared to the stability of the Np(V)- and Pa(V)-DTPA complexes. The stability of the 3+ complexes prevents the extraction of the Pu and Am into the solvent to a greater extent. The actinide distribution coefficients decreased with decreasing pH and increasing temperature. The decrease in the distribution coefficients with pH is due to the protonation of the HDEHP solvent which reduces the number of available complexation (i.e., ion exchange) sites. The decrease in the distribution coefficients with temperature is due to the exothermic nature of the extraction process. At pH 3.5, the conditional enthalpies of extraction were approximately -10 kJ/mole for Pu(III) and Am(III), -40 kJ/mol for Np(V), and -48 kJ/mol for Pa(V). The entropies of extraction were negative which results in more positive free energies of extraction as the temperature increases. The uncertainties associated with the majority of the conditional thermodynamic properties varied between approximately 10 and 50%. The nonlinearity in the data was attributed to changes in the enthalpy of extraction over the temperature range; although, the instability of Np(V) and Pu(III) likely contributed to the variance.

Fuel Cycle Research and Development Separations

DISTRIBUTION OF ACTINIDES BETWEEN THE AQUEOUS AND ORGANIC PHASES IN THE TALSPEAK PROCESS

INTRODUCTION

Background

Used reactor fuels are currently reprocessed in multiple countries using the PUREX process [2] to recover the U and Pu for future use. However, the small amounts of Np, Am, and Cm (minor actinides) produced during fuel irradiation are not recovered and are currently discarded with the fission products as high level waste. If desired, Np produced in irradiated fuels can be recovered by making slight modifications to the PUREX process to control the Np valence and extraction into the tributyl phosphate solvent.[3,4] For complete closure of the nuclear fuel cycle, the Am and Cm isotopes produced during fuel irradiation must also be recovered. The isolation and purification of the minor actinides would allow additional energy production following fabrication of fuels or targets for advanced reactors using these materials. The elimination of essentially all of the actinide materials from the high level waste generated during fuel reprocessing would also improve the performance of a geologic repository by removing radiotoxic, long-lived transuranic isotopes from the waste and reducing the heat generated by radioactive decay.

An efficient separation process which recovers Am and Cm during the reprocessing of nuclear reactor fuels has not been demonstrated on an industrial scale. One of the issues with the recovery of Am and Cm in a single process is the similarity of the chemistry of the lanthanide fission products. Solvent extraction processes have been developed which allow the separation of Am, Cm, and the lanthanide elements from other waste components using extractants such as malonamids (the DIAMEX process) or phosphine oxides (the TRUEX or TRPO processes).[5] The subsequent separation of the Am and Cm from the lanthanide fission products requires a separate process. In 1964, Weaver and Kappelmann [6] reported the development of a process to separate transplutonium elements from the lanthanides by preferentially extracting the lanthanides from an aqueous solution containing lactic acid and the sodium salt of DTPA into HDEHP. The process was titled TALSPEAK for Trivalent Actinide Lanthanide Separation with Phosphorous-reagent Extraction from Aqueous Komplexes. Under optimal conditions for the TALSPEAK process, Nd was the least extractable of the lanthanides and Cf was the most extractable of the transplutonium elements. The process can also be performed in a reverse mode in which the transplutonium elements and the lanthanide fission products are extracted into the HDEHP solvent and the transplutonium elements are stripped using a solution containing lactic acid and DTPA.

With the increased interest in the development of technology to allow closure of the nuclear fuel cycle, the TALSPEAK process is being considered for the separation of Am and Cm from the lanthanide fission products in a next generation reprocessing plant. However, at this time, the level of understanding associated with the chemistry and the control of the process variables is not acceptable for deployment of the process on an industrial scale. One issue of concern is the lack of understanding associated with the thermodynamic and kinetic driving forces of the separation. To address this issue, DOE-NE is supporting basic scientific studies focused on the TALSPEAK process through its Fuel Cycle R&D program. One element of these studies is the measurement of actinide distribution coefficients in the TALSPEAK process as a function of temperature so thermodynamic properties can be calculated using the van't Hoff equation.[7] Of particular concern, is the distribution of Pu(III) between the aqueous and organic phases. A small amount of Pu and Np would be present in the feed to the TALSPEAK process due to process losses from prior recovery operations. If the TRUEX process is used to separate the lanthanide fission products and the transuranic elements from other fission products, the Pu and Np oxidation states must be adjusted to Pu(III) and Np(IV) for efficient extraction.[8] The actinide elements are stripped from the TRUEX solvent using a buffered lactate solution containing DTPA at approximately pH 5. Following the adjustment of the solution pH (to 2.8), the product from the TRUEX process becomes the feed to the TALSPEAK process.[9]

Objectives

To better understand the thermodynamic driving force for the extraction of transuranic elements in the TALSPEAK process, a series of experiments was performed to measure the distribution of Np(V), Pu(III), Am(III), and Pa(V) between the aqueous and organic phases as a function of temperature. The van't Hoff equation was then used to calculate the conditional enthalpies and entropies of extraction. The thermodynamic properties were considered conditional, since they were based on the variation of distribution coefficients as a function of temperature, rather than the extraction equilibrium constant.[5] Prior to measuring the actinide distribution coefficients it was necessary to demonstrate the stability of Pu(III) in a buffered lactate solution containing DTPA. Plutonium (III) was prepared using both HAN and FS as reductants. Ultraviolet-visible spectroscopy was used to determine the valence of both Np and Pu over time during the stability experiments. The experimental methods used to perform the distribution coefficient measurements and stability experiments and a discussion of the results are presented in the following sections.

EXPERIMENTAL

Valence Adjustment Study

Actinide elements such as Np and Pu have multiple stable oxidation states in aqueous solutions; therefore, the oxidation state for these elements must be controlled in the TALSPEAK process, as the extraction chemistry is dependent upon the actinide's valence. Since our plans included the measurement of Pu(III) distribution coefficients using a Np(V) solution containing small amounts of ²³⁸Pu, it was necessary to demonstrate that the desired oxidation states of Np and Pu are produced and could be stabilized in a buffered lactate solution containing DTPA. To accomplish this task, Np and Pu were added to solutions containing either HAN or FS as the reductant and nominally 1.5 M lactic acid/0.05 M DTPA. The pH of the solution was subsequently adjusted to nominally 2.8, consistent with the TALSPEAK process operating conditions. The predominant valences of the actinides were then determined by UV-vis spectroscopy. The details of the experimental procedures are discussed in the following sections.

Nuclear Materials

The Np and Pu solutions used for the valence adjustment studies were initially purified by anion exchange. A characterization of each solution is provided in Table 1.

Table 1 Actinide stock solution concentrations

Element	Concentration		HNO ₃ (M)
	g/L	dpm/mL	
Np	32.0	5.00E+07	1.5
Pu	45.3	6.65E+09	1.0

The Np and Pu solutions used in the study were more concentrated than the solution used to measure distribution coefficients to ensure that the spectrometer sensitivity was sufficient to obtain representative spectra. The Pu used in the study was weapons grade (i.e., nominally 94% ²³⁹Pu and 6% ²⁴⁰Pu).

Solution Preparation

Since UV-vis spectra of Np and Pu in buffered lactate solutions containing DTPA were not available as references, the spectrum of four actinide-containing solutions were initially recorded with increasing complexity to understand the changes in the spectra due to each component. The four solutions included: (1) 0.1 M HNO₃, (2) 1.5 M lactic acid, (3) 1.5 lactic acid/0.05 M DTPA, and (4) 1.5 M lactic acid/0.05 M DTPA/0.1 M HAN. Four solution containing nominally 3 g/L Np and four solutions containing nominally 4 g/L Pu were prepared. The Np and Pu concentrations were held constant by adding 1 mL of the actinide-containing solution to 10 mL of the four solutions.

Since we planned to adjust the pH of the actinide solutions to 2.8 prior to measuring the distribution coefficients, the pH of the buffered solutions was also adjusted to the same value using 3.9 M NH₄OH prior to recording the spectrum. To estimate the volume of NH₄OH required to adjust the pH to the desired value following the addition of 1 mL of the Np solution (containing 1.5 M HNO₃) or 1 mL of the Pu solution (containing 1.0 M HNO₃), a 1.5 M lactic acid solution containing 0.05 M DTPA was prepared to simulate the adjustments. When 1 mL additions of 1.5 and 1.0 M HNO₃ were added to 10 mL aliquots of a 1.5 M lactic acid/0.05 M DTPA solution, the volumes of 3.9 M NH₄OH required to adjust the pH back to 2.8 were 0.2 and 0.3 mL, respectively. Dilution of the lactic acid and DTPA due to the addition of the actinide solution and the subsequent adjustment of the pH were taken into account during the preparation of the solutions. The preparation of the four solutions including the pH adjustments is described in Appendix DA.

The UV-vis spectra were recorded using a Zeiss diode array spectrometer controlled by a Windows NT-based computer. We used a 1 cm path length cuvette holder with 1 cm disposable cuvettes inside a radiological glovebox. The cuvette holder was connected to the spectrometer using fiber optic cables. A detailed list of the spectrometer components is provided below.

- Spectrometer: Diode array spectrometer based on the Zeiss MCS module (190-1024 nm range, approximately 0.8 nm/pixel); interfaced to computer through Hamamatsu C4070 driver/amplifier board; power supply – Condor D.C. Power Supplies model MTL-5W-A.
- Fiber optic cable: Ceramoptec or Polymicro, IR grade, 400 micron low-OH core with SMA fittings on each end.
- Computer: Texas Micro industrial PC, IPC-6806P.233MHz , Windows NT.
- Data acquisition card: National Instruments AT-AI-16XE-10 Multiple I/O Board (16-bit resolution, 16 analog and 8 digital inputs).
- Light source: Ocean Optics Tungsten Halogen Lamp Housing, LS-1.
- Variable attenuator: Oz Optics Part # BB-200-55-300 600-SP to adjust light levels.
- Cuvette block: SRNL fabricated plexiglass cuvette holders with two lenses.

During the preparation of solution (4), the required volume of HAN was combined with the lactic acid/DTPA solution prior to the addition of the Np or Pu. When the Pu was added to the solution, we did not observe a color change. Solutions containing Pu(III) are blue when viewed by reflected light.[10] When the spectra of the solutions which contained Pu in 1.5 M lactic acid/0.05 M DTPA and 1.5 M lactic acid/0.05 M DTPA/0.1 M HAN were compared, they were essentially the same which indicated that the HAN had not reduced the Pu (see the Results and Discussion section for more detail). Since the Pu was not reduced by HAN in the buffered lactate solution containing DTPA, we chose to prepare solutions in which either HAN or FS was added to the Np and Pu solutions prior to combining with the lactic acid and DTPA. Both HAN and FS will reduce Pu(IV) to Pu(III) and FS will reduce Np(V) to Np(IV).[11-12] The four solutions prepared for study included: (1a) Np + HAN added to 1.5 M lactic acid/0.05 M DTPA, (2a) Pu + HAN added to 1.5 M lactic acid/0.05M DTPA, (3a) Np + FS added to 1.5 M lactic acid/0.05 M DTPA, and (4a) Pu + FS added to 1.5 M lactic acid/0.05 M DTPA. Prior to recording the UV-vis spectrum of each solution, the pH was adjusted to nominally 2.8. The preparation of the four solutions including the pH adjustments is described in Appendix DA. The spectrum of the four solutions was recorded within 90 min of preparation and after nominally 1, 2, 3, 7, and 8 days.

Distribution Coefficient Measurements

The distribution of Np(V), Pu(III), Am(III), and Pa(V) between 1 M HDEHP (in dodecane) and an aqueous phase containing a 1.5 M lactic acid/ammonium lactate buffer and 0.05 M DTPA was measured as a function of temperature. The experimental methods used to perform this work are described below.

Nuclear Materials

The actinide distribution coefficient measurements were made using dilute solutions of the nuclear materials. To achieve good counting statistics, the desired range of activities for the Np, Pu, and Am were 10^5 - 10^6 , 10^8 - 10^9 , and 10^4 - 10^5 dpm/mL, respectively. The Pa distribution coefficients were measured using the activity (10^5 - 10^6 dpm/mL) which was in secular equilibrium with the ^{237}Np . The Np used for the measurements was initially purified by anion exchange. Since the Np was previously used to produce ^{238}Pu oxide, the alpha activity of the solution was primarily from this isotope. The characterization of the Np/Pu stock solution used to provide the actinide tracers is shown in Table 2.

Table 2 Np/Pu stock solution concentrations

Np		Pu		Nitric Acid
(M)	(dpm/mL)	(M)	(dpm/mL)	(M)
1.35×10^{-1}	4.98×10^7	4.88×10^{-4}	4.42×10^9	1.5

The ^{241}Am used for the distribution coefficient measurements was initially purified using a chromatographic resin. A stock solution was prepared by diluting a 0.1 mL aliquot of a 1.30×10^9 dpm/mL solution with 10 mL of 0.1 M HNO_3 . The final Am and HNO_3 concentrations were 1.28×10^7 dpm/mL (6.98×10^{-6} M) and 0.11 M, respectively.

Solvent Preparation

The organic phase used for all distribution coefficient measurements was 1 M HDEHP. The desired concentration of HDEHP was prepared by diluting with dodecane. To prepare the solution, the target mass of HDEHP was transferred to a volumetric flask which was diluted to volume with dodecane.

Extraction Experiments

The aqueous phase used for the actinide distribution coefficient measurements was prepared by initially adding a 250 μL aliquot of the Am stock solution to 1 mL of the Np/Pu stock solution. A 100 μL aliquot of 1.77 M HAN was subsequently added to reduce the Pu to Pu(III). The combined solutions were swirled to ensure that the HAN and the actinides were well mixed. No color change was observed due to the dilute concentration of the Pu. The actinide solution was then combined with an 11.4 mL aliquot of a 1.9 M lactic acid/0.06 M DTPA solution. All transfers of solution were performed using calibrated pipettes with precisions and accuracies typically $< 1\%$. Following the combination of the solutions, the pH was adjusted to either 2.8 or 3.5 by the addition of 3.9 M NH_4OH . The pH of the solution was measured using an Accumet[®] Basic AB15 pH meter which was calibrated using pH 1, 3, and 6 buffer solutions. The preparation of the lactic acid/DTPA solution and calculations summarizing the final composition of the aqueous phase used in the TALSPEAK extractions are presented in Appendix DA.

The actinide distribution coefficients were measured as a function of pH and temperature. The temperatures were selected to bracket the potential operating range. The conditions for each series of measurements are summarized in Table 3.

Table 3 Conditions for distribution coefficient measurements

Experiment	pH	Temperature ($^{\circ}\text{C}$)
TAL-1	2.8	20.0
TAL-2	2.8	59.0
TAL-3	3.5	20.0
TAL-4	3.5	59.5
TAL-5	3.5	40.0

To perform a series of extractions, 2 mL of the aqueous phase (containing the actinide elements in the 1.5 M lactic acid/ammonium lactate buffer and 0.05 M DTPA) were combined with 2 mL of the HDEHP solvent. This organic to aqueous ratio was used for all extractions. Two milliliters of the aqueous and organic phases were added to six, 15 mL centrifuge tubes. The centrifuge tubes were capped and placed in a Eppendorf Thermomixer R, heating/cooling block to maintain the extraction temperature at the

desired value. The heating/cooling block also provided agitation at a maximum of 750 RPM. Once the extraction temperature was reached, the aqueous and organic phases were mixed for 1 h. Since the intensity of the mixing was not sufficient to form an emulsion at the conical end of the centrifuge tubes, each tube was removed from heating/cooling block and manually mixed by shaking the tube. Manual mixing was performed at 15, 30, and 45 min into the extraction period. Once the extraction period was complete, the phases were allowed to equilibrate at temperature for 1 h. At the beginning of the equilibration period, a cap was removed from one of the centrifuge tubes to allow insertion of a calibrated thermometer. The extraction temperatures given in Table 3 were recorded using this thermometer.

To ensure that the extraction temperature remained constant during sampling, a procedure was developed to remove a sample of the organic and aqueous phases using a disposable transfer pipette without removing the centrifuge tube from the heating/cooling block. The procedure involved premarking pipettes at a height which placed the tip at the middle of the organic phase when the mark was even with the top of the centrifuge tube. This procedure allowed the removal of an approximate 1 mL sample of the organic phase. To remove a sample of the aqueous phase, the pipette bulb was compressed and inserted into the centrifuge tube until the tip touched the bottom. An approximate 1 mL sample of the aqueous phase was then removed from the bottom of the tube by releasing the bulb. The Np, Pu, Am, and Pa activities in the aqueous and organic phases were measured by Gamma Pulse Height Analysis (GPHA).

RESULTS AND DISCUSSION

Valence Adjustment Study

The UV-vis spectra of Np and Pu in buffered lactate solutions containing DTPA were not available as references; therefore, spectra were initially recorded with increasing solution complexity to understand the changes in the spectra due to the addition of the lactate buffer, DTPA, and HAN. Reference spectra for Np and Pu are provided in Figures 1 and 2, respectively. The solutions for which spectra were recorded included each actinide in solutions containing (1) 0.1 M HNO₃, (2) 1.5 M lactic acid, (3) 1.5 M lactic acid/0.05 M DTPA, and (4) 1.5 M lactic acid/0.05 M DTPA/0.1 M HAN.

Np Reference Spectra

The UV-vis spectrum of Np in 0.1 M HNO₃ (Figure 1) showed that essentially all of the Np was initially present as Np(V). Characteristic Np(V) peaks at 615 and 980 nm were observed. The UV-vis spectra of Np(IV) solutions also have a characteristic peak between 960 and 980 nm (depending upon the HNO₃ concentration); however, we attribute the peak in this spectrum to Np(V) due to the absence of the characteristic Np(IV) peak at 700 nm. When the 0.1 M HNO₃ was replaced with 1.5 M lactic acid/ammonium lactate, the spectrum changed very little. Neptunium (V) was still the predominate valence state. However, when 0.05 M DTPA was added to the solution, the spectrum became much more complicated. A new peak appeared at 741 nm which was attributed to Np(IV). The reduction of Np(V) to Np(IV) was due to the stability of Np(IV)-DTPA complex compared to the Np(V)-DTPA complex. It should be noted that the spectrum of this solution was recorded approximately 18 h following preparation. The equilibrium constants (log K) for the Np(IV)-DTPA complex in 0.5 and 1.0 M NaClO₄ are 29.29 ± 0.02 and 30.33 ± 0.12 , respectively.[13] The equilibrium constant for the Np(V)-DTPA complex is not reported; however, equilibrium constants for both the Np(IV) and Np(V)-ethylenediaminetetraacetic acid (EDTA) complexes are available. The (log K) value for the Np(IV) complex in 1.0 M NaClO₄ is 24.55 ± 0.03 while the (log K) value for the Np(V) complex in 0.1 M NaClO₄ is only 7.33 ± 0.06 . [13] By analogy, the equilibrium constant for the Np(IV)-DTPA complex should also be orders of magnitude larger than the equilibrium constant for the Np(V)-DTPA complex. The stability of the Np(IV) complex lowers the Np(IV) activity which results in the slow

reduction of Np(V) to the more stable valence state. When HAN was added to the lactic acid/ammonium lactate solution containing DTPA, the Np spectrum did not change. Hydroxylamine nitrate does not reduce Np(V) to Np(IV); [11] therefore, this result is expected.

Pu Reference Spectra

The UV-vis spectrum of Pu in 0.1 M HNO₃ (Figure 2) showed the presence of Pu(III) (peaks at 560, 600, and 663 nm), Pu(IV) (peak at 470 nm), and Pu(VI) (peak at 831 nm); although, the predominate valence was Pu(IV). When the 0.1 M HNO₃ was replaced with 1.5 M lactic acid/ammonium lactate, the Pu(IV) peak became larger and shifted to 485 nm. The peaks which were attributed to Pu(III) and Pu(VI) disappeared and a number of other peaks appeared. When 0.05 M DTPA was added to the buffered lactate solution, the spectrum became even more complicated. The Pu(IV) peak shifted to 498 nm and additional peaks appeared in the spectrum. The addition of HAN to the Pu-containing solution had essentially no effect on the spectrum. This supports our visual observation (based on the solution color not changing to blue) that HAN will not reduce Pu(IV) to Pu(III) in a solution containing a lactic acid buffer and DTPA.

Reduction of Actinide Valences Using HAN and FS

Since Pu was not reduced by HAN in the buffered lactate solution containing DTPA, solutions were prepared in which HAN and FS were added to aliquots of the Np and Pu stock solutions prior to combining with the lactic acid and DTPA. When either the HAN or FS was added to the Pu solution, the solution turned blue which is indicative of Pu(III).[10] After combination with the lactic acid and DTPA, the UV-vis spectrum for each solution was recorded. The Np (see Figures 3 and 4) and Pu (see Figures 5 and 6) spectra are compared with the spectra of the Np and Pu solutions (from Figures 1 and 2, respectively) in which HAN was added to the buffered DTPA solution prior to adding the actinides.

Figure 3 compares the UV-vis spectra of Np solutions in which HAN was added to an aliquot of the Np stock solution prior to combining with the lactic acid and DTPA and in which Np was added to a solution containing lactic acid, DTPA, and HAN. The spectrum of the solution in which HAN was added to an aliquot of the Np stock solution showed that the predominate Np valence was still Np(V). The spectrum of this solution was recorded within approximately 90 min of the solution preparation. Therefore, only a small portion of the Np(V) had been reduced to Np(IV) due to the stability of the Np(IV)-DTPA complex. The spectrum of the solution in which Np was added to a solution containing lactic acid, DTPA, and HAN was recorded approximately 18 h following preparation and showed the presence of significantly more Np(IV). The HAN had no effect on the distribution of Np valences. Figure 4 compares the UV-vis spectra of Np solutions in which FS was added to an aliquot of the Np stock solution prior to combining with the lactic acid and DTPA and in which Np was added to a solution containing lactic acid, DTPA, and HAN. The spectrum of the solution containing FS shows that the predominate Np valence was Np(IV). Ferrous sulfamate has historically been used to reduce Np(V) to Np(IV) in both ion exchange and solvent extraction applications.[12] The two Np spectra presented on Figure 4 are very similar, except for the very broad peak centered at approximately 425 nm which can be attributed to Fe(II) in the solution.

Figure 5 compares the UV-vis spectra of Pu solutions in which HAN was added to an aliquot of the Pu stock solution prior to combining with the lactic acid and DTPA and in which Pu was added to a solution containing lactic acid, DTPA, and HAN. When the Pu and HAN were combined, the solution turned blue which indicated the presence of Pu(III). The spectrum of the solution which resulted from combining the Pu(III) with lactic acid and DTPA is significantly different from the spectrum of the solution in which the Pu was added to a solution containing lactic acid, DTPA, and HAN. The three peaks between 550 and 630 nm were attributed to the presence of Pu(III) in the lactic acid/DTPA solution. It should be noted that the spectrum of this solution was recorded within approximately 90 min of preparation. Although, the spectrum was recorded shortly after the solution was prepared, a small peak at 498 nm was observed which can be attributed to Pu(IV). Figure 6 compares the UV-vis spectra of Pu

solutions in which FS and HAN were added to aliquots of the Pu stock solution prior to combining with lactic acid and DTPA with the spectrum of the solution in which Pu was simultaneously combined with lactic acid, DTPA, and HAN. As with HAN, it is well documented that FS will reduce Pu to Pu(III).[12] The spectra of the solutions which resulted from the addition of Pu(III) to the lactic acid and DTPA are very similar. Both spectra contain the three peaks between 550 and 630 nm which were attributed to Pu(III). Even though the spectrum of the solution in which the Pu was reduced using FS was recorded within approximately 90 min of preparation, a small peak attributed to Pu(IV) at 498 nm was observed.

Stability of Np(V) and Pu(III) in Lactic Acid/DTPA Solutions

The reference spectra of Np in lactic acid/DTPA solutions demonstrated that Np(V) is not stable in this matrix. The Np(V) was slowly reduced to Np(IV) due to the stability of the Np(IV)-DTPA complex. In addition, the spectra of the Pu(III) solutions generated by the addition of either HAN or FS showed the presence of Pu(IV). Therefore, the spectra of the Np and Pu solutions in which HAN and FS were added prior to combining with lactic acid and DTPA were recorded as a function of time to assess the stability of the Pu(III) and Np(V). The UV-vis spectra of the four solutions were recorded following nominally 1, 2, 3, 7, and 8 days after preparation. The Np spectra of the solutions containing HAN and FS are shown on Figures 7 and 8, respectively, and the Pu spectra of solutions containing HAN and FS are shown on Figures 9 and 10, respectively.

The stability of Np(V) in the lactic acid/DTPA/HAN solution is illustrated in Figure 7. The baseline UV-vis spectrum was recorded within about 90 min of the solution preparation. At this time, Np(V) was the predominate valence in the solution. Within approximately 24 h, a significant amount (perhaps as high as 50%) of the Np(V) was reduced to Np(IV). The fraction of Np(V) in the solution continued to diminish with time and was essentially reduced to Np(IV) after one week. Figure 8 illustrates the stability of Np(IV) in the buffered lactate/DTPA solution following reduction of the Np with FS. The baseline spectrum was recorded within approximately 90 min of the solution preparation and showed complete reduction of the Np. Over the next 8 days, the spectrum was essentially unchanged. Neptunium (IV) is the preferred valence in this system due to the stability of the Np(IV)-DTPA complex.

The stability of Pu(III) in the lactic acid/DTPA/HAN solution is illustrated in Figure 9. The baseline UV-vis spectrum was recorded within approximately 90 min of the solution preparation. Plutonium (III) is clearly the predominate valence at this time; although, the small peak at 498 nm indicates the presence of Pu(IV). After one day, the three peaks between 550 and 630 nm (which are attributed to Pu(III)) are still visible, but significantly reduced. After 2 days, the peaks have nearly disappeared and after 3 days, the peaks are gone. Therefore, it appears that the Pu(III) completely oxidized to Pu(IV) after approximately 3 days. The oxidation of Pu(III) to Pu(IV) can be explained in an analogous manner to the reduction of Np(V) to Np(IV). The Pu(IV)-DTPA complex is much more stable than the Pu(III)-DTPA complex. The equilibrium constants (log K) for the Pu(IV)- and Pu(III)-DTPA complexes are 35.39 and 29.5, respectively.[14] The stability of the Pu(IV) complex lowers the Pu(IV) activity which results in the slow oxidation of the Pu(III) to the more stable valence state. The stability of Pu(III) in the lactic acid DTPA solution which was produced by reduction with FS is shown on Figure 10. The baseline UV-vis spectrum was recorded within approximately 90 min of the solution preparation. The peaks between 550 and 630 nm show that Pu(III) was initially the predominate valence in the solution; although a small Pu(IV) peak was also observed at 498 nm. The Pu(III) peaks are not as well defined as in the spectrum of the solution in which the Pu was reduced with HAN. However, the spectra recorded following one, two, and three days after preparation of the solution continued to show some sign of Pu(III) in solution. The Pu(III) was completely oxidized to Pu(IV) after approximately 4 days.

The two series of UV-vis spectra demonstrated that Np(V) and Pu(III) are the predominate valences in the lactic acid/DTPA solution for the better part of a day following solution preparation. It is necessary to reduce the Pu to Pu(III) using either HAN or FS prior to combining with the lactic acid and DTPA. Stable Np(IV) is produced in the lactic acid/DTPA solution if FS is initially combined with the Np prior

to solution preparation. Based on these results, we chose to initially add HAN to the actinide tracer solution prepared for the distribution coefficient measurements (to produce Pu(III)) prior to combining with lactic acid and DTPA. The distribution coefficient measurements were expected to be complete in 2-3 h; therefore, Np(V) and Pu(III) valences would predominate during this time.

Distribution Coefficient Measurements

Actinide Distribution Coefficients

The activity of Np, Pu, Am, and Pa measured in the aqueous and organic phases during the TALSPEAK extraction experiments are shown in Appendix DC. The activity of the actinides in each phase were subsequently used to calculate distribution coefficients ($D_{An,o/a}$) which are defined as the ratio of the activity of the actinide element in the organic phase ($A_{An,o}$) to the activity of the actinide element in the aqueous phase ($A_{An,a}$) (equation 1).

$$D_{An,o/a} = \frac{A_{An,o}}{A_{An,a}} \quad (1)$$

The actinide distribution coefficients for the triplicate extraction experiments at each pH for the range of temperatures are given in Appendix DC. The average values are shown in Tables 4 and 5 for the experiments performed at pH 2.8 and 3.5, respectively.

Table 4 Actinide Distribution Coefficients in the TALSPEAK Process at pH 2.8

Element	20.0 °C		59.0 °C	
	$D_{An, o/a}$	Relative Std. Dev. (%)	$D_{An, o/a}$	Relative Std. Dev. (%)
Np	9.17E+00	3.6	1.15E+00	20.7
Pu	7.56E-02	10.8	4.06E-02	20.7
Am	3.89E+00	5.4	1.48E+00	4.7
Pa	1.14E+02	15.3	2.95E+01	25.3

Table 5 Actinide Distribution Coefficients in the TALSPEAK Process at pH 3.5

Element	20.0 °C		40.0 °C		59.5 °C	
	$D_{An, o/a}$	Relative Std. Dev. (%)	$D_{An, o/a}$	Relative Std. Dev. (%)	$D_{An, o/a}$	Relative Std. Dev. (%)
Np	4.45E+00	7.9	2.36E+00	10.2	5.88E-01	7.8
Pu	4.58E-02	8.7	5.06E-02	5.0	2.56E-02	29.4
Am	5.19E-01	3.6	4.49E-01	9.0	2.98E-01	3.8
Pa	9.45E+01	5.4	5.68E+01	33.9	7.62E+00	13.5

The initial TALSPEAK extraction experiments were performed at pH 2.8 based on the acidity of the feed solution used by Argonne National Laboratory in a series of process demonstrations.[9] However, the measured distribution coefficients for Am were greater than unity indicating that a majority of the Am was extracted into the solvent. Since the objective of the TALSPEAK process is to retain the Am in the aqueous phase, we chose to increase the pH (to 3.5) in subsequent extractions to lower the distribution

coefficients. Inspection of the Am data in Tables 4 and 5 shows an approximate order of magnitude decrease in the distribution coefficients when the pH was increased from 2.8 to 3.5. However, the distribution coefficient measured for Am at 20 °C (and pH 3.5) is still larger than the value (6.5E-02) reported by Nilsson et al. [5] for similar conditions. In future work, it would be beneficial to perform additional measurements without the presence of HAN in the aqueous phase to ensure that its presence had no effect on the extraction of Am into the HDEHP solvent.

The actinide distribution coefficients in Tables 4 and 5 show that Np(V) and Pa(V) were more strongly extracted into the HDEHP solvent than Pu(III) and Am(III). The increased extraction of Np and Pa can be attributed to the stability of the Pu(III)- and Am(III)-DTPA complexes compared to the Np(V)- and Pa(V)-DTPA complexes. The stability of the 3+ complexes prevents their extraction into the solvent to a much greater extent. The distribution coefficients for each actinide decreased with decreasing pH and increasing temperature. The decrease in the distribution coefficients with pH is due to the protonation of the HDEHP solvent which reduces the number of available complexation (i.e., ion exchange) sites. The decrease in the distribution coefficients with temperature is due to the exothermic nature of the extraction process. The enthalpies of extraction calculated using the van't Hoff analysis (see following section) are exothermic.

The uncertainty in the distribution coefficients generally increase at the highest temperature used for the extractions. This is likely due to the increased temperature gradient in the Thermomixer R heating/cooling block. Above 45 °C, the uncertainty in the temperature control increases from ± 0.5 to ± 2 °C. The instability of the Np(V) and Pu(III) at approximately 60 °C may also contribute to the uncertainty for these elements. At this temperature, the reduction of Np and the oxidation of Pu would proceed at faster rates; therefore, the difference in the distribution of Np and Pu valences between the first and last sample removed from the heating/cooling block would be greater, which would change the distribution between phases.

Thermodynamic Properties

The actinide distribution coefficients measured at different temperatures can be used to calculate conditional enthalpies (ΔH^0) and entropies (ΔS^0) of extraction. The thermodynamic properties are considered conditional, since they are based on the variation of distribution coefficients as a function of temperature, rather than the extraction equilibrium constant (K).[5]

The free energy of extraction is defined by equations 2 and 3.

$$\Delta G^0 = \Delta H^0 - T\Delta S^0 \quad (2)$$

$$\Delta G^0 = -RT \ln K \quad (3)$$

Combining the equations and rearrangement results in equation 4,

$$\ln K = -\frac{\Delta H^0}{RT} + \frac{\Delta S^0}{R} \quad (4)$$

which shows that a plot of the natural log of the extraction equilibrium constant as a function of the reciprocal thermodynamic temperature should be linear with a slope of $-\Delta H^0/R$ and a y-intercept of $\Delta S^0/R$. To calculate the conditional enthalpies and entropies of extraction for the TALSPEAK process, the natural log of the actinide distribution coefficients were plotted as a function of the reciprocal thermodynamic extraction temperature on Figures 11 and 12 for the series of experiments performed at pH 3.5 and 2.8, respectively. The thermodynamic properties calculated from the van't Hoff analysis are provided in Table 6 (see Appendix DC for calculations).

The uncertainties associated with the majority of the conditional thermodynamic properties given in Table 6 vary between approximately 10 and 50%. Inspection of the data at pH 3.5 on Figure 11 and the

correlation coefficients for the regression analysis (Appendix DC) show varying degrees of nonlinearity including curvature. The plots at pH 2.8 include six extractions for each actinide; however, the experiments were only performed at two temperatures and would likely show curvature over the temperature range as observed for pH 3.5. The UV-vis spectra recorded to investigate the stability of Np(V) and Pu(III) in lactic acid/DTPA solutions showed that Np(IV) and Pu(IV) are the most stable valences. The reduction of Np(V) and the oxidation of Pu(III), especially at the highest extraction temperature, would result in changes to the distribution of Np and Pu valences which contribute to the uncertainty in the van't Hoff analysis. However, the extractions were performed and samples removed within 2-3 h, and as a result, the majority of the Np and Pu should have still been present as Np(V) and Pu(III). To understand the rates at which Np(V) is reduced and Pu(III) is oxidized in lactic acid/DTPA solutions, an investigation of the oxidation/reduction kinetics should be performed as future work.

Table 6 Thermodynamic properties calculated from van't Hoff analysis

pH	Element	ΔH^0	Std. Dev.	Rel. Std. Dev.	ΔS^0	Std. Dev.	Rel. Std. Dev.
		(kJ/mol)	ΔH^0 (kJ/mol)	ΔH^0 (%)	(J/mol K)	ΔS^0 (J/mol K)	ΔS^0 (%)
3.5	Np	-39.6	4.9	12.3	-122	16	12.9
	Pu	-10.5	5.0	47.4	-60.4	16.0	26.6
	Am	-10.7	1.9	17.5	-41.6	6.1	14.6
	Pa	-48.3	9.0	18.7	-125	29	23.3
2.8	Np	-43.0	2.6	6.1	-128	8	6.6
	Pu	-13.0	2.8	21.3	-65.7	8.9	13.5
	Am	-19.8	0.8	4.3	-56.3	2.7	4.8
	Pa	-28.0	3.5	12.4	-56.2	11.1	19.8

Since the van't Hoff plots for Am and Pa (see Figure 11) also show the same curvature and the Am(III) and Pa(V) valences are stable, it is likely that the enthalpy of extraction for the actinides is not constant over the temperature range. Integration of the van't Hoff equation assumes that the enthalpy of reaction is temperature-independent. Changes in enthalpy with temperature can be addressed using either a change in heat capacity (Δc_p) term or the use of an empirical power series in temperature for the heat capacity.[7] Naghibi et al. [15] emphasized that when calorimetric data are subjected to nonlinear least-squares analysis using the integrated form of the van't Hoff equation with a nonvanishing but temperature-independent heat capacity change, the curvature of the van't Hoff plot becomes evident.

Another possibility which could affect the linearity of the van't Hoff plots are changes in the chemistry which occur due to changes in the lactic acid protonation with temperature. Rao [16] has measured the protonation constants of lactic acid as a functions of temperature. Results from this study are shown in Table 7.

Table 7 Protonation constants of lactic acid

Reaction	log β				
	10 °C	25 °C	40 °C	55 °C	70 °C
$L^- + H^+ = HL$	3.46	3.67	3.68	3.70	3.72

L \equiv lactate

ionic strength = 1.0 M NaClO₄

Small changes in the protonation constants of lactic acid occurred as the temperature was increased from 25 to 55 °C; however, these small changes would not be expected to have a significant effect on the extraction of the actinides into HDEHP.

To address the nonlinearity of the data associated with the van't Hoff plots, future distribution coefficient measurements for the extraction of the actinide elements in the TALSPEAK process should permit the regression analysis to be performed over a more narrow temperature range. Changes in the enthalpy of extraction with temperature are likely responsible for the curvature observed in the distribution data; therefore, the evaluation of data measured over a narrow temperature range should result in a more accurate analysis. The instability of Pu(III) and Np(V) in lactic acid/DTPA solutions is not an issue in the TALSPEAK process; however, any hold-up in processing the feed solution would ensure that significant amounts (if not all) of the Pu and Np are present as the more stable Pu(IV) and Np(IV) valences. Therefore, measuring the distribution of Np(IV) and Pu(IV) between the TALSPEAK aqueous and organic phases and performing the van't Hoff analysis would be an appropriate focus of future studies.

CONCLUSIONS

To better understand the thermodynamic driving force for the extraction of actinide elements in the TALSPEAK process, an experimental study was performed to measure the distribution of Np(V), Pu(III), Am(III), and Pa(V) between the aqueous and organic phases as a function of temperature. The conditional enthalpies and entropies of extraction were subsequently calculated by van't Hoff analysis. Prior to performing the extraction studies, the stability of Np(V) and Pu(III) in lactic acid/DTPA solutions was evaluated by UV-vis spectroscopy. We found that it was necessary to reduce Pu to Pu(III) prior to combining with the lactic acid and DTPA. The reduction was performed using either HAN or FS. When FS was used, Np was reduced to Np(IV). The spectroscopic studies showed that Np(V) and Pu(III) are not stable in the lactic acid/DTPA solutions used as the aqueous phase in the TALSPEAK process. The stability of Np(IV)-DTPA and Pu(IV)-DTPA complexes are much greater than the stability of the Np(V)-DTPA and Pu(III)-DTPA complexes, and as a result, Np is slowly reduced to Np(IV) and Pu is slowly oxidized to Pu(IV) due to the reduced activity of the stable complexes. When Np(V) was added to a solution containing a 1.5 M lactic acid/ammonium lactate buffer and 0.05 M DTPA, approximately 50% of the Np was reduced to Np(IV) in the first day. The fraction of Np(V) in the solution continued to diminish with time and was essentially reduced to Np(IV) after one week. When Pu(III) was added to a lactic acid/DTPA solution of the same composition, the spectrum recorded following at least two days after preparation of the solution continued to show some sign of Pu(III). The Pu(III) was completely oxidized to Pu(IV) after 3-4 days.

The actinide distribution coefficient measurements showed that the 5+ actinides (Np and Pa) were more strongly extracted into the HDEHP solvent than the 3+ actinides (Pu and Am). The increased extraction of Np and Pa was attributed to the increased affinity of the DTPA for the 3+ actinides compared to the 5+ actinides. The stability of the 3+ DTPA complexes prevents the extraction of Pu and Am into the solvent to a greater extent. The actinide distribution coefficients decreased with decreasing pH and increasing temperature. These trends in the data are due to the protonation of the HDEHP solvent (which reduces the number of complexation sites) and the exothermic nature of the extraction process. At pH 3.5, the conditional enthalpies of extraction were approximately -10 kJ/mole for Pu(III) and Am(III), -40 kJ/mol for Np(V), and -48 kJ/mol for Pa(V). The entropies of extraction were negative which results in more positive free energies of extraction as the temperature increases. The uncertainties associated with the majority of the conditional thermodynamic properties varied between approximately 10 and 50%. The nonlinearity in the data is primarily attributed to changes in the enthalpy of extraction over the temperature range; although, the instability of Np(V) and Pu(III) likely contributed to the variance.

FUTURE WORK

Recommendations for areas of additional study to follow the actinide distribution coefficient measurements and thermodynamic analysis discussed in this report fall into two distinct areas. The spectroscopic studies showed that Np(V) and Pu(III) are not stable in lactic acid/DTPA solutions. To understand the rates at which Np(V) is reduced and Pu(III) is oxidized in these solution, an investigation of the oxidation/reduction kinetics should be performed as future work. The measurement of additional distribution coefficients for Np, Pu, Am, and Pa is also recommended. Since we demonstrated that the most stable Np and Pu valences in lactic acid/DTPA solutions are Np(IV) and Pu(IV), measuring distribution coefficients for the 4+ oxidation states in the TALSPEAK process and performing the van't Hoff analysis would be an appropriate focus of future work. It would also be beneficial to perform additional measurements for Am without the presence of HAN in the aqueous phase to ensure that its presence had no effect on the extraction of Am into the HDEHP solvent.

REFERENCES

1. Nuclear Energy Research and Development Roadmap – Report to Congress, United States Department of Energy Office of Nuclear Energy, Washington, DC (2010).
2. L. R. Morss, N. M. Edelstein, and J. Fuger, Eds., *The Chemistry of the Actinide and Transactinide Elements*, 3rd ed., Springer, Dordrecht, The Netherlands, Vol. 2, pp 841-844 (2006).
3. L. R. Morss et al., pp 704-705.
4. M. L. Hyder, W. C. Perkins, M. C. Thompson, G. A. Burney, E. R. Russell, H. P. Holcomb, and L. F. Landon, *Processing of Irradiated Enriched Uranium Fuels at the Savannah River Plant*, DP-1500, E. I. du Pont de Nemours & Co., Aiken, SC (1979).
5. M. Nilsson and K. L. Nash, *Review Article: A Review of the Development and Operational Characteristics of the TALSPEAK Process*, *Solvent Extr Ion Exc*, 25, pp 665–701 (2007).
6. B. Weaver and F. A. Kappelmann, *Talspeak, A new method of separating americium and curium from the lanthanides by extraction from an aqueous solution of an aminopolyacetic acid complex with a monoacetic organophosphate or phosphonate*, ORNL-3559, Union Carbide Corporation, Oak Ridge, TN (1964).
7. K. Denbigh, *The Principles of Chemical Equilibrium*, 3rd ed., Cambridge University Press, Cambridge, United Kingdom, pp. 143-144 (1971).
8. L. R. Morss et al., pp 707-708.
9. C. Pereira, L. E. Maggos, G. F. Vandegrift, M. C. Regalbuto, K. Alford, A. Bakel, D. Bowers, J. P. Byrnes, M. A. Clark, J. R. Falkenberg, A. V. Gelis, L. Hafenrichter, A. S. Hebden, M. Kalensky, J. F. Krebs, R. A. Leonard, A. Leyva, K. J. Quigley, D. Stepinski, Y. Tsai, and V. S. Sullivan, *Results of the 2007 TALSPEAK Spent Fuel Demonstration*, Letter Report, Argonne National Laboratory, Argonne, IL (2007).
10. J. M. Cleveland, *The Chemistry of Plutonium*, American Nuclear Society, La Grange Park, IL, p 12 (1979).

11. M. C. Thompson and T. S. Rudisill, *Literature Review of Complexants and Reductants for Plutonium and Neptunium for the UREX Process*, Letter Report, Savannah River Technology Center, Aiken, SC (2002).
12. G. F. Kessinger, E. A. Kyser and P. M. Almond, *Literature Review: Reduction of Np(V) to Np(IV) – Alternatives to Ferrous Sulfamate*, SRNL-STI-2009-00610, Savannah River Nuclear Solutions, Aiken, SC (2009).
13. L. R. Morss et al., p 780.
14. L. R. Morss et al., p 1178.
15. H. Naghibi, A. Tamura, and J. M. Sturtevant, *Significant discrepancies between van't Hoff and calorimetric enthalpies*, Proc Natl Acad Sci USA, 92, pp 5597-5599 (1995).
16. L. Rao, *Understanding Actinide/Lanthanide Speciation under TALSPEAK Conditions*, AFCI-SEPA-PMO-MI-DV-2009-000xxx, Lawrence Berkeley National Laboratory, Berkeley, CA (2009).

Figure 1 Reference Spectra for Np in buffered lactic acid/DTPA systems

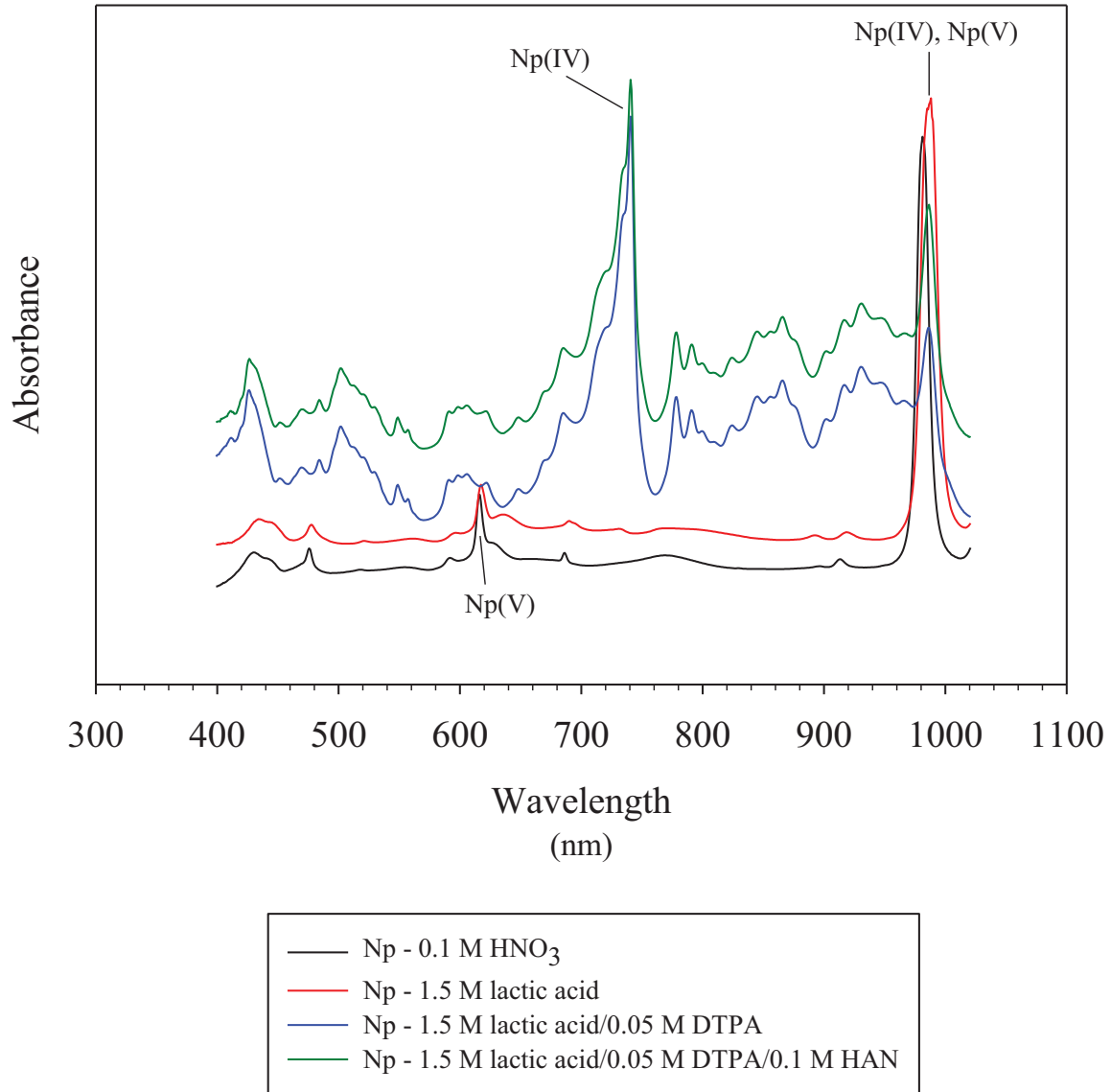


Figure 2 Reference Spectra for Pu in buffered lactic acid/DTPA systems

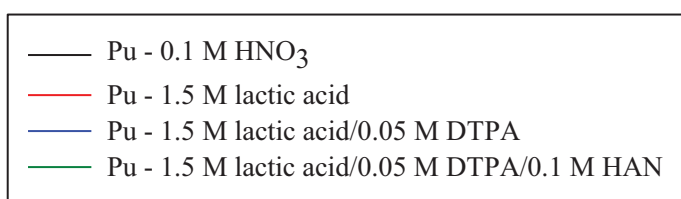
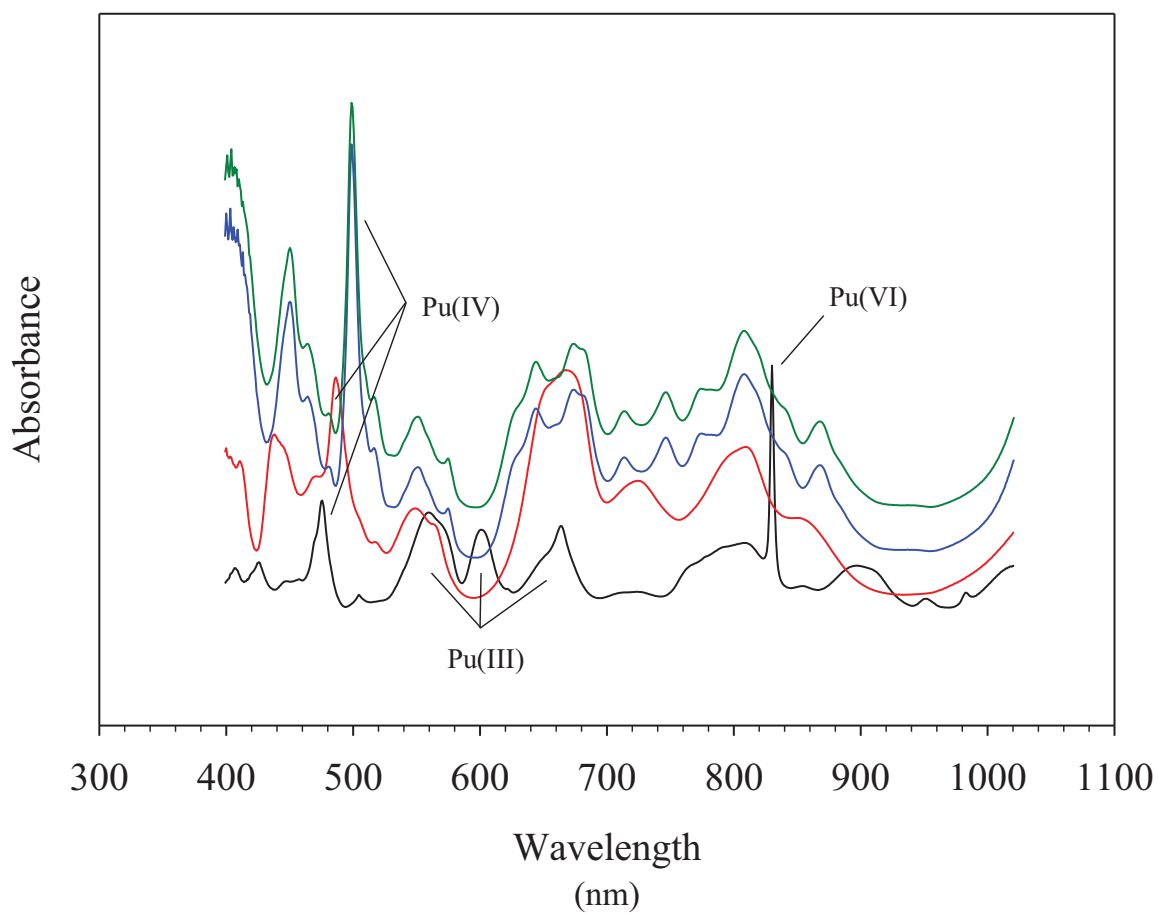


Figure 3 UV-vis spectrum of Np + 0.1 M HAN added to 1.5 M lactic acid/0.05 M DTPA

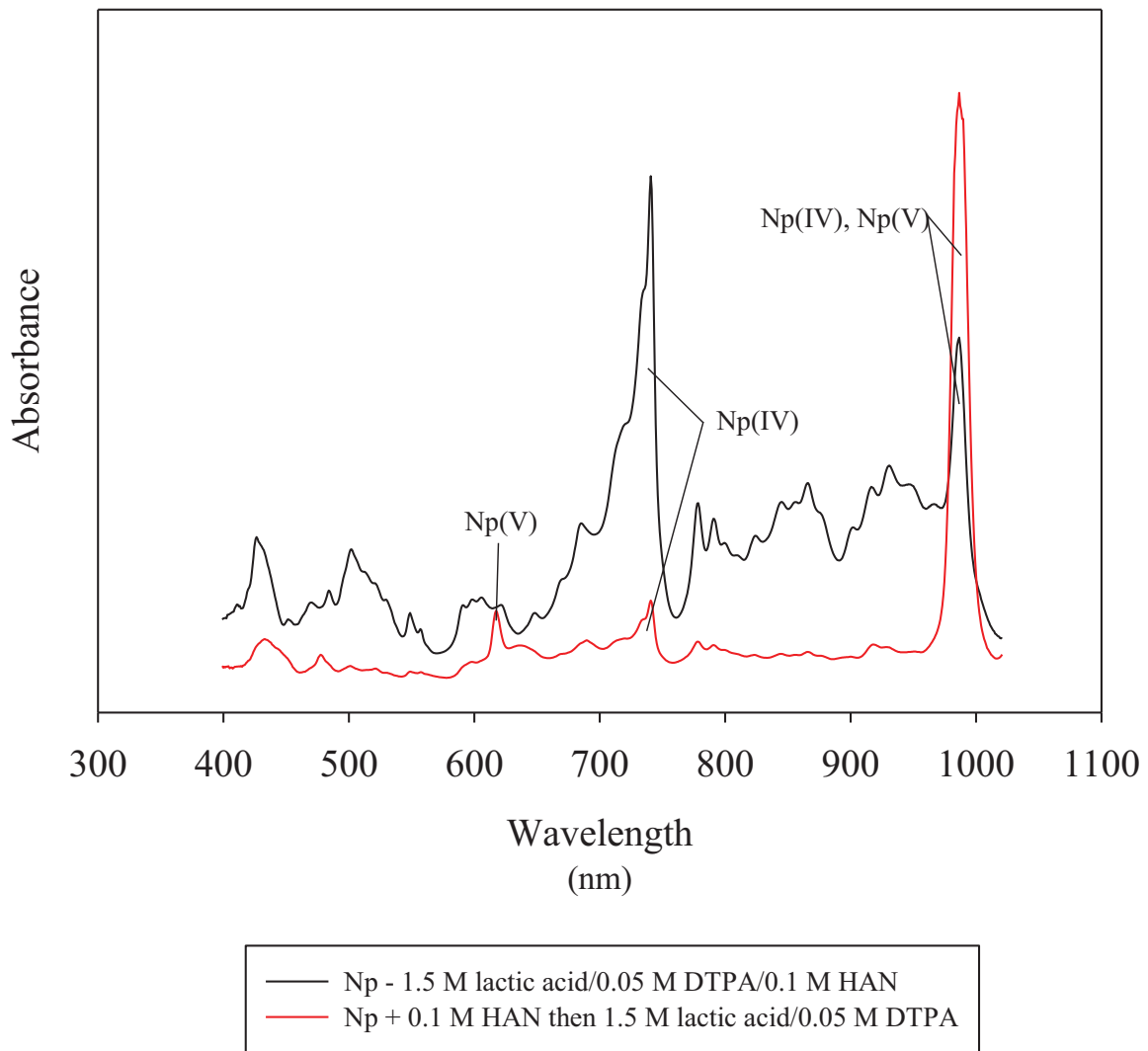


Figure 4 UV-vis spectrum of Np + 0.1 M FS added to 1.5 M lactic acid/0.05 M DTPA

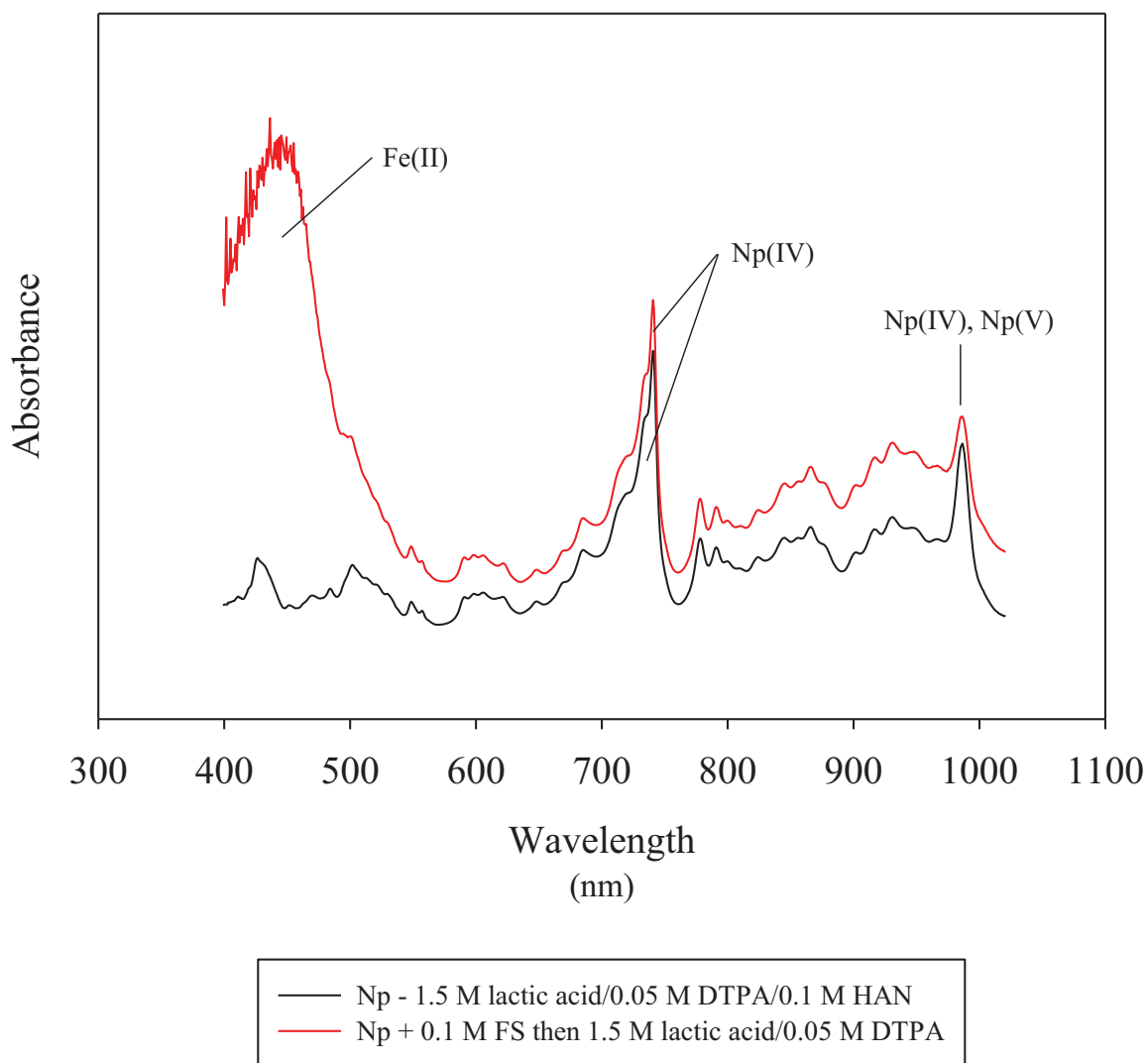


Figure 5 UV-vis spectrum of Pu + 0.1 M HAN added to 1.5 M lactic acid/0.05 M DTPA

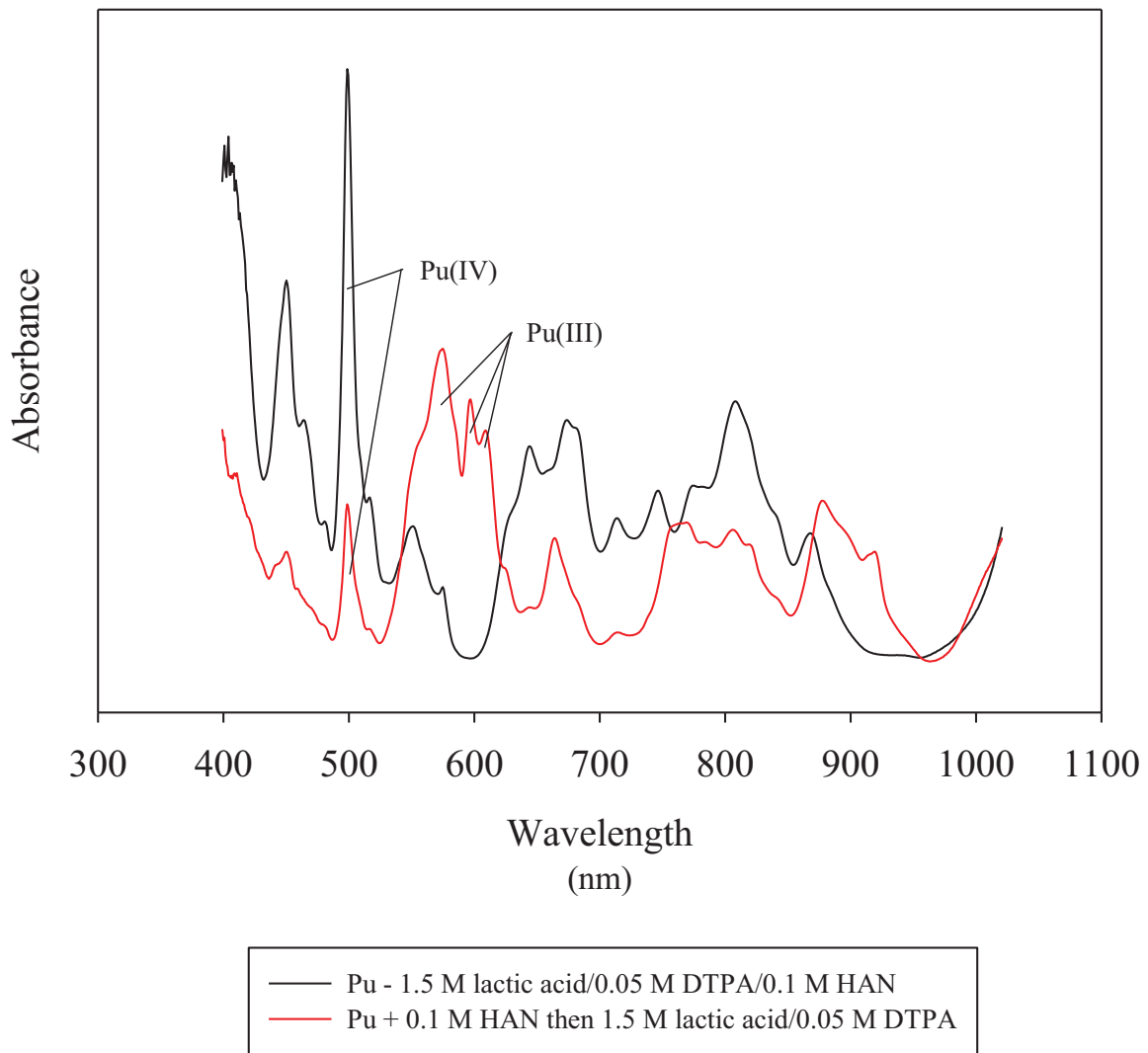


Figure 6 UV-vis spectrum of Pu + 0.1 M FS added to 1.5 M lactic acid/0.05 M DTPA

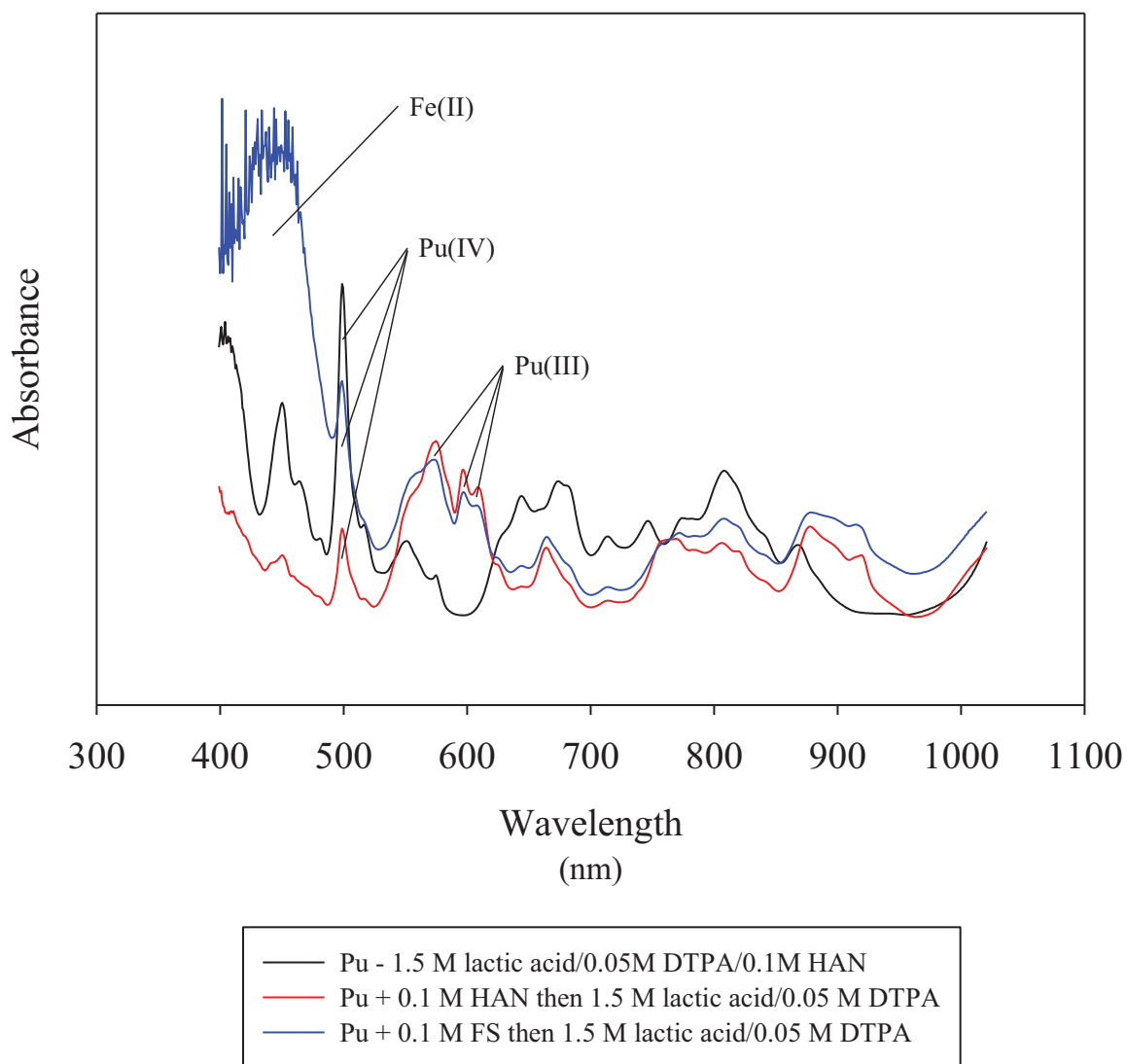


Figure 7 UV-vis spectra of Np(V)/HAN/lactic acid/DTPA solution

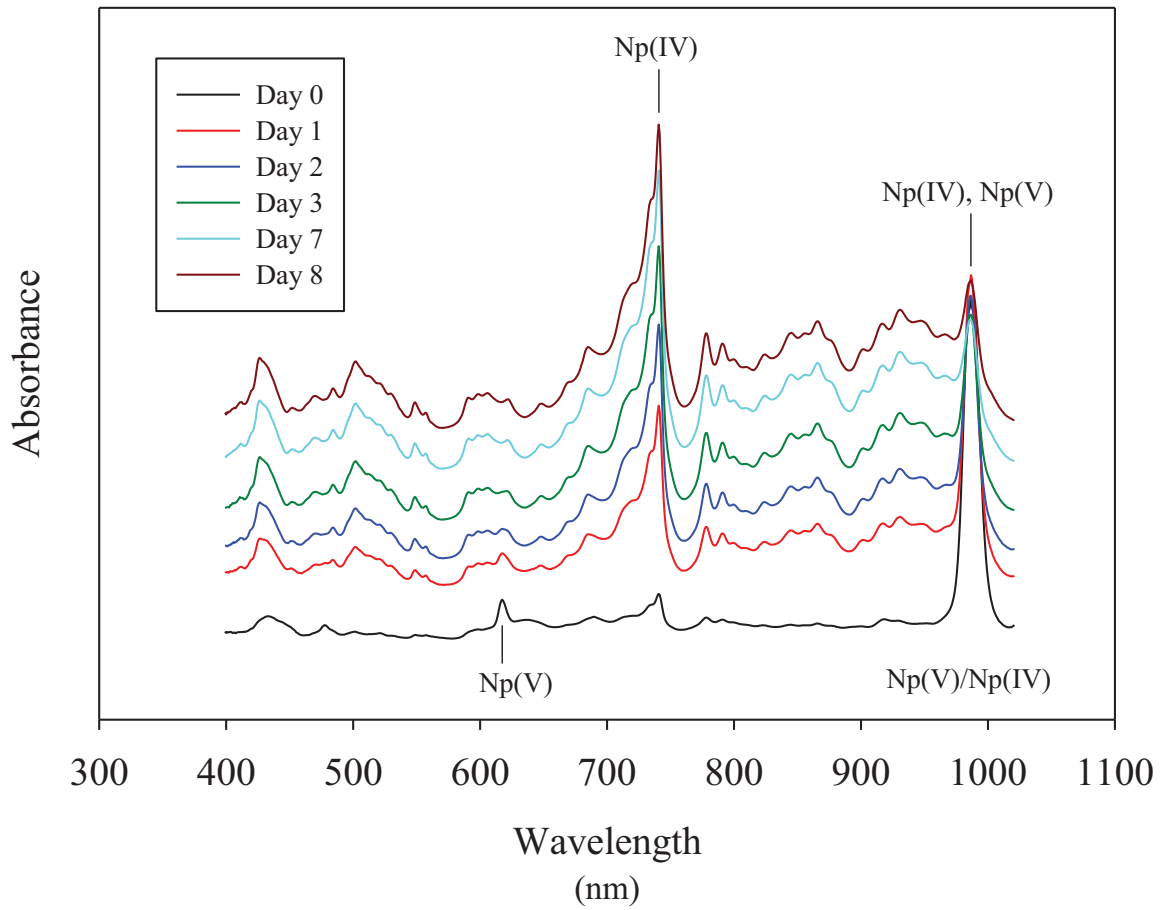


Figure 8 UV-vis spectra of Np(V)/FS/lactic acid/DTPA solution

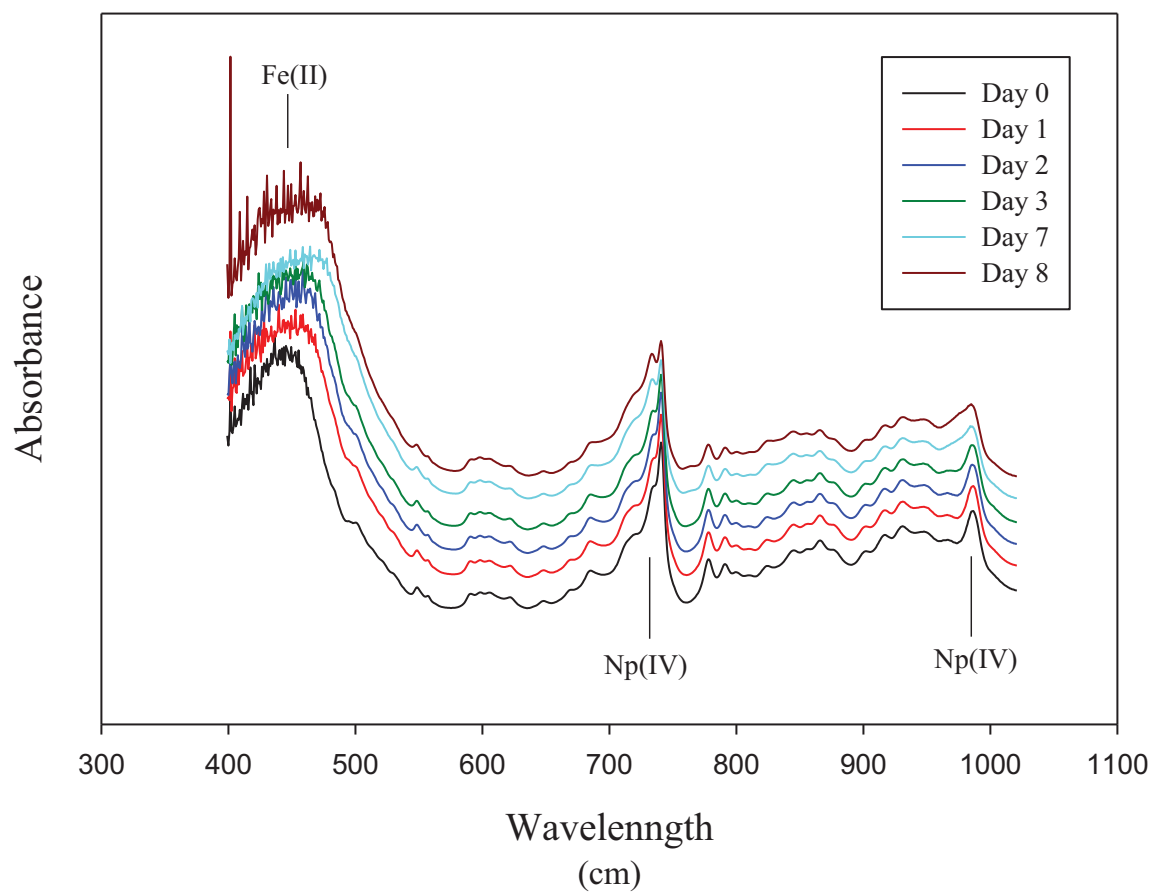


Figure 9 UV-vis spectra of Pu(III)/HAN/lactic acid/DTPA solution

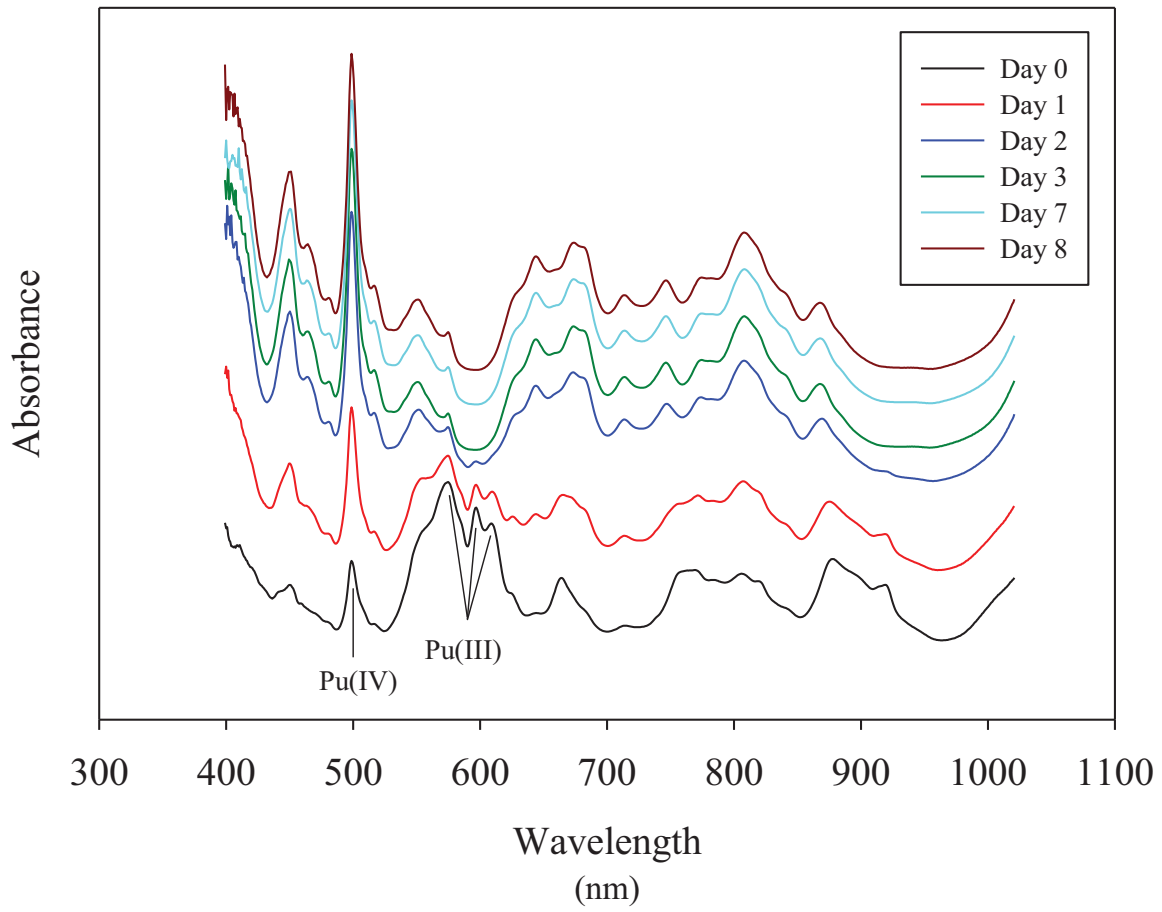


Figure 10 UV-vis spectra of Pu(III)/FS/lactic acid/DTPA solution

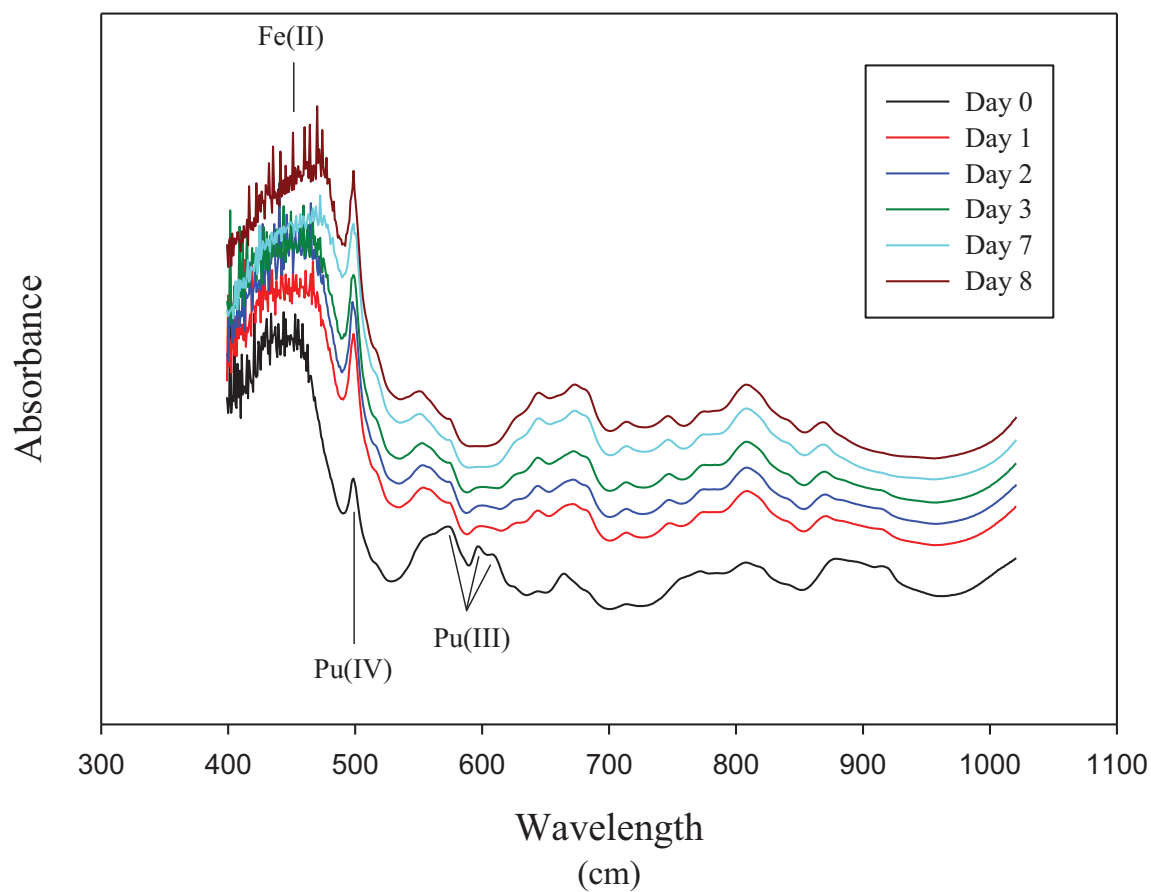


Figure 11 van't Hoff analysis for TALSPEAK extractions at pH 3.5

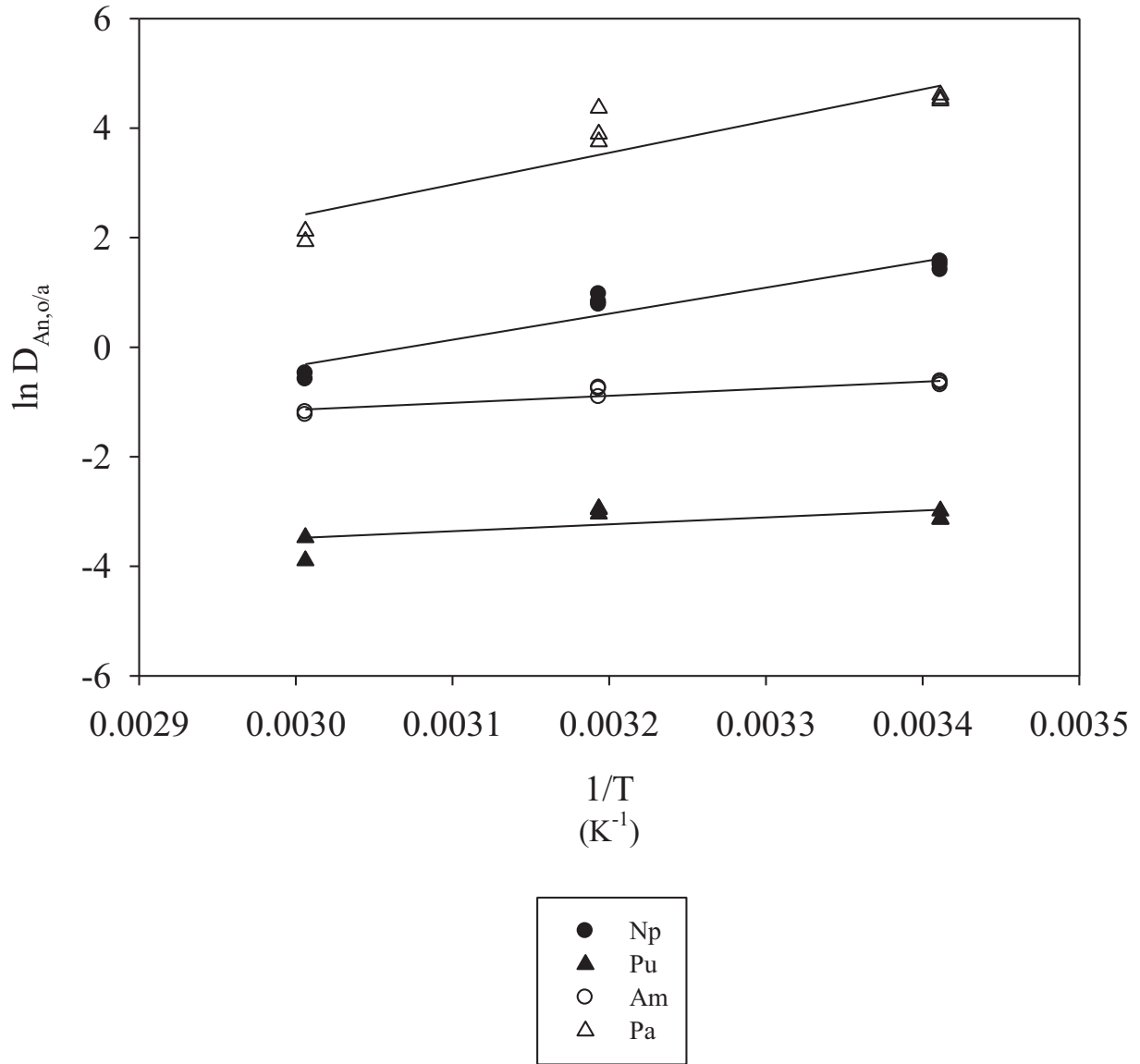
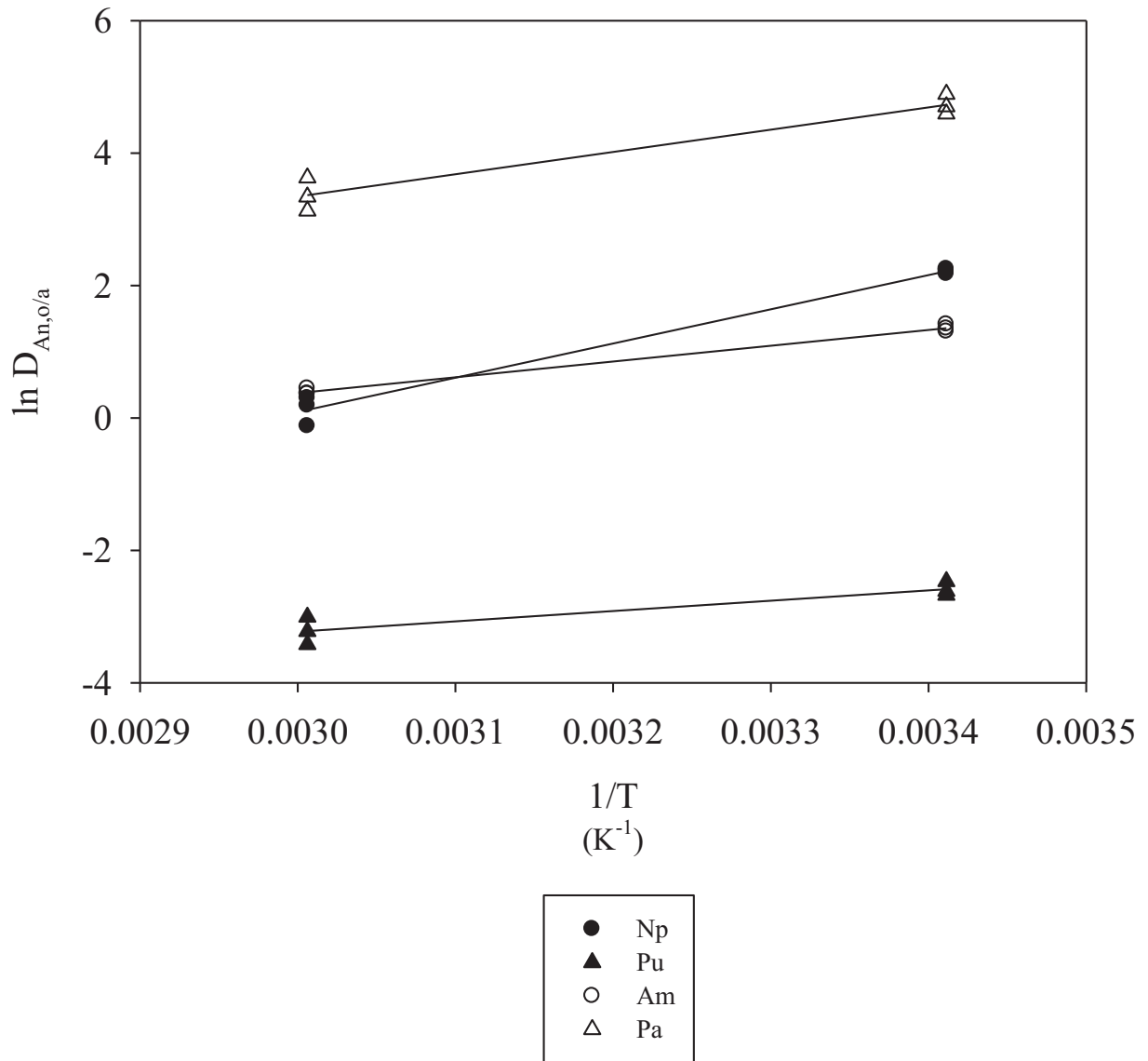


Figure 12 van't Hoff analysis for TALSPEAK extractions at pH 2.8



Appendix DA

Solution Preparation for Valence Adjustment Study

Chemical Reagents

The manufacturer and purity information for the chemicals used in the valence adjustment study and distribution coefficient measurements are provided in Table A.1.

Table A.1 Chemical manufacturer and purity information

Chemical	Manufacturer	Concentration	Purity
lactic acid	Sigma Aldrich	85 wt %	(1)
DTPA	Aldrich		97 wt %
NH ₄ OH	Fisher Scientific	29.05 wt % (7.8 M)	(2)
HNO ₃	Fisher Scientific	15.0 M ⁽³⁾	(2)
HAN	(4)	1.77 M	N/A
FS	(4)	~ 2.4 M	N/A
HDEHP	Sigma Aldrich		97 wt %
Dodecane	Sigma Aldrich		> 99 wt %

(1) ACS Reagent

(2) Certified ACS PLUS

(3) Analyzed by titration.

(4) Manufacturer is unknown; reductant was obtained from the SRS H-Canyon facility.

Solution Preparation for UV-vis Spectroscopy

0.1 M HNO₃ Solution

A 1.0 M HNO₃ stock solution was initially prepared by diluting concentrated (15 M) HNO₃ with deionized water. To obtain a 0.1 M HNO₃ solution once the Np or Pu was added and the pH was adjusted to 2.8, it was necessary to initially prepare a solution containing 0.11 M HNO₃. The solution was prepared by diluting a portion of the 1.0 M HNO₃ stock solution to the desired concentration with deionized water.

1.5 M Lactic Acid Solution

To obtain a 1.5 M lactic acid solution once the Np or Pu was added and the pH was adjusted to 2.8, it was necessary to initially prepare a solution containing 1.7 M lactic acid. One hundred milliliters of 1.7 M lactic acid were prepared by transferring 17.8006 g of 85 wt % lactic acid to a volumetric flask and diluting the flask to volume with deionized water. The pH of the lactic acid solution was preadjusted to nominally 2.8 by adding approximately 2.5 mL of 7.8 M NH₄OH. The pH of the solution was measured using an Accumet[®] Basic AB15 pH meter which was calibrated using pH 1, 3, and 6 buffer solutions.

1.5 M lactic acid/0.05 M DTPA Solution

To obtain a 1.5 M lactic acid/0.05 M DTPA solution once the Np or Pu was added and the pH was adjusted to 2.8, 1.7 M lactic acid was used to prepare a solution containing 0.06 M DTPA. To prepare 50 mL of the solution, 1.1004 g of DTPA were transferred to a 100 mL beaker. Approximately 40 mL of 1.7 M lactic acid were added. The solution was stirred using a magnetic stir bar and heated at 70-80 °C. A watch glass containing water was placed on the beaker to reduce evaporation losses. To dissolve the solids, it was necessary to increase the pH by adding 4.40 mL of 3.9 M NH₄OH. The solution was

transferred to a 50 mL volumetric flask which was diluted to volume with 1.7 M lactic acid. The pH of the lactic acid/DTPA solution was preadjusted to nominally 2.8 by adding approximately 0.25 mL of 7.8 M NH_4OH .

1.5 M lactic acid/0.05 M DTPA/0.1 M HAN Solution

To obtain a 1.5 M lactic acid/0.05 M DTPA solution once the Np or Pu and HAN were added and the pH was adjusted to 2.8, it was necessary to initially prepare a solution containing 1.8 M lactic acid and 0.06 M DTPA. One hundred milliliters of 1.8 M lactic acid were prepared by transferring 19.0578 g of 85 wt % lactic acid to a volumetric flask and diluting the flask to volume with deionized water. To prepare 50 mL of solution containing 1.8 M lactic acid/0.06 M DTPA, 1.1778 g of DTPA were initially transferred to a 100 mL beaker. Approximately 40 mL of 1.8 M lactic acid were added. The solution was stirred using a magnetic stir bar and heated. A watch glass containing water was placed on the beaker to reduce evaporation losses. To dissolve the solids, it was necessary to increase the pH by adding 2.5 mL of 3.9 M NH_4OH . The solution was transferred to a 50 mL volumetric flask which was diluted to volume with 1.8 M lactic acid. The pH of the lactic acid/DTPA solution was nominally 2.8 and was not adjusted. To achieve 0.1 M HAN in the final solution, a 0.65 mL aliquot of a 1.77 M solution was added to 9.35 mL of the 1.8 M lactic acid/0.06 M DTPA solution.

Test Solution Preparation

The assembly of the four Np and Pu test solutions prepared for the valence adjustment study are summarized below.

Solution 1 (Np) – 0.10 M HNO_3 /3 g/L Np

Preparation: 10 mL 0.11 M HNO_3 + 1 mL 32.0 g/L Np

Solution 1 (Pu) – 0.10 M HNO_3 /4 g/L Pu

Preparation: 10 mL 0.11 M HNO_3 + 1 mL 45.3 g/L Pu

Solution 2 (Np) – 1.5 M lactic acid/3 g/L Np

Preparation: 10 mL 1.7 M lactic acid + 1 mL 32.0 g/L Np

Solution 2 (Pu) – 1.5 M lactic acid/4 g/L Pu

Preparation: 10 mL 1.7 M lactic acid + 1 mL 45.3 g/L Pu

Solution 3 (Np) – 1.5 M lactic acid/0.05 M DTPA/3 g/L Np

Preparation: 10 mL 1.7 M lactic acid/0.06 M DTPA + 1 mL 32.0 g/L Np

Solution 3 (Pu) – 1.5 M lactic acid/0.05 M DTPA/4 g/L Pu

Preparation: 10 mL 1.7 M lactic acid/0.06 M DTPA + 1 mL 45.3 g/L Pu

Solution 4 (Np) – 1.5 M lactic acid/0.05 M DTPA/0.1 M HAN/3 g/L Np

Preparation: 9.35 mL 1.8 M lactic acid/0.06 M DTPA + 0.65 mL HAN + 1 mL 32.0 g/L Np

Solution 4 (Pu) – 1.5 M lactic acid/0.05 M DTPA / 0.1 M HAN/4 g/L Pu

Preparation: 9.35 mL 1.8 M lactic acid/0.06 M DTPA + 0.65 mL HAN + 1 mL 45.3 g/L Pu

pH Adjustment

The pH of the buffered solutions (numbers 2-4) was adjusted to nominally 2.8 using 3.8 M NH_4OH . The NH_4OH was added drop-wise using a disposable transfer pipette. A Thermo Scientific Orion 3 Star pH meter was used for the measurements. The instrument was calibrated using pH 2, 4, and 7 buffer solutions. The pH adjustments are summarized in Table A.2.

Table A.2 pH adjustment of buffered lactate solutions

Solution No.	Composition	Initial pH	Drops NH ₄ OH Added	Final pH
2	Pu – 1.5 M lactic acid	2.35	9	2.76
2	Np – 1.5 M lactic acid	1.31	20	2.77
3	Pu – 1.5 M lactic acid/0.05 M DTPA	2.46	8	2.77
3	Np – 1.5 M lactic acid/0.05 M DTPA	1.92	15	2.79
4	Pu – 1.5 M lactic acid/0.05 M DTPA/0.1 M HAN	2.21	13	2.77
4	Np – 1.5 M lactic acid/0.05 M DTPA/0.1 M HAN	1.55	28	2.78

Preparation of Additional Solutions for UV-vis Spectroscopy

Four additional solutions were prepared for analysis by UV-vis spectroscopy in which the reductant was added to the actinide solution prior to combining with the buffered lactate solution containing DTPA. Both HAN and FS were used as reductants. The four solutions prepared for study included: (1a) Np + HAN added to 1.5 M lactic acid/0.05 M DTPA, (2a) Pu + HAN added to 1.5 M lactic acid/0.05M DTPA, (3a) Np + FS added to 1.5 M lactic acid/0.05 M DTPA, and (4a) Pu + FS added to 1.5 M lactic acid/0.05 M DTPA. The volume of the HAN and FS stock solutions added to the actinide solutions was sufficient to achieve a concentration of 0.1 M when combined with the lactic acid and the DTPA. The lactic acid/DTPA solutions prepared for the initial spectroscopic studies were used to prepare the four solutions. The assembly of the test solutions are summarized below.

Solution 1a (Np/HAN) – 1.5 M lactic acid/0.05 M DTPA/0.1 M HAN/3 g/L Np
 Preparation: 1 mL 32.0 g/L Np + 0.65 mL HAN added to 9.35 mL 1.8 M lactic acid/0.06 M DTPA

Solution 2a (Pu/HAN) – 1.5 M lactic acid/0.05 M DTPA/0.1 M HAN/3 g/L Pu
 Preparation: 1 mL 45.3 g/L Pu + 0.65 mL HAN added to 9.35 mL 1.8 M lactic acid/0.06 M DTPA

Solution 3a (Np/FS) – 1.5 M lactic acid/0.05 M DTPA/0.1 M FS/3 g/L Np⁽¹⁾
 Preparation: 1 mL 32.0 g/L Np + 0.65 mL FS added to 9.35 mL 1.7 M lactic acid/0.06 M DTPA

Solution 4a (Pu/FS) – 1.5 M lactic acid/0.05 M DTPA/0.1 M FS/3 g/L Pu
 Preparation: 1 mL 45.3 g/L Pu + 0.65 mL FS added to 9.35 mL 1.8 M lactic acid/0.06 M DTPA

(1) The amount of 1.8 M lactic acid/0.06 M DTPA available was not sufficient to prepare the FS-containing solution; therefore, the solution was prepared using the 1.7 M lactic acid/0.06 M DTPA stock solution instead. The final concentration of lactic acid was approximately the same.

The pH of the buffered solutions was adjusted to nominally 2.8 using 3.8 M NH₄OH. The NH₄OH was added drop-wise using a disposable transfer pipette. The pH adjustments are summarized in Table A.3.

Table A.3 pH adjustment of actinide solutions containing HAN and FS

Solution No.	Composition	Initial pH	Drops NH ₄ OH Added	Final pH
1a	(Np + 0.1 M HAN) + 1.5 M lactic acid/0.05 M DTPA	2.07	16	2.79
2a	(Pu + 0.1 M HAN) + 1.5 M lactic acid/0.05M DTP	1.77	22	2.76
3a	(Np + 0.1 M FS) + 1.5 M lactic acid/0.05 M DTPA	2.71	31	2.77
4a	(Pu + 0.1 M FS) + 1.5 M lactic acid/0.05 M DTPA	1.24	45	2.78

Appendix DB

Solution Preparation for Distribution Coefficient Measurements

Chemical Reagents

The manufacturer and purity information for the chemicals used in the distribution coefficient measurements is provided in Table A.1.

Preparation of 1.9 M lactic acid/0.05 M DTPA

To obtain a 1.5 M lactic acid/0.05 M DTPA solution once the Np or Pu and HAN were added and the pH was adjusted to 2.8 (or 3.5), it was necessary to initially prepare a solution containing 1.9 M lactic acid and 0.06 M DTPA. Two hundred milliliters of 1.9 M lactic acid were prepared by transferring 40.6831 g of 85 wt % lactic acid to a volumetric flask and diluting the flask to volume with deionized water. To prepare 200 mL of solution containing 1.9 M lactic acid/0.06 M DTPA, 4.9567 g of DTPA were initially transferred to a 250 mL beaker. Approximately 150 mL of 1.9 M lactic acid were added. The solution was stirred using a magnetic stir bar and heated. A watch glass containing water was placed on the beaker to reduce evaporation losses. To dissolve the solids, it was necessary to increase the pH by adding 4.4 mL of 7.8 M NH₄OH. The solution was transferred to a 200 mL volumetric flask which was diluted to volume with 1.9 M lactic acid. The pH of the solution was subsequently adjusted from 2.58 to 2.80 by the addition of 55 drops of 7.8 M NH₄OH.

TALSPEAK Extractions

The activities of the Np, Pu, and Am in the stock solutions are summarized in Table A.4.

Table A.4 Actinide concentrations in stock solutions

Np/Pu Solution		Am Solution	
Element	Activity (dpm/mL)	Element	Activity (dpm/mL)
Np	4.98×10^7	Am	1.28×10^7
Pu	4.42×10^9		

To prepare the actinide solution for subsequent addition to the lactic acid/DTPA solution, a 250 μ L aliquot of the Am stock solution was combined with 1 mL of the Np/Pu stock solution. A 100 μ L aliquot of 1.77 M HAN was then added to reduce the Pu to Pu(III). The concentrations of Np (C_{Np}), Pu (C_{Pu}), Am (C_{Am}), and HAN (C_{HAN}) in this solution are calculated by equations A.1-A.4, respectively.

$$C_{\text{Np}} = \frac{\left(4.98 \times 10^7 \frac{\text{dpm}}{\text{mL}}\right)(1.0 \text{ mL})}{(1.0 \text{ mL} + 0.25 \text{ mL} + 0.10 \text{ mL})} = 3.69 \times 10^7 \frac{\text{dpm}}{\text{mL}} \quad \text{A.1}$$

$$C_{\text{Pu}} = \frac{\left(4.42 \times 10^9 \frac{\text{dpm}}{\text{mL}}\right)(1.0 \text{ mL})}{(1.0 \text{ mL} + 0.25 \text{ mL} + 0.10 \text{ mL})} = 3.28 \times 10^9 \frac{\text{dpm}}{\text{mL}} \quad \text{A.2}$$

$$C_{Am} = \frac{\left(1.28 \times 10^7 \frac{\text{dpm}}{\text{mL}}\right)(0.25 \text{ mL})}{(1.0 \text{ mL} + 0.25 \text{ mL} + 0.10 \text{ mL})} = 2.38 \times 10^6 \frac{\text{dpm}}{\text{mL}} \quad \text{A.3}$$

$$C_{HAN} = \frac{\left(1.77 \frac{\text{mol}}{\text{L}}\right)\left(\frac{1 \text{ L}}{1000 \text{ mL}}\right)(0.10 \text{ mL})}{(1.0 \text{ mL} + 0.25 \text{ mL} + 0.10 \text{ mL})\left(\frac{1 \text{ L}}{1000 \text{ mL}}\right)} = 0.13 \frac{\text{mol}}{\text{L}}$$

The actinide solution was then combined with an 11.4 mL aliquot of 1.9 M lactic acid/0.06 M DTPA to prepare the aqueous phase for the extractions. Once the solutions were combined, the pH was adjusted to nominally 2.8 or 3.5 using 3.9 M NH₄OH. The pH of the solution was measured using an Accumet[®] Basic AB15 pH meter which was calibrated using pH 1, 3, and 6 buffer solutions. During the preparation of the lactic acid/DTPA solution, we assumed that approximately 1.5 mL of NH₄OH would be required to adjust the pH to the desired value. The number of drops of NH₄OH required to perform the adjustment and the initial and final pH of the aqueous phase are provided in Table A.5 for each series of measurements.

Table A.5 Aqueous phase pH adjustment for TALSPEAK extractions

Experiment	Drops NH ₄ OH Added	Initial pH	Final pH
TAL-1	20	< 2.41 ⁽¹⁾	2.93
TAL-2	14	2.12	2.81
TAL-3	37	2.10	3.49
TAL-4	40	2.18	3.50
TAL-5	42	2.08	3.49

(1) Initial reading was incorrect due to electrode position.

The final concentrations of each component (Np, Pu, Am, HAN, lactic acid (C_{LA}), and DTPA (C_{DTPA})) in the aqueous phase are calculated by equations A.5-A.10. The calculations assume that nominally 1.5 mL of 3.9 M NH₄OH were added during the pH adjustments.

$$C_{Np} = \frac{\left(3.69 \times 10^7 \frac{\text{dpm}}{\text{mL}}\right)(1.35 \text{ mL})}{(1.35 \text{ mL} + 11.40 \text{ mL} + 1.50 \text{ mL})} = 3.50 \times 10^6 \frac{\text{dpm}}{\text{mL}} \quad \text{A.5}$$

$$C_{Pu} = \frac{\left(3.28 \times 10^9 \frac{\text{dpm}}{\text{mL}}\right)(1.35 \text{ mL})}{(1.35 \text{ mL} + 11.40 \text{ mL} + 1.50 \text{ mL})} = 3.10 \times 10^8 \frac{\text{dpm}}{\text{mL}} \quad \text{A.6}$$

$$C_{Am} = \frac{\left(2.38 \times 10^6 \frac{\text{dpm}}{\text{mL}}\right)(1.35 \text{ mL})}{(1.35 \text{ mL} + 11.40 \text{ mL} + 1.50 \text{ mL})} = 2.25 \times 10^5 \frac{\text{dpm}}{\text{mL}} \quad \text{A.7}$$

$$C_{\text{HAN}} = \frac{\left(0.13 \frac{\text{mol}}{\text{L}}\right)\left(\frac{1 \text{ L}}{1000 \text{ mL}}\right)(1.35 \text{ mL})}{(1.35 \text{ mL} + 11.40 \text{ mL} + 1.50 \text{ mL})\left(\frac{1 \text{ L}}{1000 \text{ mL}}\right)} = 0.0124 \frac{\text{mol}}{\text{L}} \quad \text{A.8}$$

$$C_{\text{LA}} = \frac{\left(1.9 \frac{\text{mol}}{\text{L}}\right)\left(\frac{1 \text{ L}}{1000 \text{ mL}}\right)(11.4 \text{ mL})}{(1.35 \text{ mL} + 11.40 \text{ mL} + 1.50 \text{ mL})\left(\frac{1 \text{ L}}{1000 \text{ mL}}\right)} = 1.5 \frac{\text{mol}}{\text{L}} \quad \text{A.9}$$

$$C_{\text{DTPA}} = \frac{\left(0.06 \frac{\text{mol}}{\text{L}}\right)\left(\frac{1 \text{ L}}{1000 \text{ mL}}\right)(11.4 \text{ mL})}{(1.35 \text{ mL} + 11.40 \text{ mL} + 1.50 \text{ mL})\left(\frac{1 \text{ L}}{1000 \text{ mL}}\right)} = 0.05 \frac{\text{mol}}{\text{L}} \quad \text{A.10}$$

Appendix DC

Np and Pu Distribution Coefficients

Measured Actinide Activities in the TALSPEAK Organic and Aqueous Phases

TALSPEAK extraction experiments were performed using an aqueous phase containing a 1.5 M lactic acid/ammonium lactate buffer and 0.05 M DTPA. The aqueous phase was adjusted to either pH 2.8 or 3.5. At pH 2.8, extraction experiments were performed at 20.0 and 59.0 °C. The experiments at pH 3.5 were performed at 20.0, 40.0, and 59.5 °C. The organic phase used for each extraction experiments was 1.0 M HDEHP in dodecane. Each experiment was performed in triplicate. The Np, Pu, Am, and Pa activities measured in each series of experiments are given in Tables C.1-C.5.

Table C.1 Activity measurements for Experiment TAL-1
(pH 2.8, temperature 20.0 °C)

Element	Organic Counts (dpm/mL)	1 sigma uncertainty (%)	Aqueous Counts (dpm/mL)	1 sigma uncertainty (%)
Np	1.12E+06	0.10	1.27E+05	0.37
Np	1.28E+06	0.10	1.35E+05	0.37
Np	1.16E+06	0.10	1.26E+05	0.37
Pu	1.82E+04	2.70	2.64E+05	0.26
Pu	2.27E+04	2.30	2.68E+05	0.20
Pu	1.90E+04	2.70	2.60E+05	0.25
Am	2.35E+05	0.30	6.37E+04	0.41
Am	2.71E+05	0.30	6.59E+04	0.40
Am	2.44E+05	0.30	6.32E+04	0.41
Pa	5.14E+05	0.10	4.66E+03	1.62
Pa	5.90E+05	0.10	5.97E+03	1.53
Pa	5.32E+05	0.14	3.99E+03	1.78

Table C.2 Activity measurements for Experiment TAL-2
 (pH 2.8, temperature 59.0 °C)

Element	Organic Counts (dpm/mL)	1 sigma uncertainty (%)	Aqueous Counts (dmp/mL)	1 sigma uncertainty (%)
Np	2.57E+05	0.20	2.13E+05	0.20
Np	2.72E+05	0.20	2.02E+05	0.20
Np	2.14E+05	0.20	2.42E+05	0.20
Pu	5.01E+03	4.91	1.26E+05	0.40
Pu	5.88E+03	5.30	1.19E+05	0.40
Pu	4.05E+03	5.30	1.24E+05	0.40
Am	5.24E+04	0.60	3.63E+04	0.60
Am	5.26E+04	0.70	3.37E+04	0.70
Am	5.11E+04	0.70	3.56E+04	0.70
Pa	2.62E+05	0.20	6.97E+03	1.20
Pa	2.58E+05	0.20	1.13E+04	1.00
Pa	2.48E+05	0.20	8.80E+03	1.10

Table C.3 Activity measurements for Experiment TAL-3
 (pH 3.5, temperature 20.0 °C)

Element	Organic Counts (dpm/mL)	1 sigma uncertainty (%)	Aqueous Counts (dmp/mL)	1 sigma uncertainty (%)
Np	3.76E+05	0.174	7.86E+04	0.411
Np	3.41E+05	0.176	8.36E+04	0.397
Np	3.51E+05	0.221	7.83E+04	0.410
Pu	5.14E+03	2.25	1.19E+05	0.352
Pu	5.34E+03	4.25	1.22E+05	0.341
Pu	5.84E+03	4.09	1.16E+05	0.359
Am	2.89E+04	1.11	5.57E+04	0.430
Am	2.82E+04	1.05	5.64E+04	0.507
Am	2.86E+04	1.18	5.32E+04	0.489
Pa	2.70E+05	0.198	2.70E+03	2.02
Pa	2.61E+05	0.202	2.79E+03	2.01
Pa	2.68E+05	0.200	2.98E+03	2.04

Table C.4 Activity measurements for Experiment TAL-4
(pH 3.5, temperature 59.5 °C)

Element	Organic Counts (dpm/mL)	1 sigma uncertainty (%)	Aqueous Counts (dmp/mL)	1 sigma uncertainty (%)
Np	1.29E+05	0.289	2.08E+05	0.246
Np	1.06E+05	0.320	1.04E+05	0.324
Np	1.11E+05	0.313	2.00E+05	0.249
Pu	2.62E+03	8.13	8.46E+04	0.497
Pu	1.98E+03	10.8	2.25E+03	9.01
Pu	1.64E+03	13.1	8.07E+04	0.510
Am	1.44E+04	1.70	4.70E+04	0.638
Am	1.43E+04	1.72	1.41E+04	2.00
Am	1.31E+04	1.71	4.51E+04	0.597
Pa	1.92E+05	0.240	2.30E+04	0.738
Pa	1.83E+05	0.248	1.79E+05	0.246
Pa	1.71E+05	0.256	2.48E+04	0.694

Table C.5 Activity measurements for Experiment TAL-5
(pH 3.5, temperature 40.0 °C)

Element	Organic Counts (dpm/mL)	1 sigma uncertainty (%)	Aqueous Counts (dmp/mL)	1 sigma uncertainty (%)
Np	2.95E+05	0.157	1.12E+05	0.373
Np	2.62E+05	0.208	1.15E+05	0.362
Np	2.76E+05	0.195	1.27E+05	0.354
Pu	4.94E+03	5.36	9.54E+04	0.443
Pu	4.85E+03	5.68	9.25E+04	0.450
Pu	5.01E+03	5.34	1.05E+05	0.436
Am	2.27E+04	1.30	4.76E+04	0.577
Am	2.19E+04	1.27	4.69E+04	0.584
Am	2.11E+04	1.29	5.24E+04	0.566
Pa	1.74E+05	0.254	2.21E+03	2.94
Pa	1.69E+05	0.257	3.45E+03	1.88
Pa	1.68E+05	0.258	3.94E+03	1.77

Calculated Distribution Coefficients

The actinide distribution coefficients were calculated for each of the extraction experiments using equation 1. The values are given in Tables C.6-C.10.

Table C.6 Calculated distribution coefficients for Experiment TAL-1
 (pH 2.8, temperature 20.0 °C)

Element	$D_{An, o/a}$	1 sigma uncertainty (%)
Np	8.82E+00	0.39
Np	9.48E+00	0.39
Np	9.21E+00	0.39
Pu	6.89E-02	2.71
Pu	8.47E-02	2.30
Pu	7.31E-02	2.71
Am	3.69E+00	0.52
Am	4.11E+00	0.48
Am	3.86E+00	0.50
Pa	1.10E+02	1.62
Pa	9.88E+01	1.54
Pa	1.33E+02	1.78

Table C.7 Calculated distribution coefficients for Experiment TAL-2
 (pH 2.8, temperature 59.0 °C)

Element	$D_{An, o/a}$	1 sigma uncertainty (%)
Np	1.21E+00	0.31
Np	1.35E+00	0.32
Np	8.84E-01	0.31
Pu	3.98E-02	4.92
Pu	4.94E-02	5.36
Pu	3.27E-02	5.35
Am	1.44E+00	0.89
Am	1.56E+00	1.00
Am	1.44E+00	1.00
Pa	3.76E+01	1.26
Pa	2.28E+01	1.02
Pa	2.82E+01	1.14

Table C.8 Calculated distribution coefficients for Experiment TAL-3
(pH 3.5, temperature 20.0 °C)

Element	$D_{An, o/a}$	1 sigma uncertainty (%)
Np	4.78E+00	0.45
Np	4.08E+00	0.43
Np	4.48E+00	0.47
Pu	4.32E-02	2.28
Pu	4.38E-02	4.26
Pu	5.03E-02	4.11
Am	5.19E-01	1.19
Am	5.00E-01	1.17
Am	5.38E-01	1.28
Pa	1.00E+02	2.03
Pa	9.35E+01	2.02
Pa	8.99E+01	2.05

Table C.9 Calculated distribution coefficients for Experiment TAL-4
(pH 3.5, temperature 59.5 °C)

Element	$D_{An, o/a}$	1 sigma uncertainty (%)
Np	6.20E-01	0.38
Np ⁽¹⁾	1.02E+00	0.46
Np	5.55E-01	0.40
Pu	3.10E-02	8.14
Pu ⁽¹⁾	8.80E-01	14.1
Pu	2.03E-02	13.2
Am	3.06E-01	1.82
Am ⁽¹⁾	1.01E+00	2.64
Am	2.90E-01	1.81
Pa	8.35E+00	0.78
Pa ⁽¹⁾	1.02E+00	0.35
Pa	6.90E+00	0.74

(1) Second replication is an outlying data point.

Table C.10 Calculated distribution coefficients for Experiment TAL-5
 (pH 3.5, temperature 40.0 °C)

Element	D _{An, o/a}	1 sigma uncertainty (%)
Np	2.63E+00	0.40
Np	2.28E+00	0.42
Np	2.17E+00	0.40
Pu	5.18E-02	5.37
Pu	5.24E-02	5.69
Pu	4.77E-02	5.36
Am	4.77E-01	1.42
Am	4.67E-01	1.40
Am	4.03E-01	1.41
Pa	7.87E+01	2.95
Pa	4.90E+01	1.90
Pa	4.26E+01	1.79

van't Hoff Analysis

The slope and y-intercept from the linear regressions performed to calculate the conditional enthalpies and entropies of extraction from the TALSPEAK distribution data are summarized in Table C.11.

Table C.11 Linear regressions results from van't Hoff analysis

pH	Element	Slope	Standard Deviation Slope	y-intercept	Standard Deviation y-intercept	Correlation Coefficient
3.5	Np	4762	584	-14.63	1.89	0.9578
	Pu	1261	597	-7.268	1.930	0.6529
	Am	1287	225	-5.004	0.729	0.9189
	Pa	5806	1085	-15.03	3.506	0.9093
2.8	Np	5173	315	-15.43	1.01	0.9927
	Pu	1559	332	-7.905	1.067	0.9201
	Am	2384	102	-6.774	0.328	0.9964
	Pa	3367	416	-6.756	1.338	0.9708

The conditional enthalpies and entropies of extraction for the actinide elements were calculated using equations C.1 and C.2, respectively,

$$\Delta H^0 = -(\text{slope}) R \tag{C.1}$$

$$\Delta S^0 = (\text{y-intercept}) R \tag{C.2}$$

where R is the ideal gas constant. The values are shown in Table 7 for each of the actinide element.